

**Engineering Poly(ethylene glycol) hydrogel microenvironment for  
osteogenic differentiation of human mesenchymal stem cells**

by

Navakanth Reddy Gandavarapu

B.Tech (Hons)., Indian Institute of Technology, Kharagpur, India. 2007

A thesis submitted to the  
Faculty of the Graduate School of the  
University of Colorado in partial fulfillment  
of the requirement for the degree of  
Doctor of Philosophy  
Department of Chemical and Biological Engineering  
2013

This thesis entitled:  
Engineering Poly(ethylene glycol) hydrogel microenvironment for osteogenic  
differentiation of human mesenchymal stem cells

written by Navakanth Reddy. Gandavarapu  
has been approved for the Department of Chemical and Biological Engineering

---

Dr. Kristi S. Anseth

---

Dr. Jefferey Stansbury

Date\_\_\_\_\_

The final copy of this thesis has been examined by the signatories, and we  
Find that both the content and the form meet acceptable presentation standards  
Of scholarly work in the above mentioned discipline.

## ABSTRACT

Gandavarapu, Navakanth Reddy (Ph.D., Chemical and Biological Engineering)

Engineering Poly(ethylene glycol) hydrogel microenvironment for osteogenic differentiation of human mesenchymal stem cells

Thesis directed by Professor Kristi S. Anseth

Poly(ethylene glycol) (PEG)-based hydrogels have emerged as important class of biomaterials for use as cell and drug delivery vehicles for tissue engineering and also as two- and three-dimensional cell culture substrates. PEG is commonly used due to its hydrophilic and bio-inert properties. The versatility of PEG chemistry allows for independent tailoring of biophysical properties and biochemical functionalization of the microenvironment experienced by cells allowing researchers to conduct systematic studies, *in vitro*, to study and understand the role of physiological cues experienced by cells in a biologically relevant fashion. The main goal of this thesis is to design appropriate hydrogel substrates to design biomaterials platforms to study and understand the role of extracellular matrix (ECM) cues on osteogenic differentiation of human mesenchymal stem cells.

First, the role of phosphate functional groups, found abundantly in the mineral phase of bone, on osteogenic differentiation of hMSCs in the absence of osteogenic supplements was studied. Role of sequestered serum proteins in mediating the adhesion and interaction of hMSCs with the phosphate functional groups was characterized. The role of focal adhesion kinase (FAK) mediated integrin signaling on inducing osteogenic differentiation in hMSCs cultured on phosphate functionalized hydrogels was assessed.

Second, thiol-ene photopolymerization chemistry was exploited to synthesize  $\alpha 5$  integrin priming hydrogels and the role of substrate elasticity on osteogenic differentiation of hMSCs induced by  $\alpha 5\beta 1$  signaling was studied.  $\text{cyl(RRETAWA)}$  peptide that specifically binds to  $\alpha 5$  integrin was synthesized and the effect on soluble delivery to hMSCs was assessed by measuring ALP activity. Hydrogel formulations were identified to independently control their peptide functionalization and elasticity. The interplay of substrate elasticity and peptide functionalization on hMSC adhesion and focal adhesions formation was quantified. Towards understanding the role of substrate elasticity on osteogenic differentiation of hMSCs induced by  $\alpha 5\beta 1$  integrin signaling, the ALP activity of the cultures as a function of substrate elasticity and peptide concentration was measured.

Last, towards development of chemical strategies that allow dynamic tunability of biochemical environment experienced by cells, we have designed and synthesized addition-fragmentation-chain transfer capable allyl sulfide functionalized PEG hydrogel networks. Biochemical patterning via photo-initiated thiol-ene reactions on allyl sulfide was studied and characterized with fibronectin based CRGDS motif as a model thiol containing bioactive compound. The ability to reversibly exchange any thiol containing biochemical cues in these hydrogels was demonstrated and the kinetics of exchange reactions was characterized.

*na hi jnanena sadrsam  
pavitram iha vidyate*

*To my parents*

## ACKNOWLEDGEMENTS

This thesis work would not have been possible without the generous support and encouragement from large number of incredible individuals. First and most importantly, I would like to thank my advisor Prof. Kristi Anseth for all her support, encouragement and advice. Her vision and mentorship has shaped this work into a product I am extremely proud of. Next, I would like to thank my thesis committee members, Prof. Stephanie Bryant, Prof. Jeffrey Stansbury, Prof. Joel Kaar, Prof. Virginia Ferguson for all the advice throughout the years. I would also like to thank my alma mater, Indian Institute of Technology-Kharagpur for installing in me confidence and strength to pursue graduate studies.

I have had the pleasure of working with and learning from several extra-ordinary and creative people within the Anseth group. In particular, I would like to thank Dr. Michael Schwartz and Dr. Peter Mariner for their help on initial conception and direction of my PhD project. I would like to thank Dr. Sarah Anderson for teaching me all the techniques of molecular biology used in this thesis and patiently answering my questions related to biology. In addition I would like to thank my collaborators Dr. Malar Azhagarsamy and Dr. Daniel Alge for their guidance and assistance with the projects. Dr. Malar Azagarsamy has taught me all I know about organic synthesis and Dr. Daniel Alge has taught me a lot about the peptide chemistry. This thesis would not have been possible without help from these supportive scientists.

As a graduate student I have pleasure of working with many talented graduate students who have helped me in and out of lab. I would like to thank fellow graduate students,

Josh McCall, Mark Tibbitt, Abigail Bernard, Dan McKinnon, Celia Xue who made valuable contributions to my research and made my graduate school experience wonderful.

I would like to acknowledge the financial support I've had throughout the years of my graduate work. Funding was provided by National Institutes of Health and Howard Hughes Medical Institute.

I would like to thank all my Boulder friends particularly Raveesh Shenoy, Vamshidhar Dantu, Kaniska Mohanty, Prasanna Madhusudhanan, Parag Shah, Sri Haritha, Prasanna Pavani, Rakesh Kiran for all their good times and support right from my first day in USA to date. Finally, I am grateful to my family for all their care and support throughout the years. Dad, you are my inspiration and special thanks for your help and support. Mom, you are my strength and your constant push for me to shoot for the stars has installed in me attitude to only aim for the best. Sister, you have been a special companion throughout my childhood.

## TABLE OF CONTENTS

LIST OF TABLES	xi
LIST OF FIGURES AND SCHEMES	xii
CHAPTER 1 – INTRODUCTION AND BACKGROUND	1
1.1 Human mesenchymal stem cells for bone regeneration	1
1.1.1 <i>In vitro</i> osteogenic differentiation of hMSCs	2
1.2 Bioactive signals of bone extra-cellular matrix that influence osteogenic differentiation of hMSCs	4
1.2.1 Role of integrin signaling in osteogenic differentiation in hMSCs	5
1.3 Bio-physical signals that influence osteogenic differentiation of hMSCs	9
1.3.1 Influence of matrix mechanics	9
1.3.2 Cell shape and geometry	13
1.4 PEG hydrogels as a platform to culture and study hMSCs	17
1.4.1 Crosslinking PEG using chain and step growth polymerization	17
1.4.2 Creating bioactive PEG hydrogels	20
1.4.3 Dynamic regulation of biochemical signals	22
1.5 Research summary	27
1.6 References	28
CHAPTER 2 – OBJECTIVES	40
2.1 References	45
CHAPTER 3 – Extra-cellular matrix protein adsorption to phosphate-functionalized hydrogels from serum promotes osteogenic differentiation of human mesenchymal stem cells (hMSCs)	46
3.1 Abstract	46
3.2 Introduction	47
3.3 Materials and Methods	51
3.3.1 Cell culture	51
3.3.2 Phosphate functionalized poly(ethylene glycol) gels	51
3.3.3 Quantification of protein adsorption	52
3.3.4 Focal adhesion staining and calculating cell shape parameters	52
3.3.5 Adhesion blocking and integrin blocking experiments	53
3.3.6 Role of focal adhesion kinase (FAK) in osteogenesis of hMSCs on phosphate gels	54
3.3.7 Alkaline phosphatase (ALP) production of hMSCs cultured on phosphate gels	54
3.3.8 Gene expression of hMSCs cultured on phosphate gels	55
3.3.9 Statistical Analysis	56
3.4 Results	
3.4.1 Serum proteins facilitate hMSC attachment and spreading on PO <sub>4</sub> -PEG hydrogels	57



3.4.2 hMSC attachment is mediated by ECM protein-integrin interactions	59
3.4.3 Focal adhesion kinase (FAK) signaling is required for PO <sub>4</sub> -PEG hydrogel induced osteogenesis	61
3.5 Discussion	66
3.6 Conclusions	73
3.7 Acknowledgements	73
3.8 References	74
CHAPTER 4 – Osteogenic differentiation of human mesenchymal stem cells on $\alpha 5$ integrin binding peptide hydrogels is dependent on substrate elasticity	80
4.1 Introduction	80
4.2 Materials and Methods	83
4.2.1 Cell culture	83
4.2.2 Synthesis of cyl(RRETAWA) and CRGDS	83
4.2.3 Synthesis of PEG-Norbornene	85
4.2.4 Rheological characterization of peptide hydrogels	85
4.2.5 Preparation of thiolated glass coverslips	86
4.2.6 Preparation of peptide functionalized hydrogels for cell culture	86
4.2.7 Integrin blocking experiments	87
4.2.8 Focal adhesion staining and determination of cell area, aspect ratio and focal adhesion area	87
4.2.9 Alkaline phosphatase (ALP) production of hMSCs on peptide functionalized gels	88
4.3 Results	89
4.3.1 Synthesis and characterization of $\alpha 5$ binding peptide	90
4.3.2 Soluble delivery of cyl(RRETAWA) induces osteogenic differentiation in hMSCs	91
4.3.3 hMSCs bind to cyl(RRETAWA) gels via $\alpha 5$ integrin	92
4.3.4 Effect of substrate elasticity and peptide concentration on hMSC adhesion to cyl(RRETAWA) gels	94
4.3.5 Osteogenic differentiation of hMSCs on cyl(RRETAWA) functionalized gels	99
4.4 Discussion	100
4.5 References	104
CHAPTER 5 – Photo-click living strategy for controlled reversible exchange of biochemical ligands	106
5.1 Introduction	106
5.2 Results and Discussion	109
5.2.1 Synthesis and biochemical patterning of <i>allyl sulfide</i> functionalized PEG-hydrogel networks	110
5.2.2 Kinetics of biochemical patterning in <i>allyl sulfide</i> functionalized PEG-hydrogel networks	113
5.2.3 Reversible exchange of biochemical moieties in <i>allyl sulfide</i>	117

functionalized hydrogels	
5.2.4 Kinetics of exchange of biochemical moieties in <i>allyl sulfide</i>	120
functionalized hydrogels	
5.3 Materials and Methods	123
5.3.1 Synthesis of 1a (PEG-tetra-azide)	123
5.3.2 Synthesis of 1b	123
5.3.3 Synthesis of 1c	124
5.3.4 Synthesis of peptides	125
5.3.5 Synthesis of fluorescently labeled peptides	125
5.3.6 Hydrogel synthesis	125
5.3.7 Biochemical patterning	126
5.4 References	127
5.5 Supplementary Information	130
5.5.1 Derivation of Rate of addition to allyl sulfide containing networks	130
CHAPTER 6 – Conclusions and Recommendations	132
6.1 References	142
CHAPTER 7 – Bibliography	145

## List of Tables

<b>Table 3.1</b> Primers used for RT-PCR studies	56
<b>Table 4.1</b> Macromolecular monomer compositions for the preparation of cyl(RRETAW) functionalized PEG gels used in the study to form soft and stiff gels and their corresponding modulus	95

## List of Figures and Schemes

**Figure 1.1.** Schematic showing the pathways that mesenchymal stem cells have been shown to differentiate *in vitro*. The image also depicts the shapes of the lineage specific cells typically observed after differentiation of the spindly shaped mesenchymal stem cells. 2

**Figure 1.2.** Generalized timeline for various indicators of osteogenic differentiation of hMSCs (a) Time line for gene expression of Col1, ALP, Cbfa1, OPN and proliferation of hMSCs. (b) Phenotypic changes during osteogenic differentiation of hMSCs. 4

**Figure 1.3.** (a) The schematic depicting integrin signaling events and actin organization inside cells. Upon binding to ECM fibers, integrins initiate formation of focal adhesions (components of focal adhesions are shown in inset), which include focal adhesion kinase (FAK) and vinculin (Vin). Focal adhesions initiate intracellular signaling events that ultimately converge in the nucleus. Focal adhesions also support actin monomer polymerization to form actin-cytoskeleton fibers. The schematic also depicts the role of ECM elasticity on integrin binding and actin organization. Higher ECM elasticity allows for increased integrin clustering and highly developed actin cytoskeleton organization. (b) Immunostaining images demonstrating focal adhesions (characterized by Vinculin in green) and actin cytoskeleton (red) in hMSCs cultured on TCPS. Note the dashed morphology of the focal adhesions at the tips of actin fibers. Scale bar = 50  $\mu\text{m}$ . 7

**Figure 1.4.** Substrate elasticity directs hMSCs differentiation fate as studied by Engler *et al.* hMSCs cultured on poly(acrylamide) gels of Young's modulus (E) 0.1-1 kPa (soft), 8-17 kPa (intermediate), 25-40 kPa (Stiff) underwent neurogenic, myogenic and osteogenic differentiation respectively, in the absence of soluble cues. Immunostained images show the expression of  $\beta 3$  tubulin (corresponding to neurogenic differentiation), MyoD (corresponding to myogenic differentiation) and CBFA-1 (corresponding to osteogenic differentiation) in green and nucleus in blue. Scale bar = 20  $\mu\text{m}$ . 11

**Figure 1.5.** Cell shape and geometry influence hMSCs differentiation fate. A) Role of cell shape on hMSC differentiation as studied by McBeath *et al.* hMSCs cultured on square fibronectin islands of area 1024  $\mu\text{m}^2$  and 10000  $\mu\text{m}^2$  undergo adipogenic and osteogenic differentiation, respectively. B) Role of geometry on hMSC differentiation as studied by Kilian *et al.* hMSCs cultured on flower shaped pattern preferred adipogenic differentiation while those on star shaped pattern preferred osteogenic differentiation. Figures show immunostaining for f-

actin(green), vinculin (red) and nuclei (blue) 16

**Figure 1.6.** Schematic showing the structure of PEG hydrogels formed via (a) Chain growth polymerization and (b) Step growth polymerization 20

**Figure 1.7.** Dynamic regulation of presentation of biochemical ligands. a) 2-photon photopatterning of biochemical ligands using unreactive acrylate functionalities as studied by Hoffman and West. PEG hydrogel is soaked in solution containing biochemical ligand and initiator and subsequently specific regions were exposed to multi-photon light using confocal microscope to form desired 3D patterns. b) Reversible photo-patterning of small peptides achieved by dual wavelength responsive systems. Addition to the network is achieved via thiol-ene photoclick chemistry at 460 nm and removal of the ligands is achieved via cleavage of o-nitrobenzyl moiety upon exposure to 365 nm light. 26

**Figure 3.1.** Serum components mediate hMSC attachment and spreading on  $\text{PO}_4$ -PEG gels ( $[\text{PO}_4] = 50\text{mM}$ ) (A) Effect of seeding conditions on hMSC adhesion to gels. Average number of cells per area attached to PEGDM and  $\text{PO}_4$ -PEG gels when seeded in serum containing media (black bar), pre-incubated with serum containing media and seeded in serum free media (white bar, textured), and seeded in serum free media (grey bar). (# indicates significant difference compared to that on control gels (PEGDM);  $p < 0.05$ , Data represents averages of  $N=3$  different experiments with  $n = 3$  replicates during each experiments). (B). Cell shape parameters; average cell area (filled black bars) and average aspect ratio (striped bars) when cultured for 24 h on different gels as indicated. Cell shape parameters of hMSCs on TCPS were also included for comparison. Phosphate functional groups promote cell spreading similar to cells cultured on tissue culture polystyrene (TCPS) when seeded in growth media. Error bars represent standard deviations for  $N=150-250$  cells. 58

**Figure 3.2. Effect of  $[\text{PO}_4]$  concentration on total protein adsorbed from serum.** Total protein adsorbed was significantly higher on phosphate gels compared to the control ( $[\text{PO}_4] = 0 \text{ mM}$ ) gels. Increasing the concentration of  $[\text{PO}_4]$  in the gels did not result in any significant increase in protein adsorption. Total protein adsorbed on TCPS under similar conditions is  $0.5 \mu\text{g}/\text{cm}^2$  (#, indicates significant difference compared to the control ( $[\text{PO}_4] = 0 \text{ mM}$ ) gel; Data represent averages of  $N=3$  different experiments with 4 replicates in each experiment.  $p < 0.05$ ). 59

**Figure 3.3.** ECM proteins are differentially adsorbed on to  $\text{PO}_4$ -PEG gels ( $[\text{PO}_4] = 50\text{mM}$ ). Blocking cell adhesion sites corresponding to specific ECM proteins (Fibro = Fibronectin, Coll-1 = Collagen-1) adsorbed onto the  $\text{PO}_4$ -PEG gel influences cell attachment. Average number of cells that remained attached to  $\text{PO}_4$ -PEG gels upon blocking were counted and reported as a percentage compared to control. # indicates significant difference compared to control  $p < 0.05$ . (Data represent averages of  $N=3$  different experiments with 3 replicates

in each experiment.)

60

**Figure 3.4.** hMSC interaction with the PO<sub>4</sub>-PEG gels ([PO<sub>4</sub>] = 50mM) is mediated through β1 and β3 integrins. (A) Integrin blocking studies. Cells were incubated with β1, β3, β1+ β3 or control (IgG) antibodies for 30 min and seeded onto phosphate gels. Average number of cells attached were counted and reported as a percentage compared to control. Data represent averages of N=3 different experiments with 3 replicates in each experiment. (B-I). Immunostaining for vinculin (green, B, F), actin (red, C, G), nuclei (blue, D, H) and overlay (E, I) of hMSCs seeded on PO<sub>4</sub>-PEG gels (B-E) and on TCPS (F-I) shows the presence of well-developed focal adhesion plaques. (Scale bar = 50μm). # indicates significant difference compared to control, p<=0.05.

63

**Figure 3.5.** Effect of inhibition of FAK phosphorylation on ALP activity of hMSCs. (A) Total cell number of hMSCs on PO<sub>4</sub>-PEG gels ([PO<sub>4</sub>] = 50mM) in growth media with (45° striped bar) and without (white bar) pFAK inhibitor. Total cell number of hMSCs on TCPS in OS media with (135° striped bar) and without (black bar) pFAK inhibitor. (B) ALP activity profiles of hMSCs cultured on PO<sub>4</sub>-PEG gels ([PO<sub>4</sub>] = 50mM) in growth media with (filled circles) or without (open circles) PF-573228 normalized to cell number. Positive control cultures of hMSCs on TCPS with osteogenic supplements (OS) and with (filled squares) or without (open squares) PF-573228 are also shown. # indicates significant difference compared to hMSC cultures on PO<sub>4</sub>-PEG gel without pFAK inhibitor, (\*) indicates significant difference compared to hMSC cultures on TCPS with OS. Data represent averages of normalized ALP activity of N=3 different experiments with n=3 replicates (C-K). Addition of pFAK inhibitor, PF-573228, doesn't affect the formation of focal adhesion plaques. Immunostained images for vinculin (green, C,F,I), actin (red, D,G,J), overlay (E,H,K) of hMSCs at day1 (C-E), day 7 (F-H), day 14 (I-K) cultured on PO<sub>4</sub>-PEG constructs in the presence of FAK inhibitor. Vinculin staining shows the presence of well-developed focal adhesion plaques upon inhibiting phosphorylation of FAK. (Scale bar= 100μm)

65

**Figure 3.6.** Effect of inhibition of phosphorylation of FAK on expression of osteogenic related genes in hMSCs. hMSCs cultured on PO<sub>4</sub>-PEG gels ([PO<sub>4</sub>] = 50mM) in growth media on TCPS in OS media in the presence (black bars) or absence (white bars) of FAK inhibitor (PF-573228). All data are normalized to GAPDH gene and further normalized to a corresponding TCPS, growth media control. Data are shown for OS genes, a) Collagen-1 (COLL-1), b) CBFA1, c) Osteopontin (OPN). # indicates significant difference compared to cultures that did not receive pFAK inhibitor p<=0.05. Data represent fold increase averaged over N=3 biological replicates with n=2 technical replicates of each.

66

**Figure 4.1. Schematic of synthesis of c(RRETAWA) peptide (B) via lactam bridge formation.** On-resin cyclization of (A) CAhxK(Alloc)RRETAWAE(ODmab). i) Deprotection of ODmab in 2% Hydrazine in DMF, ii) Deprotection of Alloc in 0.1 eq Pd(PPh<sub>3</sub>), in DCM, iii) HOBt/HBTU coupling to form the lactam bridge, iv) Peptide cleavage from resin

in trifluoroacetic acid, tri-isopropyl silane and phenol.

90

**Figure 4.2. Priming  $\alpha 5$  integrin induces osteogenic differentiation in hMSCs.**

Figure shows the ALP activity of hMSCs at day 7 and 14 cultured on TCPS in growth media supplemented with 10  $\mu\text{g}/\text{ml}$  (●) or 100  $\mu\text{g}/\text{ml}$  (■) c(RRETAWA) peptide. Normalized ALP activity of hMSCs cultured on TCPS in osteogenic media (◆) without the peptide is also included as positive control. Normalized ALP activity was calculated by normalizing the measured ALP activity to that of day 1.

92

**Figure 4.3. Interaction of hMSCs with c(RRETAWA) gels occurs via  $\alpha 5$  integrin.**

A) Effect of blocking  $\alpha 5$  integrin and  $\alpha V\beta 3$  on hMSC adhesion to c(RRETAWA) gels. hMSCs were incubated with corresponding antibodies for 30 mins to allow for binding of the antibodies to integrins and seeded onto 1 mM c(RRETAWA) gels and the number of hMSCs that remain attached were measured and reported as percentage compared to the control. Isotype antibody was used as a control antibody. Blocking with  $\alpha 5$  integrin antibody significantly reduced the binding of hMSCs to the gels. B-D: Immunostaining for  $\alpha 5$  integrin (green, B,D), f-actin (red, C,D) and combined (D) in hMSCs cultured on 1mM c(RRETAWA) PEG gels. Images clearly show the localization of  $\alpha 5$  integrin as dashed shaped structures at the edge of actin fibers. Scale bar = 100  $\mu\text{m}$ .

93

**Figure 4.4: Effect of substrate elasticity and ligand concentration on hMSC adhesion to c(RRETAWA) gels.** A) Cell adhesion density B) Cell area C) Aspect ratio of hMSCs on soft and stiff gels at 0.1 and 1 mM c(RRETAWA) concentration. Both substrate elasticity and ligand concentration affected hMSC attachment. Stiff gels supported significantly higher cell attachment at both the concentrations studied. Cell area and aspect ratio results demonstrate that hMSCs show well-spread morphology on stiffer substrates. hMSC spreading was enhanced on stiffer substrates and also by the c(RRETAWA) peptide. (\*) indicates statistical significance between different ligand concentration at similar stiffness. (#) indicates statistical significance between different stiffness at similar ligand concentration. 97

**Figure 4.5 Effect of substrate elasticity and ligand concentration on focal adhesion formation.** A-L) Immunostaining for focal adhesions (vinculin, green A,D,G,J), f-actin (red, B,E,H,K) and combined (C,F,I,L) of hMSCs on soft (A-F) and stiff (G-L) gels at 0.1 mM (A-C, G-I) and 1 mM (D-F, J-L) c(RRETAWA) (ligand). hMSCs showed diffused f-actin and did not form any focal adhesions on soft gels at 0.1 mM ligand concentration and poor organization of f-actin and small focal adhesions at 1mM peptide concentration. hMSCs formed well developed f-actin organization on stiff gels at both the concentrations while prominent focal adhesions were only formed at 1mM peptide concentration. Scale bar = 50  $\mu$ m. 98

**Figure 4.6. Effect of substrate elasticity and c(RRETAWA) (ligand) concentration on focal adhesion area (A) and focal adhesion density (B).** A) Average area of focal adhesions formed by hMSCs on soft and stiffer substrates at 0.1 and 1 mM ligand concentrations were measured using ImageJ. hMSCs developed significantly larger focal adhesions on stiff gels at 1 mM compared to 0.1 mM ligand concentration. On softer substrates hMSCs formed small but significantly larger focal adhesions only at 1mM ligand concentrations. # denotes significant difference with 1mM soft gels. (\*) denotes significant difference from 0.1mM stiff gels. B) Focal adhesion density was calculated as fraction of focal adhesions occupied in the cell area. Focal adhesion density did not show any dependence on stiffness or ligand concentration. 99

**Figure 4.7 Osteogenic differentiation of hMSCs on c(RRETAWA) functionalized PEG gels.** A) ALP activity of hMSCs cultured on stiff (■,◆) and soft (□,◇) gels at 0.1mM (diamonds) and 1 mM (squares) . ALP activity was significantly increased only in hMSCs cultured on stiff substrates. Higher c(RRETAWA) concentration induced higher ALP activity in hMSCs on stiff substrates. Normalized gene expression profiles at day 14 of B) CBFA-1, C) Osteopontin (OPN) and D) Coll-1a genes in hMSCs cultured on soft and stiff gels at 0.1 mM (white bars) and 1 mM (black bars) c(RRETAWA) concentrations. hMSCs upregulated osteogenic genes only on stiff gels in a concentration dependent manner. All data are normalized with GAPDH and further normalized with corresponding expression of hMSCs on TCPS in growth media. &,#



indicates significant difference compared to 0.1 mM soft, 1 mM soft gels respectively. (\*) indicates significant difference between 1mM and 0.1 mM ligand concentration at same stiffness 100

**Scheme 5.1.** Mechanism of addition fragmentation chain transfer of an allyl sulfide functional group upon attack by a thiyl radical. 110

**Figure 5.1.** Structures of monomers used to form the hydrogel networks. 1a: 4-arm-poly(ethylene glycol)-tetra azide. 1b: 2-methylene-propane-1,3-bis(thioethyl 4-pentynoate). 1c: Benzoic acid-3,5-bis( 4-pentynoate). 111

**Figure 5.2.** Biochemical patterning of allyl sulfide functionalized PEG hydrogels. A) Exposing specific regions of networks formed from 1a and 1b to 365 nm wavelength light results in mass loss in exposed regions due to the  $\beta$ -scission of allyl sulfide functional group resulting in degradation of the crosslinks. B) Image demonstrates the mass loss of hydrogel in the exposed regions. After patterning, the gel was swollen in AF555 solution and imaged under confocal microscope. Black regions represent the degraded regions of the hydrogel. C) Exposing specific regions of networks formed from 1a, 1b and 1c result in stable patterning of the biochemical ligand as opposed to degradation in (A). D) Confocal image of array of 100  $\mu\text{m}$  square patterns formed by exposing specific regions of the network to 365 nm light in the presence of patterning conditions. Scale bar = 50  $\mu\text{m}$ . 113

**Figure 5.3.** Kinetics of thiol-ene photopatterning of allyl sulfide functionalized PEG hydrogel networks. A) Reaction mechanism of addition of a thiol containing compound to the allyl sulphide functionalized hydrogel. B) Concentration of patterned peptide as a function of time of exposure shows that the rate of addition is directly proportional to the time of exposure. C) Concentration of patterned peptide as a function of initiator concentration at different light intensities used at 10 min exposure times. The figure shows linear dependence of rate of addition on both initiator concentration and light intensity. 116

**Figure 5.4. Photoclick living strategy allows reversible exchange of biochemical ligands.** A) Mechanism of replacement of a thiol-containing compound on allyl sulphide functional group. B) Schematic of replacement of biochemical ligand. C-K) Demonstration of reversible exchange of thiol containing peptides. (C-E) 250 $\mu\text{m}$  square pattern of AF<sub>555</sub>AhxRGDSC. (F-H) Buffalo logo was formed by replacing AF<sub>555</sub>AhxRGDSC with AF<sub>488</sub>AhxRGDSC resulting in appearance of green fluorescence and disappearance of red fluorescence only in the exposed regions. (I-K) Demonstration of further replacement on living allyl sulfide: Letters 'CU' inside the buffalo logo were exposed to 720 nm light to photo-exchange with non-fluorescent AhxRGDSC peptide. Photo-exchange of peptides was confirmed by removal of green fluorescent (J) only at the exposed regions. Scale bar = 100  $\mu\text{m}$ . 119

**Figure 5.5. Kinetics of exchange of biochemical ligands in AFCT capable hydrogels.** A) Amount of AF<sub>555</sub>AhxRGDSC remained attached to the network after the photo-exchange reaction as a function of dosage at different laser scanning speeds. B) Amount of AF<sub>488</sub>AhxRGDSC photo-coupled to the network due to the exchange as a function of dosage at different laser scanning speeds. (pixel dwell times for laser scan speed 2 = 36.67  $\mu\text{sec}/\mu\text{m}^2$ , 4 = 9.17  $\mu\text{sec}/\mu\text{m}^2$ , 6 = 2.3  $\mu\text{sec}/\mu\text{m}^2$ ) C-E) Simultaneous generation of opposing gradient patterns of two different biomacromolecules. (C) AF<sub>555</sub>, (D) AF<sub>488</sub>RGDS and (E) combined. Gradient pattern is formed by exposing a uniform 250  $\mu\text{m}$  square pattern to radially increasing laser power at scan speed 2. 122

**Figure S5.1.** Amount of AF<sub>555</sub>AhxRGDSC photopatterned into the network as a function of  $[I]_0I_0$ . All the data points collapse onto a straight line validating Equation 6. 131

**Figure 6.1.** a) Development of addition-fragmentation-chain transfer (AFCT) capable hydrogels to achieve independent control of reversible patterning and substrate elasticity. A cyclic allyl sulfide can be covalently tethered to the cross-linker used to form the hydrogels reported in Chapter 5. b) Controlling the direction of  $\beta$ -scission of allyl sulfide intermediate upon attack by a thyl radical. Asymmetric allyl sulfide functional group (i) upon attack by thiyl radical forms an intermediate (ii) that undergoes  $\beta$ -scission only in the direction of sulphur atom resulting in (iii) 138

**Figure 6.2. Adhesive patterns define actin-organization maintaining the geometric shape of cell.** Brightfield images (a,c,e,g) show geometric shapes of adhesive patterns. Immunostained images (b,d,f,h) show vinculin (green) and f-actin (red) organization in on different geometric patterns studied. Images clearly show variation of f-actin organization and focal adhesion localization in retinal pigment epithelial cells with same geometric shape. 140

**Figure 6.3. Two-dimensional modulation of f-actin and vinculin organization maintaining the geometric shape.** A) Cells can be initially seeded onto adhesive patterns (e.g. pentagon pattern shown) formed on allyl sulfide containing PEG gels. At a later time point, specific regions of the adhesive pattern can be exchanged with a non-adhesive peptide in the presence of cells, resulting in a new pattern. Cells should re-modulate the f-actin and vinculin organization. Such dynamic modulation of f-actin organization could be used to study the interplay of cell geometry and f-actin organization on hMSC differentiation. 141

**Figure 6.4. Mapping osteogenic differentiation of hMSCs on  $\alpha 5$  integrin priming cyl(RRETAWA) gels.** At specific time points, cyl(RRETAWA) peptide can be exchanged with a non-specific integrin binding CRGDS peptide, and osteogenic differentiation assayed to map osteogenic differentiation of hMSCs induced by  $\alpha 5$  integrin signaling. 142

## CHAPTER 1

### INTRODUCTION AND BACKGROUND

---

#### 1.1 Human mesenchymal stem cells for bone regeneration

Human mesenchymal stem cells are fibroblast-like multipotent cell populations that reside in a bone marrow niche.<sup>1</sup> When isolated from bone marrow and expanded *ex vivo*, these cells have been shown to be capable of differentiating down osteogenic, adipogenic and chondrogenic lineages,<sup>2</sup> as well as several other pathways (Figure 1.1). From the time of establishment of *in vitro* protocols for differentiation of hMSCs down specific lineages by Pittenger *et al.*,<sup>2</sup> there has been a growing interest in the use of hMSCs for applications in regenerative medicine. Their ease of isolation, expansion and differentiation potential has rendered them particularly attractive for use in several cell-based therapies for regenerating cartilage and bone *in vivo*.<sup>3-5</sup> For example, these cells have been shown to engraft and promote bone growth in children with osteogenesis imperfecta.<sup>4</sup>

Traditionally, hMSCs are expanded as monolayers on tissue culture polystyrene (TCPS) in growth media supplemented with fetal bovine serum (FBS). Several growth factors and small chemical molecules have been identified that promote proliferation (e.g., FGF-2),<sup>6-13</sup> differentiation (e.g., TGF- $\beta$  for chondrogenic differentiation, dexamethasone for osteogenic differentiation, isobutyl methylxanthine for adipogenic differentiation),<sup>2,6,8,14-25</sup> and migration (e.g., TNF- $\alpha$ )<sup>26-30</sup> of hMSCs *in vitro*. In lineage-

specific culture conditions, hMSCs up-regulate lineage specific genes and also secrete extracellular matrix molecules that can be tissue specific.<sup>2</sup>

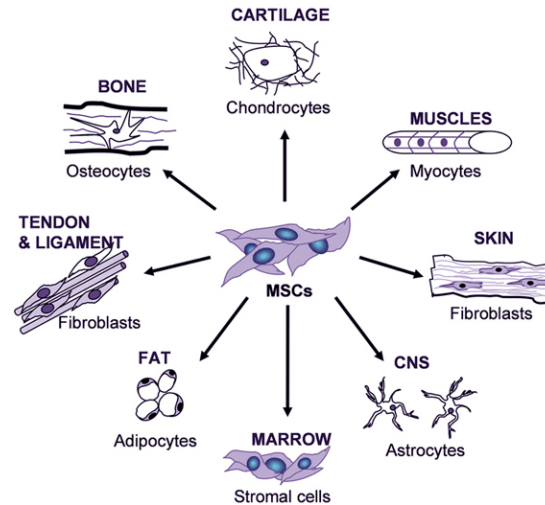


**Figure 1.1.** Schematic showing the pathways that mesenchymal stem cells have been shown to differentiate *in vitro*. The image also depicts the shapes of the lineage specific cells typically observed after differentiation of the spindly shaped mesenchymal stem cells. [Adopted from <http://www.stem-cell-solutions.com.au/test/training/research/111-adult-mesenchymal-stem-cells>].

### 1.1.1 *In vitro* osteogenic differentiation of hMSCs

*In vitro*, hMSCs have been shown to differentiate into bone producing osteoblasts upon induction with a ‘cocktail’ of soluble factors, consisting of growth factors and chemical molecules added to the growth medium. This cocktail is usually comprised of dexamethasone,  $\beta$ -glycerol phosphate, and ascorbic acid 2-phosphate, or alternatively bone morphogenetic proteins (BMPs). The progression of hMSCs towards the osteogenic lineage is characterized by several distinguishing characteristics, which include elevated alkaline phosphatase (ALP) secretion, up-regulation of core binding factor alpha-1 (CBFA1), ALP, collagen type 1 (Coll-1), osteopontin (OPN), and osteocalcin (OCN)

genes, and transition from an elongated, spindle morphology to one that is more cuboidal. The transcription factor, CBFA1, is considered to be an early and specific marker indicative of the osteoblast lineage, as it controls the expression of several of osteogenic related genes.<sup>31</sup> Biochemical pathways that are stimulated by soluble factors converge to phosphorylate CBFA1 transcription factor present inside the nucleus that then further controls the expression of osteogenic genes. Hence, up-regulation of CBFA1 is considered to be one of the early essential markers for progression of hMSCs down an osteogenic lineage.

Figure 1.2 shows a schematic representing lineage progression of hMSCs during osteogenic differentiation *in vitro* with respect to cell number and the expression of CBFA1, ALP, Coll-1 and OPN. Initially, hMSCs undergo an exponential growth phase until they become confluent. Upon reaching confluency, expression of Coll-1 increases as cells secrete and deposit an extracellular matrix. During this time, hMSCs also secrete ALP, which reaches a maximum and then decreases before matrix mineralization. Later stages of the differentiation program are then characterized by up-regulation of OPN expression and the resulting mineralization of the proteinaceous matrix.

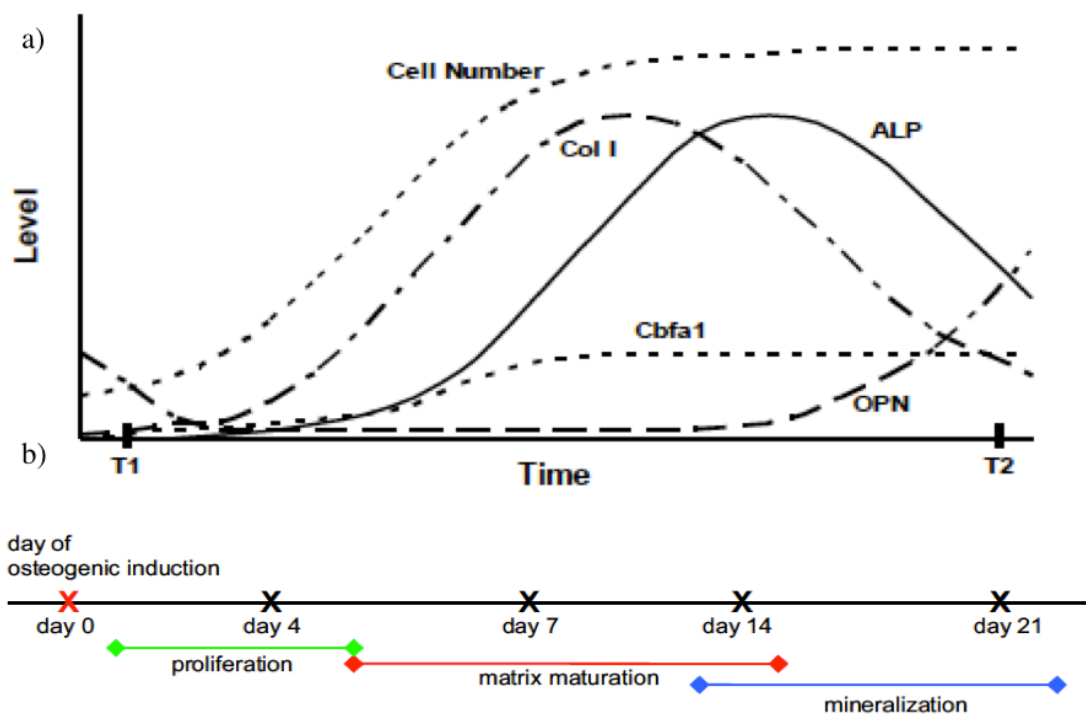


**Figure 1.2. Generalized timeline for various indicators of osteogenic differentiation of hMSCs** (a) Time line for gene expression of Col1, ALP, Cbfa1, OPN and proliferation of hMSCs.<sup>32</sup> (b) Phenotypic changes during osteogenic differentiation of hMSCs.<sup>33</sup>

## 1.2 Bioactive signals of Bone Extra-Cellular Matrix (ECM) that influence osteogenic differentiation of hMSCs.

*In vivo* cells reside in a complex biological macromolecular scaffold, termed the extracellular matrix (ECM), that is comprised of multiple types of insoluble molecules, such as adhesive proteins (e.g., fibronectin, collagen-1) and proteoglycans that synergize to form a tight meshwork that provides physical support to the cells and also sequesters biological signals.<sup>34</sup> Cells constantly interact with this matrix scaffold, receiving signals that in turn result in remodeling of the surrounding ECM, ultimately creating a highly dynamic, bioactive tissue environment. Since the establishment of *in vitro* culture

conditions to define the differentiation program in hMSCs, there has been significant interest in studying the role of cell-ECM interactions, referred to as insoluble cues in this thesis, in the differentiation of hMSCs. Of all the diverse ECM molecules, interaction of hMSCs with adhesive proteins has been of significant interest for bone tissue engineering applications, as the organic phase of bone ECM is ~20% of the bone mass, is composed of ~90% collagen<sup>35</sup> and ~5% of other adhesive proteins (e.g., fibronectin, vitronectin, osteopontin).

Many cellular processes like morphology, survival, growth, differentiation, migration and apoptosis are dependent on the continuous dialog between cells and their surrounding ECM. Hence, studying the role of these insoluble cues in hMSC differentiation provides new avenues for biomedical researchers interested in designing biomaterial platforms and learning about which functional cues are necessary to elicit desired cellular functions.

### **1.2.1 Role of integrin signaling in osteogenic differentiation of hMSCs:**

Integrins are heterodimeric transmembrane receptors consisting of  $\alpha$  and  $\beta$  subunits that primarily mediate the adhesion of cells to the surrounding ECM adhesive proteins.<sup>36-</sup>  
<sup>38</sup> Currently, 8 $\beta$  and 18 $\alpha$  integrin subunits have been identified, and they associate to form 24 distinct  $\alpha\beta$  integrins, each with different binding characteristics. Upon binding to ECM ligands, integrins cluster and initiate recruitment of cytoskeletal and intracellular signaling molecules to form macromolecular aggregates, termed focal adhesions (Figure 1.3),<sup>39</sup> that initiate a cascade of signaling pathways such as FAK, Rac, Rho, MAPK pathways. These pathways are known to be critical for survival, growth, differentiation and migration of cells.

Cultures of hMSCs expanded on TCPS have been found to express  $\alpha1\beta1$ ,  $\alpha2\beta1$ ,  $\alpha5\beta1$ ,  $\alpha6\beta1$ ,  $\alphaV\beta3$  and  $\alphaV\beta5$  integrins.<sup>40</sup> The role of the  $\beta1$  integrin subfamily in hMSCs is predominant, as they mediate adhesion to the ECM proteins fibronectin, collagen and laminin, all of which are found in bone ECM *in vivo*.<sup>38,41-46</sup> A dominant negative type  $\beta1$  subunit in mice results in reduced bone mass and a thinner and more porous bone structure.<sup>43</sup> Perturbing  $\beta1$  signaling using function-perturbing antibodies also results in lower ALP activity and matrix mineralization on biomaterial surfaces designed to promote osteogenic differentiation.<sup>40</sup> In contrast, the  $\beta3$  subunit, which includes the  $\alphaV\beta3$  integrin, has been shown to play a negative role during bone formation and healing *in vivo*. Although, the  $\alphaV\beta3$  integrin mediates adhesion to fibronectin, it has been shown to have a dominant negative effect on proliferation and osteogenic differentiation of hMSCs.<sup>47-49</sup> The negative role of the  $\beta3$  integrin is also supported by *in vivo* studies demonstrating early fracture healing and up-regulation of osteogenic related genes in  $\beta3$  null mice.<sup>50</sup> Collectively, the above studies highlight the importance of the  $\beta1$  family integrins in bone biology.



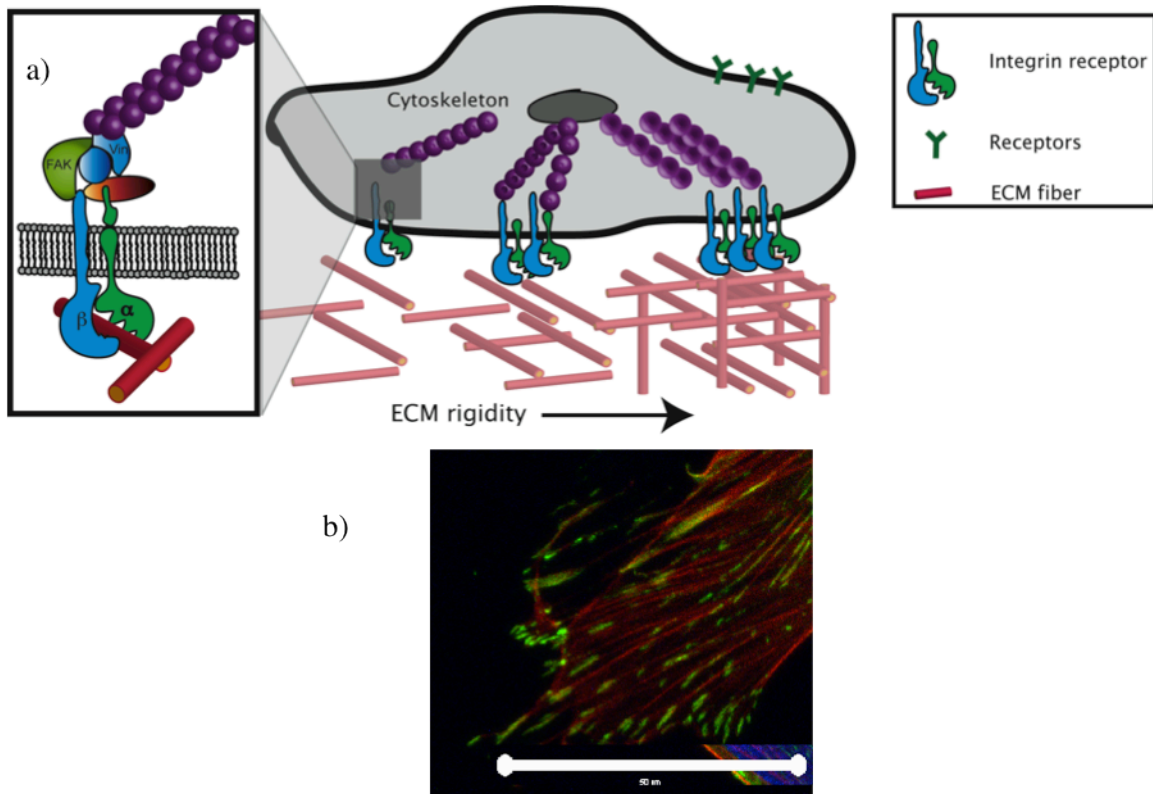


**Figure 1.3.** (a) The schematic depicting integrin signaling events and actin organization inside cells. Upon binding to ECM fibers, integrins initiate formation of focal adhesions (components of focal adhesions are shown in inset), which include focal adhesion kinase (FAK) and vinculin (Vin). Focal adhesions initiate intracellular signaling events that ultimately converge in the nucleus. Focal adhesions also support actin monomer polymerization to form actin-cytoskeleton fibers. The schematic also depicts the role of ECM elasticity on integrin binding and actin organization. Higher ECM elasticity allows for increased integrin clustering and highly developed actin cytoskeleton organization. (b) Immunostaining images demonstrating focal adhesions (characterized by Vinculin in green) and actin cytoskeleton (red) in hMSCs cultured on TCPS. Note the dashed morphology of the focal adhesions at the tips of actin fibers. Scale bar = 50  $\mu\text{m}$ .

Early studies have shown that fibronectin plays a key role in regulating survival,<sup>51</sup> adhesion,<sup>42,48,52,53</sup> matrix secretion<sup>46,48,51-53</sup> and expression of osteogenic related genes in osteoblasts,<sup>41,51</sup> a late stage functional phenotype of hMSCs differentiating down the osteogenic pathway.  $\alpha 5\beta 1$ , which predominantly mediates adhesion to fibronectin, is steadily expressed by hMSCs and has been shown to be important for their survival.<sup>42</sup> Several studies have reported that engagement of  $\alpha 5\beta 1$  integrin is strongly correlated to the ability of hMSCs to undergo osteogenic differentiation. Fibronectin fragments that promote higher and more specific interaction with  $\alpha 5\beta 1$  have been found to induce a specificity dependent increase in matrix mineralization, along with elevated expression of CBFA1, OCN and alkaline phosphatase activity. These results demonstrate a strong dependence of osteogenic differentiation of hMSCs on  $\alpha 5\beta 1$  downstream signaling.<sup>48,52,53</sup> In another study, priming  $\alpha 5\beta 1$  using antibodies or over-expression of the  $\alpha 5$  integrin resulted in enhanced alkaline phosphatase secretion and mineralization, whereas blocking the  $\alpha 5$  integrin reversed the effect in hMSCs.<sup>54,55</sup> The role of  $\alpha 5\beta 1$  in osteogenesis is further supported by *in vivo* implant studies, which found better osseointegration of titanium implants coated with a  $\alpha 5\beta 1$  specific engineered fibronectin fragment compared to uncoated ones.<sup>52</sup> Further,  $\alpha 5\beta 1$  signaling has also been correlated to a reduction in fibroblast growth factor receptor (FGFR) expression, stimulation of which has been shown to preserve the stem cell phenotype in hMSCs, in osteoblasts.<sup>56</sup> Finally, a study by Salter *et al.*<sup>57</sup> demonstrated that osteoblasts sense the mechanics of their surrounding environment using  $\alpha 5\beta 1$ , suggesting a potential role of this integrin in substrate elasticity defined osteogenic differentiation of hMSCs.

### **1.3 Bio-physical signals that influence osteogenic differentiation of hMSCs**

There is a growing body of literature demonstrating that cells are sensitive to physical factors, such as cell shape, geometry, matrix mechanics and nanotopography of the surrounding ECM.<sup>58</sup> These biophysical cues are sensed, in part, by cells using their sensory machinery, such as integrins,<sup>59,60</sup> and are transduced into regulation of downstream gene expression, a process termed as mechanotransduction. Ultimately, mechanotransduction can play a similar role to bioactive cues in determining cell fate, even differentiation of stem cells like hMSCs. However, much research is needed to improve the field's understanding as to how these external cues are translated all the way to the nucleus and the specific pathways involved.

During tissue regeneration and wound healing, the mechanics of the surrounding environment is constantly changing, structurally and mechanically; thus, mechanotransduction can play a significant role in the regeneration/repair mechanism played out by stem cells. Studies demonstrating the individual role of these cues in stem cell fate and those that foray into the underlying mechanisms have been greatly advanced by developments in biomaterial chemistries, along with micro- and nano-technology processing strategies, which enable the development of highly controlled, relevant *in vitro* models for conducting systematic studies.

#### **1.3.1 The influence of matrix mechanics**

Stem cells are mechanosensitive and mechanoresponsive, in the sense that respond to changes in elasticity of the surrounding ECM by modulating their endogenous cytoskeleton contractility which is balanced by the resistive forces of the ECM. The magnitude of this response is often regulated by the elastic modulus of the ECM and

transmitted by cell-ECM adhesions. This tensional homeostasis plays a key role in several basic cellular functions such as proliferation, apoptosis, adhesion and migration, and its dysregulation has been suggested to be involved in the pathogenesis of several human diseases, including osteoporosis, osteoarthritis and cancer.<sup>61,62</sup> The selective control over stimulation of differentiation pathways in hMSCs by substrate elasticity was only recently demonstrated. In this seminal study, Engler *et al.*<sup>63</sup> (Figure 1.4) demonstrated that in the absence of exogenous soluble factors, hMSCs cultured on poly(acrylamide) hydrogels of varying elastic modulus (soft: 0.1-1kPa, intermediate: 8-17kPa, stiff: 25-40 kPa) was sufficient to induce differentiation in hMSCs into a tissue type corresponding to the tissue's relative elasticity *in vivo* (soft: neurogenic, intermediate: myogenic, stiff: osteogenic differentiation). This study generated tremendous interest to better understand and define the role of mechanotransduction in the biology of hMSCs. Later studies have shown that substrate elasticity has a major effect on hMSCs proliferation, adhesion, intra-cellular organization of cytoskeletal elements, migration and differential response to soluble signals. For example, Winer *et al.*<sup>64</sup> demonstrated that hMSCs maintain quiescence with cell cycle arrest on 250 Pa gels, reminiscent of its bone marrow niche. These quiescent hMSCs were competent and resumed proliferation and osteogenic differentiation when in contact with stiffer substrates in growth media (i.e., in the presence of serum). Further, the quiescent hMSCs underwent adipogenic differentiation on 250 Pa gels when stimulated with adipogenic supplements, demonstrating that the hMSCs maintains their stemness on soft gels.

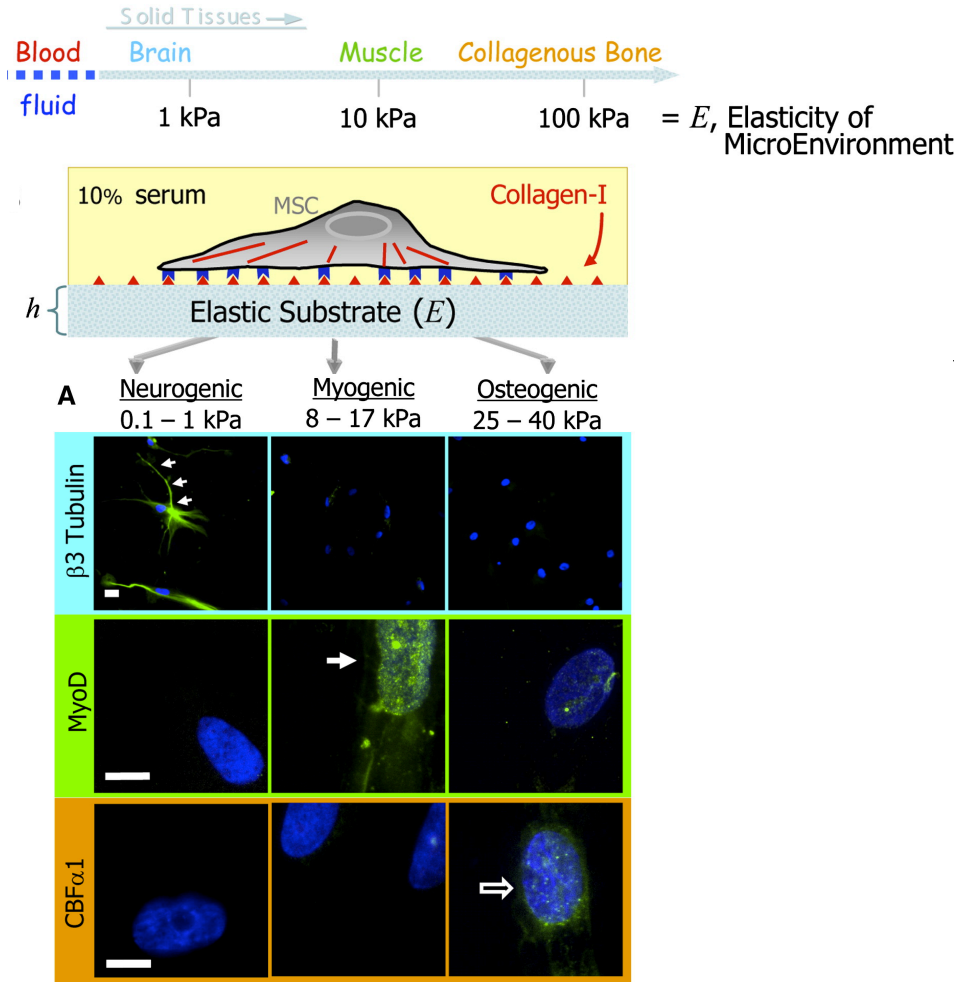


**Figure 1.4. Substrate elasticity directs hMSCs differentiation fate as studied by Engler *et al.*<sup>63</sup>** hMSCs cultured on poly(acrylamide) gels of Young's modulus ( $E$ ) 0.1-1 kPa (soft), 8-17 kPa (intermediate), 25-40 kPa (Stiff) underwent neurogenic, myogenic and osteogenic differentiation respectively, in the absence of soluble cues. Immunostained images show the expression of  $\beta 3$  tubulin (corresponding to neurogenic differentiation), MyoD (corresponding to myogenic differentiation) and CBF $\alpha$ -1 (corresponding to osteogenic differentiation) in green and nucleus in blue. Scale bar = 20  $\mu$ m.

As hMSCs egress from the bone marrow niche<sup>65</sup> and home to specific tissue environments, they encounter different ECM stiffnesses, and hence, they could also respond to gradients in stiffness. In this regard, hMSCs have been shown to migrate up an elasticity gradient in a process termed ‘durotaxis’ when presented with both physiological and pathological substrate gradients. These results implicate that hMSCs may first respond to an elasticity gradient through migration, and then differentiate after reaching the tissue site.<sup>66</sup> Substrate elasticity has also been shown to cause a dramatic effect on the adhesion of hMSCs. On soft substrates, hMSCs exhibit a rounded morphology with poor cytoskeleton development, as determined by f-actin organization and the formation of immature focal adhesions. Interestingly, hMSCs show a well spread morphology with highly organized f-actin, mature focal adhesions and higher proliferation on stiff substrates.

Adherent cells sense matrix mechanics through a force balance between the force exerted by the intracellular actomyosin contractility and the resistance offered by the surrounding environment determined by its elastic modulus. Hence, the level of cytoskeleton tension developed inside of cells, determined by organization of actomyosin fibers, is directly proportional to the substrate elasticity. This positive correlation has been demonstrated by studies observing very good organization of actin cytoskeleton at higher substrate elasticity and poor actin cytoskeleton organization on soft substrates.<sup>67-69</sup> Also, integrins act as pivot points to transmit these pulling and resistive forces between intracellular components and extracellular surroundings. Figure 1.3a depicts the effect of substrate elasticity on integrin binding and actin cytoskeleton organization. This tensional homeostasis also plays a causal role for regulating the matrix mechanics dependent

differentiation observed with hMSCs. When the ability to generate cytoskeleton tension is blocked by an inhibitor, such as blebbistatin, hMSCs do not respond to substrate stiffness, and the matrix stiffness dependent differentiation capability is obliterated.<sup>63</sup> Further studies<sup>63,70,71</sup> have revealed that matrix stiffness controls the activation of RhoA/ROCK, a key regulator of actin cytoskeleton formation and FA formation, which controls downstream signaling pathways resulting in regulation of CBFA1. Involvement of these pathways has been further verified by studies demonstrating significantly reduced gene expression levels of osteogenic genes, ALP activity and matrix mineralization of hMSCs cultured on stiff hydrogels in the presence of RhoA/ROCK inhibitor.<sup>71-74</sup> Taken together, the above studies suggest a significant role of matrix mechanics on hMSC biology and warrant biomedical researchers to incorporate this factor in designing biomaterials for tissue engineering and regenerative medicine applications.

### **1.3.2 Cell shape and geometry:**

Cells are known to adapt their shapes to accommodate their specific functions. For example, adipocytes are spherical in shape to maximize lipid vacuoles storage, and neurons have long axons to deliver signals rapidly over a long distance. Events associated with stem cell differentiation during tissue regeneration are designed to change cell shape, and those changes in shape can influence tissue structure and function. Previous research on endothelial, epithelial, and fibroblasts cells has revealed that when cells proliferate they are elongated and spread, but undergo apoptosis and die when they

are in a completely retracted state. Hence, with respect to stem cells, a natural converse question arises as to whether controlling their shape can regulate their phenotype.

Evidence for the dependence of hMSC differentiation on cell shape has been only recently demonstrated and generated huge interest to create biomaterial culture systems that manipulate and control cell shape. For example, McBeath *et al.*<sup>74</sup> constructed fibronectin islands of varying size using microcontact printing and showed that hMSCs restricted to smaller shapes differentiated into adipocytes, but preferred an osteogenic fate when allowed to spread (Figure 1.5a). These studies were conducted in the presence of media with dual soluble cues (i.e., a mixture of soluble cues that induce osteogenic and adipogenic differentiation in hMSCs), thus implicating that shapes cues may work in concert with soluble cues. Complementary to this work, Ruiz and Chen<sup>73</sup> demonstrated that the spatial position of cells residing within multicellular fibronectin islands also affected the differentiation of hMSCs: cells present in the interior of the pattern preferred adipogenic differentiation while cells present near the exterior of the patterns preferred osteogenic differentiation. Also, the hMSC differentiation patterns varied in a manner that depended on the overall geometry of the microenvironment; hMSCs towards the convex side of all the shapes preferred adipogenic differentiation while those near the concave side preferred osteogenic differentiation. Complementary traction force measurements revealed that cells present on the convex side of the patterns experienced higher stresses, while cells present on the concave side of the pattern experienced lower stresses. Thus, the authors suggested that cytoskeleton tension may play a causal role in fate decisions of hMSCs. Inhibiting actin polymerization in hMSCs with chemical inhibitors added to the media reversed the preference of osteogenesis to adipogenesis in



the convex areas that promoted osteogenesis. These studies have supported recent hypotheses that cell shape signalling and soluble inductive factor signaling converge on the actin cytoskeleton to regulate hMSC fate.

In another landmark study, Kilian *et al.*<sup>75</sup> reported that, by constructing single cell fibronectin islands, cell geometry also plays an important role in fate decisions of hMSCs. Their study demonstrated that the aspect ratio of rectangular islands correlated positively with osteogenic differentiation, and islands with a pentagonal symmetry and curvatures increased cytoskeleton tension, promoting osteogenesis relative to adipogenesis (Figure 1.5b). Further, hMSCs underwent adipogenesis when cultured in the presence of inhibitors of actin irrespective of the geometry and curvature, supporting the previous reports that cytoskeleton tension plays a causal role in hMSC fate decisions.

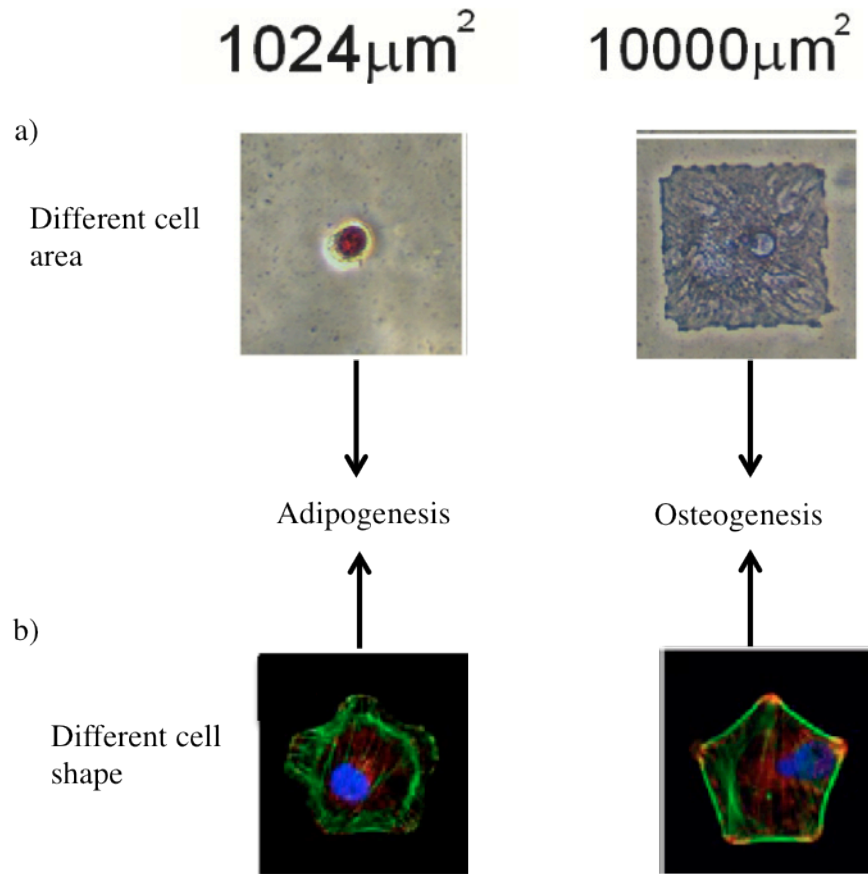


**Figure 1.5. Cell shape and geometry influence hMSCs differentiation fate.** A) Role of cell shape on hMSC differentiation as studied by McBeath *et al.*<sup>74</sup> hMSCs cultured on square fibronectin islands of area 1024 μm<sup>2</sup> and 10000 μm<sup>2</sup> undergo adipogenic and osteogenic differentiation, respectively. B) Role of geometry on hMSC differentiation as studied by Kilian *et al.*<sup>75</sup> hMSCs cultured on flower shaped pattern preferred adipogenic differentiation while those on star shaped pattern preferred osteogenic differentiation. Figures show immunostaining for f-actin (green), vinculin (red) and nuclei (blue)

## **1.4 PEG hydrogels as a platform to culture and study hMSCs**

Poly(ethylene glycol) (PEG) based hydrogels have emerged as a versatile material system for use as cell culture platforms owing to their high water content, tissue like elastic properties, and facile transport of nutrients and waste.<sup>76-80</sup> PEGs hydrophilicity and bioinert nature render this chemistry highly resistant to non-specific protein adsorption. As a result, PEG hydrogels provide a basic physical structure upon which cells can be seeded on or in, while simultaneously allowing experimenters to introduce biochemical cues in a systematic manner without confounding factors of non-specific adsorption of numerous serum proteins. The physical and mechanical properties of PEG hydrogels can be easily modified by controlling the initial monomer formulation and polymerization conditions that directly influence crosslinking density, swelling and elasticity. The result is a tunable hydrogel with elasticity ranging from that of soft tissues, such as brain, to the protein components of hard tissues such as collagenous bone.<sup>81</sup> The hydroxyl end groups that are often present on PEGs allow easy modification of linear chains or multi-arm polymers to include other chemical functionalities (e.g., acids, amine, maleimides, azides, thiols, acrylates etc) that can be subsequently used for crosslinking and also to incorporate pendant signaling moieties to promote and control cell function.<sup>82-96</sup> Several strategies have been reported for the synthesis of PEG hydrogel cell culture platforms under mild and cytocompatible conditions.<sup>82</sup>

### **1.4.1 Crosslinking PEG using chain and step growth polymerizations**

PEG hydrogels used for cell culture applications typically, with few notable exceptions, have been synthesized via free-radical chain polymerization or step growth polymerization schemes.<sup>97,98</sup> The choice of the reaction scheme and the

functionality of PEG monomers determine the structure and physical properties of the resulting polymer networks. In chain growth polymerization, the polymerization is often initiated upon attack of an initiator molecule on a monomer, resulting in the formation of reactive center on that monomer molecule. The polymer network grows upon repeated addition of the reactive functionalities on the PEG molecules to the reactive center, growing a kinetic chain.<sup>99</sup> Chain polymerization of bi-functional monomers results in the formation of linear polymers, while multi-functional monomers result in the formation of cross-linked networks. Because chain extension occurs only due to addition of functional units to the reactive center, very high molecular weight chains result at even low conversions.

In step growth polymerizations, the polymer evolves in a statistical fashion i.e. any functional group can react with the neighboring counterpart and is not restricted to an active center. Due to this mechanism, monomers react to give dimers, trimers, tetramers etc and high molecular weight polymers are obtained only at relatively high conversions. Usually, the reactive functionalities are complementary, though some step growth networks can also be formed from a single functionality, such as condensation of dicarboxylic acids to form anhydrides, oxidation of thiols to form disulfides. Mono- or bi-functional monomers result in the formation of linear or branched polymers, while multi-functional monomers (an average functionality  $> 2$ ) results in the formation of a cross-linked network.

Due to the reaction mechanisms, chain growth networks are usually characterized by an early gelation point resulting in the formation of a complex network structure with polydisperse kinetic chains connected by a long, extended PEG chains as shown in Figure

1.6a<sup>100</sup>. In contrast, step growth networks reach the gelation point at very high conversion (e.g,m as predicted by Flory-Stockmeyer equation<sup>99</sup>) and result in the formation of more ideal and uniform network structures as shown in Figure 1.6b.

This thesis research focuses on photochemical polymerizations to create PEG hydrogels, as photochemical reactions provide benefits with respect to spatiotemporal control of network formation. Photo-initiation mechanisms have been previously used to form PEG gels using both chain and step growth mechanisms. Photo-initiators, such as 2-hydroxy-1-[4-(2-hydroxyethoxy) phenyl]-2-methyl 1-propanone (I2959),<sup>101</sup> lithium phenyl-2,4,6-trimethylbenzoylphosphinate (LAP),<sup>102</sup> are water soluble, and can be used to generate radicals with 365 nm light and 405 nm light, respectively, at low light dosage (low cytotoxicity) and in buffer conditions, thus allowing formation of networks in the presence of cells, proteins and other biologically relevant molecules under cytocompatible conditions.<sup>103</sup>

A commonly used approach to form PEG hydrogels is chain growth polymerizations of multi(meth)acrylated PEG monomers. While robust and extensively studied,<sup>104,105</sup> this reaction chemistry poses additional challenges, as they are susceptible to oxygen inhibition that results in longer polymerization times and requires increased light dosage leading to undesired side effects such as damage of biomacromolecules.<sup>106</sup> There is a growing interest in formation of PEG hydrogels via step growth thiol-ene ‘click’ reactions<sup>107</sup>, as they are not oxygen inhibited and require lower radical concentrations for complete network formation. Particularly, PEGs functionalized with terminal norbornene functional groups and reacted with bis-thiol crosslinkers have been

successfully copolymerized through photoinitiation to create hydrogel systems for encapsulation and culture of fibroblasts,<sup>108</sup> pancreatic  $\beta$ -cells,<sup>80</sup> hMSCs<sup>109</sup> and proteins.<sup>110</sup>

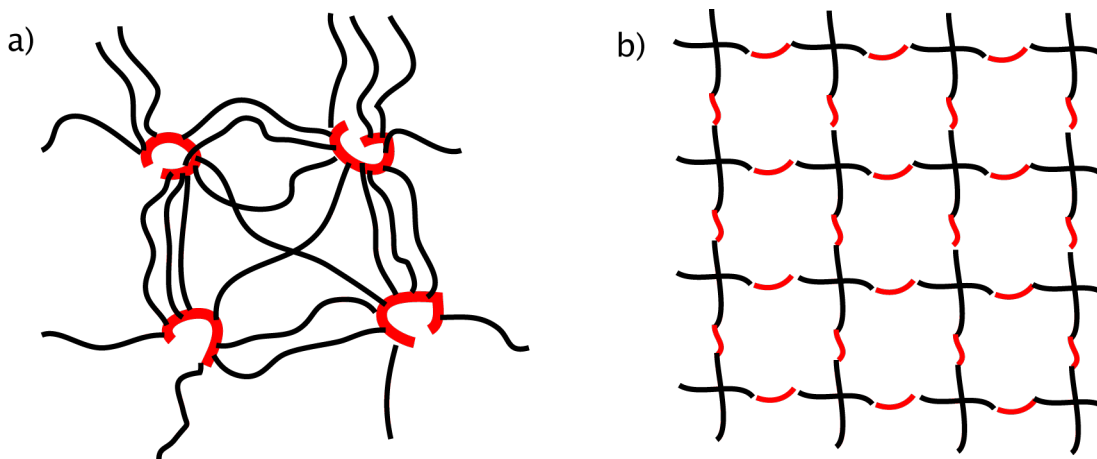


**Figure 1.6.** Schematic showing the structure of PEG hydrogels formed via (a) Chain growth polymerization and (b) Step growth polymerization (Not to scale)

#### 1.4.2 Creating bioactive PEG hydrogels:

Synthetic hydrogels have been designed to incorporate cues derived from the molecules present in the ECM to provide for integrin binding,<sup>84,111,112</sup> enzymatic degradation<sup>79,113,114</sup> and growth factor sequestering.<sup>97,115–117</sup> The most straightforward method to create a bioactive hydrogel is to simply mix the biochemical cue of interest in the monomer precursor solution to form the hydrogel, resulting in the uniform distribution of the biochemical cue throughout the network. A plethora of bio-conjugate chemistries previously developed for facile modification of biomacromolecules have been employed to attach reactive functionalities that can be used to co-polymerize into PEG hydrogels. Typically, the choice of reactive functionalities, and hence the chemistries employed to attach them to the biochemical cues, depends on the selected

polymerization scheme and PEG macromers. Acrylate conjugated peptides have been used by several different researchers to form hydrogel networks through chain copolymerization with PEG diacrylate, that supported dose dependent cell adhesion to promote vascularization and directed migration.<sup>84,118-121</sup> For example, acrylate conjugated cell adhesive peptides, such as acryoyl-PEG-RGD, synthesized by reacting acryoyl-PEG-NHS ester with the amine containing RGD peptide, have been synthesized previously and co-polymerized into PEG diacrylate hydrogels to promote osteoblast adhesion.<sup>84</sup> Alternatively, mixed mode radical chain growth polymerization involving termination of acrylate chains by a step addition of a thiol has been used to incorporate cysteine-containing peptides into hydrogel networks formed from PEG diacrylate without the need for post-synthetic modification of the peptides.<sup>122,123</sup> Radical mediated thiol-ene photoclick reactions between a thyl radical and a strained alkene, as described earlier, have also been used to introduce any thiol containing biochemical cues into the network during the synthesis of PEG hydrogels.<sup>108,109,124</sup> Base catalyzed Micheal addition between a thiol and electron deficient alkenes (such as acrylate, vinyl sulfones etc) has been used by Hubbell and co-workers to incorporate cysteine-containing peptides into the PEG hydrogel network.<sup>125</sup> These reactions, although relatively straightforward, use a base for the reaction, which can limit its use in the presence of cells and proteins. The thiol-ene and Michael addition reactions lead to similar network structures, but the thiol-ene reaction is sometimes preferred as it offers spatio-temporal control over the gel functionalization.

### 1.4.3 Dynamic regulation of biochemical signals

The techniques outlined above only allow control of the initial biochemical properties of the hydrogel. Platforms that allow subsequent tunability over presentation of multiple biochemical signals are often desirable, and particularly if they allow experimenters control over cell function at specific places and times. Towards this goal, researchers have utilized various chemical strategies to covalently attach biochemical cues of interest post synthesis of hydrogels. Approaches to conjugate biochemical cues to gels have exploited similar or orthogonal chemistries to that used to synthesize the original networks. One technique to achieve controlled and uniform surface functionalization of PEG hydrogels with adhesive peptides such as GRGDS, GYIGSR (laminin derived) etc. using carboxylic acid-amine coupling<sup>126</sup> and to covalently tether ECM proteins, like collagen, has relied on the reaction between carboxylic acid and an activated NHS ester.<sup>127</sup> In these studies, carboxylic acid functionalized monomers were added at desired concentrations, depending on the degree of peptide functionalization required, during the synthesis of the hydrogel network. Using this strategy, Hubbell and coworkers demonstrated controlled adhesion of fibroblasts through specific integrins. However, spatial and temporal control over ligand presentation is often desired and so microcontact printing has been applied in conjunction with this approach to transfer adhesive molecules through a poly(dimethoxy siloxane) (PDMS) stamp. Specific regions on hydrogel surfaces have been patterned with reactive ligands and covalently bound to gels using this conjugation reaction. Alternatively, photo-lithography has been combined with light controlled reactions to chemically bind biochemical cues only at regions where



light is delivered.<sup>92,128-139</sup> For example, photo-activatable thiol-acrylate and thiol-ene reactions were used to tether thiol-containing biomacromolecules to pre-formed PEG gels in a manner that precisely controls their introduction in 4D (i.e., xyz and time).

Photolithographic techniques rely on the ability to control the delivery of photons, either through photomasks or optical control of laser light in 3D. The West group has used such photopolymerization techniques to tether peptides and/or growth factors in PEGDA hydrogels.<sup>129,136,137</sup> Their approach has exploited acrylate functional groups that were left unreacted after the partial polymerization of PEGDA hydrogels and then a subsequent photopolymerization reaction to incorporate Acryl-PEG conjugated biochemical cues (Figure 1.7a). Using this technique, multiple cues were bound to PEG hydrogels to control the adhesion and migration of human dermal fibroblasts in 3D, as well as the angiogenic response of HUVECs. While these demonstrations were insightful to the field, the resultant pattern composition is ill-defined and difficult to characterize, which has limited its wide applicability to functionalize biomaterials. In a complementary approach, the Anseth lab has developed a versatile and more defined approach using thiol-ene photocoupling reactions to tether biochemical cues into PEG networks.<sup>92,108,138,139</sup> In their approach, thiol-ene photopolymerizations or alkyne-azide click reactions were used to form PEG hydrogels presenting pendant alkene functionalities after network formation. The alkene functionality was then used to perform subsequent thiol-ene reactions in the presence of photo-initiator and thiol containing biochemicals. This approach was used to tether peptides in complex 3D patterns that controlled the morphology of hMSCs and migration of 3T3 cells.

Although presentation of biochemical cues can be achieved at any desired time point using the above outlined strategies, they do not allow for subsequent regulation of their presentation (i.e., to either remove or exchange the functional group with another biochemical cue). Such programmable presentation of biochemical ligands is often useful to better understand ECM signaling to cells, as the cell microenvironment *in vivo* is far from static, constantly changing and influencing cell fate. Such dynamic control over the presentation of microenvironmental signals *in vitro* would allow researchers to more closely mimic and model the *in vivo* ECM and would be tremendously advantageous in various biomaterial applications, including *in vitro* stem cell expansion, 3D cell cultures for drug screening, and/or tissue engineering applications. These programmable hydrogel niches would further enable researchers to conduct unique biological characterization experiments and answer questions about the effect of dynamic regulation of information between a cell and its microenvironment. To date, only a few examples exist that allow such specific control over the presentation of biochemical cues.

Anseth and colleagues pioneered the use of dual wavelength systems that utilizes visible light wavelength to react and introduce biochemical cues in the matrix and a second, independent wavelength (e.g., 365 nm) to remove the biochemical cue independently.<sup>139</sup> In this technique, eosin initiated thiol-ene photoclick reactions were used to react in peptides, proteins and small molecules conjugated with o-nitrobenzyl moieties that could be subsequently removed using through photodegradation of the o-nitrobenzyl functional group (Figure 1.7b). This strategy is fully cytocompatible and creating localized RGD patterns led to confinement of hMSC attachment only to the

patterned regions of a gel and subsequent release and capture of sub-populations attached upon UV light induced cleavage.

Recently, Popik and colleagues have also reported an alternative strategy that relies on the equilibrium switching of unreactive 3-(hydroxymethyl)-2-naphthol and reactive o-2-naphthoquinone-3-methides (NQM) to achieve attachment, removal and reattachment of streptavidin to a thiol-derivitized glass slide.<sup>140</sup> Their approach uses base catalyzed Michael addition to couple functional groups, and 350 nm UV light to cleave NQM functionalized chemical moieties on thiol functionalized glass. While this technique demonstrates reversibility in the addition and removal of NQM derivitized biochemical moieties, it requires the use of base and 350 nm or lower wavelength light, which are more difficult to perform under cytocompatible conditions and limiting their cell culture and biomaterial applications.

Towards reversible strategies to modify polymer networks, Bowman and colleagues pioneered the development of covalently adaptable networks (CANs) that possess reversible covalent crosslinks that respond to an externally applied stimulus (e.g., the Diels-Alder/retro-Diels-Alder reaction).<sup>141,142</sup> One example demonstrate the reversible reaction between a furan with a maleimide to form bicyclic compounds at low temperatures and a retro-Diels-Alder reaction at higher temperature. A second example synthesized networks containing allyl sulfides that undergo addition-fragmentation-chain transfer upon a radical attack and was used to demonstrate how network rearrangement can be used to relieve stress developed during polymerization.<sup>143-145</sup> While these chemical strategies show great promise to achieve reversible presentation of biochemical cues, less focus has been on reactions that can be performed in the presence of cells.

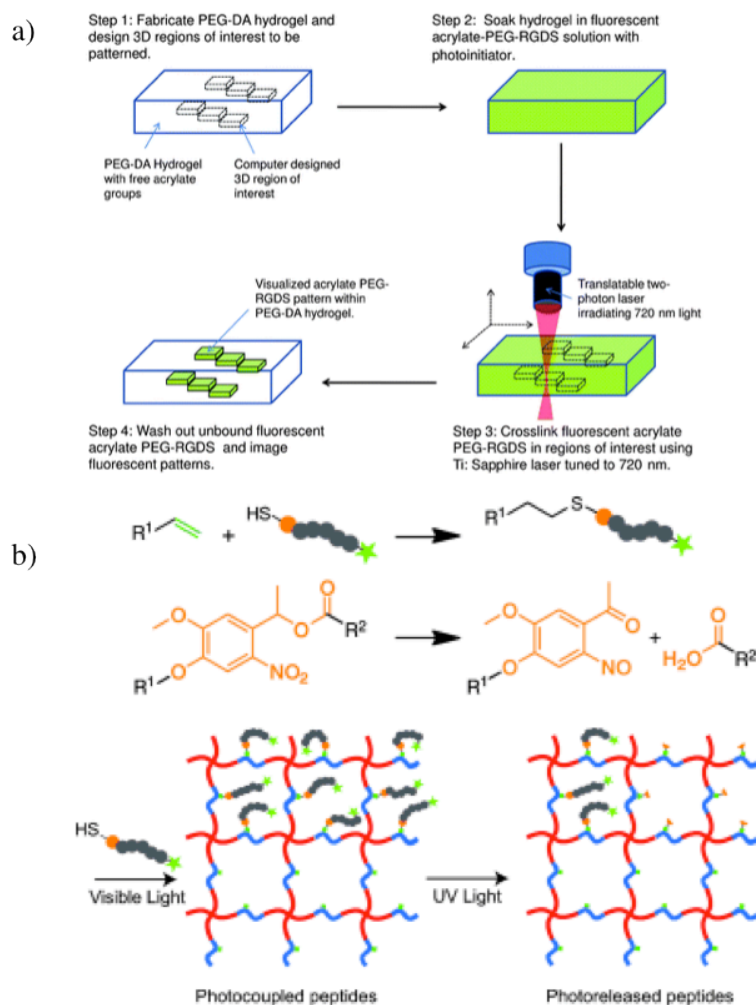


**Figure 1.7. Dynamic regulation of presentation of biochemical ligands.** a) 2-photon photopatterning of biochemical ligands using unreactive acrylate functionalities as studied by Hoffman and West.<sup>146</sup> PEG hydrogel is soaked in solution containing biochemical ligand and initiator and subsequently specific regions were exposed to multiphoton light using confocal microscope to form desired 3D patterns. b) Reversible photo-patterning of small peptides achieved by dual wavelength responsive systems. Addition to the network is achieved via thiol-ene photoclick chemistry at 460 nm and removal of the ligands is achieved via cleavage of o-nitrobenzyl moiety upon exposure to 365 nm light.<sup>139</sup>

## 1.5 Research Summary

This thesis aims to engineer PEG hydrogel platforms to study and understand the role of integrin signaling and cell shape on osteogenic differentiation of hMSCs. Towards this goal, Chapter 2 outlines the specific aims and hypotheses of this thesis work and the strategies employed to achieve these aims. This is followed by four chapters that summarize the key findings. In Chapter 3, we study and understand the molecular mechanisms involved in osteogenic differentiation of hMSCs on phosphate functionalized PEG hydrogels. Integrin mediated signaling via interaction with the adsorbed extra-cellular matrix proteins is investigated and found to be sufficient to promote osteogenic differentiation of hMSCs cultured on phosphate gels. Towards the effort to understand the role of specific integrin signaling in promoting osteogenic differentiation in hMSCs, in Chapter 4 reports the synthesis of peptide functionalized hydrogel platform to signal  $\alpha 5\beta 1$  integrin with high specificity. These gels are used to study the role of  $\alpha 5\beta 1$  integrin signaling on osteogenic differentiation of hMSCs and potential synergies involved with the underlying matrix stiffness.

Chapter 5 moves towards the synthesis and characterization of a PEG hydrogels incorporating allyl sulphide functionalities and using thiol-ene reactions to reversibly modify the hydrogels with biochemical ligands of interest for hMSC differentiation. By tuning the photo-coupling conditions, we characterize the extent of spatial control and temporal exchange of biochemical ligands in these hydrogels. Finally, Chapter 6 concludes with a summary of the progress in engineering functionalized PEG hydrogel platforms to study and control the osteogenic differentiation of hMSCs and suggests

future avenues that might be interesting to probe and understand the role of these systems in better understanding and controlling osteogenic differentiation of hMSCs.

## 1.6 References

1. Bianco, P., Reginacci, M., Gronthos, S. & Robey, P. G. Bone Marrow Stromal Stem Cells: Nature, Biology, and Potential Applications. *STEM CELLS* **19**, 180–192 (2001).
2. Pittenger, M. F. *et al.* Multilineage potential of adult human mesenchymal stem cells. *Science* **284**, 143–147 (1999).
3. Bruder, S. P., Kraus, K. H., Goldberg, V. M. & Kadiyala, S. The effect of implants loaded with autologous mesenchymal stem cells on the healing of canine segmental bone defects. *J Bone Joint Surg Am* **80**, 985–996 (1998).
4. Horwitz, E. M. *et al.* Isolated allogeneic bone marrow-derived mesenchymal cells engraft and stimulate growth in children with osteogenesis imperfecta: Implications for cell therapy of bone. *PNAS* **99**, 8932–8937 (2002).
5. Barry, F. P. & Murphy, J. M. Mesenchymal stem cells: clinical applications and biological characterization. *Int. J. Biochem. Cell Biol.* **36**, 568–584 (2004).
6. Ng, F. *et al.* PDGF, TGF-beta, and FGF signaling is important for differentiation and growth of mesenchymal stem cells (MSCs): transcriptional profiling can identify markers and signaling pathways important in differentiation of MSCs into adipogenic, chondrogenic, and osteogenic lineages. *Blood* **112**, 295–307 (2008).
7. Tsutsumi, S. *et al.* Retention of multilineage differentiation potential of mesenchymal cells during proliferation in response to FGF. *Biochem. Biophys. Res. Commun.* **288**, 413–419 (2001).
8. Jung, S., Sen, A., Rosenberg, L. & Behie, L. A. Identification of growth and attachment factors for the serum-free isolation and expansion of human mesenchymal stromal cells. *Cytotherapy* **12**, 637–657 (2010).
9. Abdelrazik, H., Spaggiari, G. M., Chiossone, L. & Moretta, L. Mesenchymal stem cells expanded in human platelet lysate display a decreased inhibitory capacity on T- and NK-cell proliferation and function. *Eur. J. Immunol.* **41**, 3281–3290 (2011).
10. Gruber, R. *et al.* Platelet-released supernatants increase migration and proliferation, and decrease osteogenic differentiation of bone marrow-derived mesenchymal progenitor cells under in vitro conditions. *Platelets* **15**, 29–35 (2004).
11. Li, Y.-M. *et al.* Effects of high glucose on mesenchymal stem cell proliferation and differentiation. *Biochem. Biophys. Res. Commun.* **363**, 209–215 (2007).

12. Solchaga, L. A., Penick, K., Goldberg, V. M., Caplan, A. I. & Welter, J. F. Fibroblast growth factor-2 enhances proliferation and delays loss of chondrogenic potential in human adult bone-marrow-derived mesenchymal stem cells. *Tissue Eng Part A* **16**, 1009–1019 (2010).
13. Choi, S.-C. *et al.* Fibroblast Growth Factor-2 and -4 Promote the Proliferation of Bone Marrow Mesenchymal Stem Cells by the Activation of the PI3K-Akt and ERK1/2 Signaling Pathways. *Stem Cells and Development* **17**, 725–736 (2008).
14. Jaiswal, N., Haynesworth, S. E., Caplan, A. I. & Bruder, S. P. Osteogenic differentiation of purified, culture-expanded human mesenchymal stem cells in vitro. *Journal of Cellular Biochemistry* **64**, 295–312 (1997).
15. Scott, M. A., Nguyen, V. T., Levi, B. & James, A. W. Current methods of adipogenic differentiation of mesenchymal stem cells. *Stem Cells Dev.* **20**, 1793–1804 (2011).
16. Tamama, K., Kawasaki, H. & Wells, A. Epidermal Growth Factor (EGF) Treatment on Multipotential Stromal Cells (MSCs). Possible Enhancement of Therapeutic Potential of MSC. *Journal of Biomedicine and Biotechnology* **2010**, 1–11 (2010).
17. Mimura, S. *et al.* Growth factor-defined culture medium for human mesenchymal stem cells. *Int. J. Dev. Biol.* **55**, 181–187 (2011).
18. Mostafa, N. Z. *et al.* Osteogenic differentiation of human mesenchymal stem cells cultured with dexamethasone, vitamin D3, basic fibroblast growth factor, and bone morphogenetic protein-2. *Connect. Tissue Res.* **53**, 117–131 (2012).
19. Fink, T. & Zachar, V. Adipogenic differentiation of human mesenchymal stem cells. *Methods Mol. Biol.* **698**, 243–251 (2011).
20. Sekiya, I., Larson, B. L., Vuoristo, J. T., Cui, J.-G. & Prockop, D. J. Adipogenic differentiation of human adult stem cells from bone marrow stroma (MSCs). *J. Bone Miner. Res.* **19**, 256–264 (2004).
21. Danišovič, L., Varga, I. & Polák, S. Growth factors and chondrogenic differentiation of mesenchymal stem cells. *Tissue Cell* **44**, 69–73 (2012).
22. Mohan, N., Nair, P. D. & Tabata, Y. A 3D biodegradable protein based matrix for cartilage tissue engineering and stem cell differentiation to cartilage. *J Mater Sci Mater Med* **20 Suppl 1**, S49–60 (2009).
23. Shintani, N. & Hunziker, E. B. Chondrogenic differentiation of bovine synovium: bone morphogenetic proteins 2 and 7 and transforming growth factor beta1 induce the formation of different types of cartilaginous tissue. *Arthritis Rheum.* **56**, 1869–1879 (2007).

24. An, C., Cheng, Y., Yuan, Q. & Li, J. IGF-1 and BMP-2 induces differentiation of adipose-derived mesenchymal stem cells into chondrocytes-like cells. *Ann Biomed Eng* **38**, 1647–1654 (2010).
25. Bai, X., Li, G., Zhao, C., Duan, H. & Qu, F. BMP7 induces the differentiation of bone marrow-derived mesenchymal cells into chondrocytes. *Med Biol Eng Comput* **49**, 687–692 (2011).
26. Lee, S. H., Lee, Y. J., Song, C. H., Ahn, Y. K. & Han, H. J. Role of FAK phosphorylation in hypoxia-induced hMSCS migration: involvement of VEGF as well as MAPKS and eNOS pathways. *Am J Physiol Cell Physiol* **298**, C847–C856 (2010).
27. Corallini, F. *et al.* TNF-alpha modulates the migratory response of mesenchymal stem cells to TRAIL. *Cell. Mol. Life Sci.* **67**, 1307–1314 (2010).
28. Fu, X. *et al.* Migration of bone marrow-derived mesenchymal stem cells induced by tumor necrosis factor-alpha and its possible role in wound healing. *Wound Repair Regen* **17**, 185–191 (2009).
29. Kollar, K., Cook, M. M., Atkinson, K. & Brooke, G. Molecular Mechanisms Involved in Mesenchymal Stem Cell Migration to the Site of Acute Myocardial Infarction. *International Journal of Cell Biology* **2009**, 1–8 (2009).
30. Neuss, S., Becher, E., Wöltje, M., Tietze, L. & Jahnen-Dechent, W. Functional expression of HGF and HGF receptor/c-met in adult human mesenchymal stem cells suggests a role in cell mobilization, tissue repair, and wound healing. *Stem Cells* **22**, 405–414 (2004).
31. Ducy, P. *et al.* A Cbfa1-dependent genetic pathway controls bone formation beyond embryonic development. *Genes Dev.* **13**, 1025–1036 (1999).
32. Extra.
33. Aubin, J. E. & Turksen, K. Monoclonal antibodies as tools for studying the osteoblast lineage. *Microscopy Research and Technique* **33**, 128–140 (1996).
34. Frantz, C., Stewart, K. M. & Weaver, V. M. The extracellular matrix at a glance. *J Cell Sci* **123**, 4195–4200 (2010).
35. Gelse, K., Pöschl, E. & Aigner, T. Collagens--structure, function, and biosynthesis. *Adv. Drug Deliv. Rev.* **55**, 1531–1546 (2003).
36. Hynes, R. O. Integrins: bidirectional, allosteric signaling machines. *Cell* **110**, 673–687 (2002).
37. Giancotti, F. G. & Ruoslahti, E. Integrin signaling. *Science* **285**, 1028–1032 (1999).



38. Humphries, J. D., Byron, A. & Humphries, M. J. Integrin ligands at a glance. *J Cell Sci* **119**, 3901–3903 (2006).
39. Petit, V. & Thiery, J. P. Focal adhesions: structure and dynamics. *Biol. Cell* **92**, 477–494 (2000).
40. Gronthos, S., Simmons, P. J., Graves, S. E. & Robey, P. G. Integrin-mediated interactions between human bone marrow stromal precursor cells and the extracellular matrix. *Bone* **28**, 174–181 (2001).
41. Moursi, A. M., Globus, R. K. & Damsky, C. H. Interactions between integrin receptors and fibronectin are required for calvarial osteoblast differentiation in vitro. *J. Cell. Sci.* **110** ( Pt 18), 2187–2196 (1997).
42. Athanassiou, G. & Deligianni, D. Adhesion strength of individual human bone marrow cells to fibronectin. Integrin beta1-mediated adhesion. *J Mater Sci Mater Med* **12**, 965–970 (2001).
43. Zimmerman, D., Jin, F., Leboy, P., Hardy, S. & Damsky, C. Impaired bone formation in transgenic mice resulting from altered integrin function in osteoblasts. *Dev. Biol.* **220**, 2–15 (2000).
44. Mizuno, M., Fujisawa, R. & Kuboki, Y. Type I collagen-induced osteoblastic differentiation of bone-marrow cells mediated by collagen-alpha2beta1 integrin interaction. *J. Cell. Physiol.* **184**, 207–213 (2000).
45. Takeuchi, Y. *et al.* Differentiation and transforming growth factor-beta receptor down-regulation by collagen-alpha2beta1 integrin interaction is mediated by focal adhesion kinase and its downstream signals in murine osteoblastic cells. *J. Biol. Chem.* **272**, 29309–29316 (1997).
46. Van der Velde-Zimmermann, D. *et al.* Fibronectin distribution in human bone marrow stroma: matrix assembly and tumor cell adhesion via alpha5 beta1 integrin. *Exp. Cell Res.* **230**, 111–120 (1997).
47. Keselowsky, B. G., Collard, D. M. & García, A. J. Integrin binding specificity regulates biomaterial surface chemistry effects on cell differentiation. *PNAS* **102**, 5953–5957 (2005).
48. Petrie, T. A., Capadona, J. R., Reyes, C. D. & García, A. J. Integrin specificity and enhanced cellular activities associated with surfaces presenting a recombinant fibronectin fragment compared to RGD supports. *Biomaterials* **27**, 5459–5470 (2006).
49. McHugh, K. P. *et al.* Mice lacking beta3 integrins are osteosclerotic because of dysfunctional osteoclasts. *J. Clin. Invest.* **105**, 433–440 (2000).

50. Hu, D. *et al.* Absence of beta3 integrin accelerates early skeletal repair. *J. Orthop. Res.* **28**, 32–37 (2010).
51. Globus, R. K. *et al.* Fibronectin is a survival factor for differentiated osteoblasts. *J. Cell. Sci.* **111** ( Pt 10), 1385–1393 (1998).
52. Petrie, T. A. *et al.* The effect of integrin-specific bioactive coatings on tissue healing and implant osseointegration. *Biomaterials* **29**, 2849–2857 (2008).
53. Martino, M. M. *et al.* Controlling integrin specificity and stem cell differentiation in 2D and 3D environments through regulation of fibronectin domain stability. *Biomaterials* **30**, 1089–1097 (2009).
54. Hamidouche, Z. *et al.* Priming integrin alpha5 promotes human mesenchymal stromal cell osteoblast differentiation and osteogenesis. *Proc. Natl. Acad. Sci. U.S.A.* **106**, 18587–18591 (2009).
55. Fromigué, O. *et al.* Peptide-based activation of alpha5 integrin for promoting osteogenesis. *J. Cell. Biochem.* **113**, 3029–3038 (2012).
56. Kaabeche, K. *et al.* Cbl-mediated ubiquitination of alpha5 integrin subunit mediates fibronectin-dependent osteoblast detachment and apoptosis induced by FGFR2 activation. *J. Cell. Sci.* **118**, 1223–1232 (2005).
57. Salter, D. M., Robb, J. E. & Wright, M. O. Electrophysiological responses of human bone cells to mechanical stimulation: evidence for specific integrin function in mechanotransduction. *J. Bone Miner. Res.* **12**, 1133–1141 (1997).
58. Vogel, V. & Sheetz, M. Local force and geometry sensing regulate cell functions. *Nat. Rev. Mol. Cell Biol.* **7**, 265–275 (2006).
59. Schwartz, M. A. & Ginsberg, M. H. Networks and crosstalk: integrin signalling spreads. *Nat. Cell Biol.* **4**, E65–68 (2002).
60. Schwartz, M. A. & DeSimone, D. W. Cell adhesion receptors in mechanotransduction. *Curr. Opin. Cell Biol.* **20**, 551–556 (2008).
61. Wozniak, M. A. & Chen, C. S. Mechanotransduction in development: a growing role for contractility. *Nat Rev Mol Cell Biol* **10**, 34–43 (2009).
62. Mammoto, T. & Ingber, D. E. Mechanical control of tissue and organ development. *Development* **137**, 1407–1420 (2010).
63. Engler, A. J., Sen, S., Sweeney, H. L. & Discher, D. E. Matrix elasticity directs stem cell lineage specification. *Cell* **126**, 677–689 (2006).

64. Winer, J. P., Janmey, P. A., McCormick, M. E. & Funaki, M. Bone marrow-derived human mesenchymal stem cells become quiescent on soft substrates but remain responsive to chemical or mechanical stimuli. *Tissue Eng Part A* **15**, 147–154 (2009).
65. Katayama, Y. *et al.* Signals from the Sympathetic Nervous System Regulate Hematopoietic Stem Cell Egress from Bone Marrow. *Cell* **124**, 407–421 (2006).
66. Tse, J. R. & Engler, A. J. Stiffness Gradients Mimicking In Vivo Tissue Variation Regulate Mesenchymal Stem Cell Fate. *PLoS ONE* **6**, e15978 (2011).
67. Walcott, S. & Sun, S. X. A mechanical model of actin stress fiber formation and substrate elasticity sensing in adherent cells. *PNAS* **107**, 7757–7762 (2010).
68. Skardal, A., Mack, D., Atala, A. & Soker, S. Substrate elasticity controls cell proliferation, surface marker expression and motile phenotype in amniotic fluid-derived stem cells. *J Mech Behav Biomed Mater* **17**, 307–316 (2013).
69. Kocgozlu, L. *et al.* Selective and uncoupled role of substrate elasticity in the regulation of replication and transcription in epithelial cells. *J. Cell. Sci.* **123**, 29–39 (2010).
70. Shih, Y.-R. V., Tseng, K.-F., Lai, H.-Y., Lin, C.-H. & Lee, O. K. Matrix stiffness regulation of integrin-mediated mechanotransduction during osteogenic differentiation of human mesenchymal stem cells. *J. Bone Miner. Res.* **26**, 730–738 (2011).
71. Xu, B. *et al.* RhoA/ROCK, cytoskeletal dynamics, and focal adhesion kinase are required for mechanical stretch-induced tenogenic differentiation of human mesenchymal stem cells. *J. Cell. Physiol.* **227**, 2722–2729 (2012).
72. Chen, Z. *et al.* Synthetic osteogenic growth peptide promotes differentiation of human bone marrow mesenchymal stem cells to osteoblasts via RhoA/ROCK pathway. *Molecular and Cellular Biochemistry* **358**, 221–227 (2011).
73. Ruiz, S. A. & Chen, C. S. Emergence of Patterned Stem Cell Differentiation Within Multicellular Structures. *STEM CELLS* **26**, 2921–2927 (2008).
74. McBeath, R., Pirone, D. M., Nelson, C. M., Bhadriraju, K. & Chen, C. S. Cell shape, cytoskeletal tension, and RhoA regulate stem cell lineage commitment. *Dev. Cell* **6**, 483–495 (2004).
75. Kilian, K. A., Bugarija, B., Lahn, B. T. & Mrksich, M. Geometric cues for directing the differentiation of mesenchymal stem cells. *PNAS* **107**, 4872–4877 (2010).
76. Ratner, B. D. & Bryant, S. J. BIOMATERIALS: Where We Have Been and Where We are Going. *Annual Review of Biomedical Engineering* **6**, 41–75 (2004).

77. Peppas, N. A., Hilt, J. Z., Khademhosseini, A. & Langer, R. Hydrogels in Biology and Medicine: From Molecular Principles to Bionanotechnology. *Advanced Materials* **18**, 1345–1360 (2006).
78. Tibbitt, M. W. & Anseth, K. S. Hydrogels as extracellular matrix mimics for 3D cell culture. *Biotechnol. Bioeng.* **103**, 655–663 (2009).
79. Lutolf, M. P. & Hubbell, J. A. Synthetic biomaterials as instructive extracellular microenvironments for morphogenesis in tissue engineering. *Nature Biotechnology* **23**, 47–55 (2005).
80. Lin, C.-C., Raza, A. & Shih, H. PEG hydrogels formed by thiol-ene photo-click chemistry and their effect on the formation and recovery of insulin-secreting cell spheroids. *Biomaterials* **32**, 9685–9695 (2011).
81. Nemir, S. & West, J. L. Synthetic materials in the study of cell response to substrate rigidity. *Ann Biomed Eng* **38**, 2–20 (2010).
82. Zhu, J. Bioactive Modification of Poly(ethylene glycol) Hydrogels for Tissue Engineering. *Biomaterials* **31**, 4639–4656 (2010).
83. Sawhney, A. S., Pathak, C. P. & Hubbell, J. A. Bioerodible hydrogels based on photopolymerized poly(ethylene glycol)-co-poly(.alpha.-hydroxy acid) diacrylate macromers. *Macromolecules* **26**, 581–587 (1993).
84. Burdick, J. A. & Anseth, K. S. Photoencapsulation of osteoblasts in injectable RGD-modified PEG hydrogels for bone tissue engineering. *Biomaterials* **23**, 4315–4323 (2002).
85. Elisseeff, J. *et al.* Transdermal photopolymerization for minimally invasive implantation. *Proc. Natl. Acad. Sci. U.S.A.* **96**, 3104–3107 (1999).
86. Buxton, A. N. *et al.* Design and characterization of poly(ethylene glycol) photopolymerizable semi-interpenetrating networks for chondrogenesis of human mesenchymal stem cells. *Tissue Eng.* **13**, 2549–2560 (2007).
87. Hahn, M. S., McHale, M. K., Wang, E., Schmedlen, R. H. & West, J. L. Physiologic pulsatile flow bioreactor conditioning of poly(ethylene glycol)-based tissue engineered vascular grafts. *Ann Biomed Eng* **35**, 190–200 (2007).
88. Beamish, J. A., Zhu, J., Kottke-Marchant, K. & Marchant, R. E. The effects of monoacrylated poly(ethylene glycol) on the properties of poly(ethylene glycol) diacrylate hydrogels used for tissue engineering. *J Biomed Mater Res A* **92**, 441–450 (2010).
89. Hubbell, J. A. Synthetic biodegradable polymers for tissue engineering and drug delivery. *Current Opinion in Solid State and Materials Science* **3**, 246–251 (1998).

90. Metters, A. & Hubbell, J. Network formation and degradation behavior of hydrogels formed by Michael-type addition reactions. *Biomacromolecules* **6**, 290–301 (2005).
91. Park, Y., Lutolf, M. P., Hubbell, J. A., Hunziker, E. B. & Wong, M. Bovine primary chondrocyte culture in synthetic matrix metalloproteinase-sensitive poly(ethylene glycol)-based hydrogels as a scaffold for cartilage repair. *Tissue Eng.* **10**, 515–522 (2004).
92. Polizzotti, B. D., Fairbanks, B. D. & Anseth, K. S. Three-dimensional biochemical patterning of click-based composite hydrogels via thiolene photopolymerization. *Biomacromolecules* **9**, 1084–1087 (2008).
93. Malkoch, M. *et al.* Synthesis of well-defined hydrogel networks using Click chemistry. *Chem. Commun.* 2774–2776 (2006).doi:10.1039/B603438A
94. Hu, B.-H., Su, J. & Messersmith, P. B. Hydrogels Cross-Linked by Native Chemical Ligation. *Biomacromolecules* **10**, 2194–2200 (2009).
95. Sanborn, T. J., Messersmith, P. B. & Barron, A. E. In situ crosslinking of a biomimetic peptide-PEG hydrogel via thermally triggered activation of factor XIII. *Biomaterials* **23**, 2703–2710 (2002).
96. Ehrbar, M. *et al.* Enzymatic formation of modular cell-instructive fibrin analogs for tissue engineering. *Biomaterials* **28**, 3856–3866 (2007).
97. Lin, C.-C. & Anseth, K. S. Controlling Affinity Binding with Peptide-Functionalized Poly(ethylene glycol) Hydrogels. *Adv Funct Mater* **19**, 2325 (2009).
98. Rydholm, A. E., Bowman, C. N. & Anseth, K. S. Degradable thiol-acrylate photopolymers: polymerization and degradation behavior of an in situ forming biomaterial. *Biomaterials* **26**, 4495–4506 (2005).
99. Odian, G. G. *Principles of polymerization.* (Wiley, 2004).at <<http://public.eblib.com/EBLPublic/PublicView.do?ptiID=469767>>
100. Lin-Gibson, S., Jones, R. L., Washburn, N. R. & Horkay, F. Structure–Property Relationships of Photopolymerizable Poly(ethylene glycol) Dimethacrylate Hydrogels. *Macromolecules* **38**, 2897–2902 (2005).
101. Bryant, S. J., Nuttelman, C. R. & Anseth, K. S. Cytocompatibility of UV and visible light photoinitiating systems on cultured NIH/3T3 fibroblasts in vitro. *J Biomater Sci Polym Ed* **11**, 439–457 (2000).
102. Fairbanks, B. D., Schwartz, M. P., Bowman, C. N. & Anseth, K. S. Photoinitiated polymerization of PEG-diacrylate with lithium phenyl-2,4,6-trimethylbenzoylphosphinate: polymerization rate and cytocompatibility. *Biomaterials* **30**, 6702–6707 (2009).

103. Fisher, J. P., Dean, D., Engel, P. S. & Mikos, A. G. Photoinitiated Polymerization of Biomaterials. *Annual Review of Materials Research* **31**, 171–181 (2001).
104. Anseth, K. S., Wang, C. M. & Bowman, C. N. Reaction behaviour and kinetic constants for photopolymerizations of multi(meth)acrylate monomers. *Polymer* **35**, 3243–3250 (1994).
105. Lin, C.-C. & Anseth, K. S. PEG hydrogels for the controlled release of biomolecules in regenerative medicine. *Pharm. Res.* **26**, 631–643 (2009).
106. Lin, C.-C., Sawicki, S. M. & Metters, A. T. Free-radical-mediated protein inactivation and recovery during protein photoencapsulation. *Biomacromolecules* **9**, 75–83 (2008).
107. Hoyle, C. E. & Bowman, C. N. Thiol–Ene Click Chemistry. *Angewandte Chemie International Edition* **49**, 1540–1573 (2010).
108. Fairbanks, B. D. *et al.* A Versatile Synthetic Extracellular Matrix Mimic via Thiol-Norbornene Photopolymerization. *Advanced Materials* **21**, 5005–5010 (2009).
109. Anderson, S. B., Lin, C.-C., Kuntzler, D. V. & Anseth, K. S. The performance of human mesenchymal stem cells encapsulated in cell-degradable polymer-peptide hydrogels. *Biomaterials* **32**, 3564–3574 (2011).
110. McCall, J. D. & Anseth, K. S. Thiol–Ene Photopolymerizations Provide a Facile Method To Encapsulate Proteins and Maintain Their Bioactivity. *Biomacromolecules* **13**, 2410–2417 (2012).
111. Hern, D. L. & Hubbell, J. A. Incorporation of adhesion peptides into nonadhesive hydrogels useful for tissue resurfacing. *J. Biomed. Mater. Res.* **39**, 266–276 (1998).
112. Schmedlen, R. H., Masters, K. S. & West, J. L. Photocrosslinkable polyvinyl alcohol hydrogels that can be modified with cell adhesion peptides for use in tissue engineering. *Biomaterials* **23**, 4325–4332 (2002).
113. Lutolf, M. P. *et al.* Synthetic matrix metalloproteinase-sensitive hydrogels for the conduction of tissue regeneration: Engineering cell-invasion characteristics. *PNAS* **100**, 5413–5418 (2003).
114. Mann, B. K., Gobin, A. S., Tsai, A. T., Schmedlen, R. H. & West, J. L. Smooth muscle cell growth in photopolymerized hydrogels with cell adhesive and proteolytically degradable domains: synthetic ECM analogs for tissue engineering. *Biomaterials* **22**, 3045–3051 (2001).
115. Lin, C.-C., Metters, A. T. & Anseth, K. S. Functional PEG-peptide hydrogels to modulate local inflammation induced by the pro-inflammatory cytokine TNFalpha. *Biomaterials* **30**, 4907–4914 (2009).

116. Tayalia, P. & Mooney, D. J. Controlled growth factor delivery for tissue engineering. *Adv. Mater. Weinheim* **21**, 3269–3285 (2009).
117. McCall, J. D., Lin, C.-C. & Anseth, K. S. Affinity Peptides Protect Transforming Growth Factor Beta During Encapsulation in Poly(ethylene glycol) Hydrogels. *Biomacromolecules* **12**, 1051–1057 (2011).
118. Roberts, M. J., Bentley, M. D. & Harris, J. M. Chemistry for peptide and protein PEGylation. *Adv. Drug Deliv. Rev.* **54**, 459–476 (2002).
119. Gobin, A. S. & West, J. L. Cell migration through defined, synthetic ECM analogs. *FASEB J.* **16**, 751–753 (2002).
120. DeLong, S. A., Moon, J. J. & West, J. L. Covalently immobilized gradients of bFGF on hydrogel scaffolds for directed cell migration. *Biomaterials* **26**, 3227–3234 (2005).
121. Weber, L. M., Hayda, K. N., Haskins, K. & Anseth, K. S. The effects of cell-matrix interactions on encapsulated beta-cell function within hydrogels functionalized with matrix-derived adhesive peptides. *Biomaterials* **28**, 3004–3011 (2007).
122. Salinas, C. N. & Anseth, K. S. Mixed Mode Thiol–Acrylate Photopolymerizations for the Synthesis of PEG–Peptide Hydrogels. *Macromolecules* **41**, 6019–6026 (2008).
123. Lin, C.-C. & Anseth, K. S. Glucagon-Like Peptide-1 Functionalized PEG Hydrogels Promote Survival and Function of Encapsulated Pancreatic  $\beta$ -Cells. *Biomacromolecules* **10**, 2460–2467 (2009).
124. Gould, S. T., Darling, N. J. & Anseth, K. S. Small peptide functionalized thiol-ene hydrogels as culture substrates for understanding valvular interstitial cell activation and de novo tissue deposition. *Acta Biomater* **8**, 3201–3209 (2012).
125. Lutolf, M. P., Tirelli, N., Cerritelli, S., Cavalli, L. & Hubbell, J. A. Systematic Modulation of Michael-Type Reactivity of Thiols through the Use of Charged Amino Acids. *Bioconjugate Chem.* **12**, 1051–1056 (2001).
126. Drumheller, P. D. & Hubbell, J. A. Polymer networks with grafted cell adhesion peptides for highly biospecific cell adhesive substrates. *Anal. Biochem.* **222**, 380–388 (1994).
127. Lee, W., Lee, T. & Koh, W. Grafting of poly(acrylic acid) on the poly(ethylene glycol) hydrogel using surface-initiated photopolymerization for covalent immobilization of collagen. *J. Ind. Eng. Chem.* **13**, 1195–1200 (2007).

128. Albrecht, D. R., Tsang, V. L., Sah, R. L. & Bhatia, S. N. Photo- and electropatterning of hydrogel-encapsulated living cell arrays. *Lab Chip* **5**, 111–118 (2005).
129. Hahn, M. S. *et al.* Photolithographic patterning of polyethylene glycol hydrogels. *Biomaterials* **27**, 2519–2524 (2006).
130. Quist, A. P., Pavlovic, E. & Oscarsson, S. Recent advances in microcontact printing. *Anal Bioanal Chem* **381**, 591–600 (2005).
131. Perl, A., Reinhoudt, D. N. & Huskens, J. Microcontact Printing: Limitations and Achievements. *Advanced Materials* **21**, 2257–2268 (2009).
132. Kobel, S., Limacher, M., Gobaa, S., Laroche, T. & Lutolf, M. P. Micropatterning of Hydrogels by Soft Embossing†. *Langmuir* **25**, 8774–8779 (2009).
133. Lutolf, M. P., Doyonnas, R., Havenstrite, K., Koleckar, K. & Blau, H. M. Perturbation of single hematopoietic stem cell fates in artificial niches. *Integr. Biol.* **1**, 59–69 (2009).
134. Leslie-Barbick, J. E., Shen, C., Chen, C. & West, J. L. Micron-scale spatially patterned, covalently immobilized vascular endothelial growth factor on hydrogels accelerates endothelial tubulogenesis and increases cellular angiogenic responses. *Tissue Eng Part A* **17**, 221–229 (2011).
135. Leslie-Barbick, J. E., Moon, J. J. & West, J. L. Covalently-immobilized vascular endothelial growth factor promotes endothelial cell tubulogenesis in poly(ethylene glycol) diacrylate hydrogels. *J Biomater Sci Polym Ed* **20**, 1763–1779 (2009).
136. Saik, J. E., Gould, D. J., Watkins, E. M., Dickinson, M. E. & West, J. L. Covalently immobilized platelet-derived growth factor-BB promotes angiogenesis in biomimetic poly(ethylene glycol) hydrogels. *Acta Biomater* **7**, 133–143 (2011).
137. Moon, J. J., Hahn, M. S., Kim, I., Nsiah, B. A. & West, J. L. Micropatterning of Poly(Ethylene Glycol) Diacrylate Hydrogels with Biomolecules to Regulate and Guide Endothelial Morphogenesis. *Tissue Engineering Part A* **15**, 579–585 (2009).
138. DeForest, C. A. & Anseth, K. S. Cytocompatible click-based hydrogels with dynamically tunable properties through orthogonal photoconjugation and photocleavage reactions. *Nature Chemistry* **3**, 925–931 (2011).
139. DeForest, C. A. & Anseth, K. S. Photoreversible Patterning of Biomolecules within Click-Based Hydrogels. *Angewandte Chemie International Edition* **51**, 1816–1819 (2012).
140. Arumugam, S. & Popik, V. V. Attach, Remove, or Replace: Reversible Surface Functionalization Using Thiol–Quinone Methide Photoclick Chemistry. *J. Am. Chem. Soc.* **134**, 8408–8411 (2012).



141. Adzima, B. J., Aguirre, H. A., Kloxin, C. J., Scott, T. F. & Bowman, C. N. Rheological and Chemical Analysis of Reverse Gelation in a Covalently Cross-Linked Diels–Alder Polymer Network. *Macromolecules* **41**, 9112–9117 (2008).
142. Kloxin, C. J., Scott, T. F., Adzima, B. J. & Bowman, C. N. Covalent Adaptable Networks (CANs): A Unique Paradigm in Cross-Linked Polymers. *Macromolecules* **43**, 2643–2653 (2010).
143. Kloxin, C. J., Scott, T. F. & Bowman, C. N. Stress relaxation via addition-fragmentation chain transfer in a thiol-ene photopolymerization. *Macromolecules* **42**, 2551–2556 (2009).
144. Kloxin, C. J., Scott, T. F., Park, H. Y. & Bowman, C. N. Mechanophotopatterning on a Photoresponsive Elastomer. *Advanced Materials* **23**, 1977–1981 (2011).
145. Scott, T. F., Schneider, A. D., Cook, W. D. & Bowman, C. N. Photoinduced Plasticity in Cross-Linked Polymers. *Science* **308**, 1615–1617 (2005).
146. Hoffmann, J. C. & West, J. L. Three-dimensional photolithographic patterning of multiple bioactive ligands in poly(ethylene glycol) hydrogels. *Soft Matter* **6**, 5056–5063 (2010).

## Chapter 2

### OBJECTIVES

---

Cells *in vivo* are in constant dialogue with their surrounding extracellular matrix (ECM) that harbors biophysical and biochemical cues that signal and control the genetic program of cells. There is a growing interest in studying and understanding how the interactions of cells with ECM influence the biological function of cells and utilizing this knowledge towards the design of more relevant biomaterial scaffolds for applications in regenerative medicine. Particularly, understanding of the effect and signaling pathways upregulated by matricellular cues to control the differentiation and fate of human mesenchymal stem cells (hMSCs) is advancing methods to expand and culture hMSCs, as well as strategies to design hMSC carriers for therapeutic applications in bone repair. This thesis research aims to design materials that incorporate specific cues found in ECM and conduct systematic studies for understanding matrix signaling mechanisms that relate to osteogenic differentiation of hMSCs. Specifically, poly(ethylene glycol) (PEG) based hydrogels are exploited as a biomaterial platform to systematically introduce matrix cues and study their influence on hMSC differentiation. Depending on the specific hydrogel formulation, PEG gels are designed to achieve specific moduli, introduce specific chemical moieties, and/or control stimuli responsiveness over nano-, micro- and macroscopic length scales relevant to hMSCs.<sup>1</sup> Building on these concepts, this thesis aims to exploit the versatility of PEG chemistry to engineer biochemical functionalization of hMSC microenvironments.

Specifically, PEG hydrogels are utilized as substrates to better understand the role of chemical cues found in the native bone matrix on hMSC osteogenic differentiation and to develop strategies that allow reversible presentation of these biochemical ligands in four dimensions (i.e., three-dimensional space; x-,y-,z and time). The first aim of this thesis examines phosphate functionalized PEG hydrogels to study and understand the mechanisms underlying how this chemistry induces osteogenic differentiation in hMSCs. We hypothesize that phosphate functional groups sequester ECM proteins present in serum and induce osteogenic differentiation in hMSCs via focal adhesion kinase dependent integrin signaling. The second aim then focuses on developing  $\alpha 5$  integrin priming PEG hydrogels to elucidate the interplay of substrate elasticity and  $\alpha 5$  integrin signaling on osteogenic differentiation of hMSCs. We hypothesize that osteogenic differentiation of hMSCs via  $\alpha 5\beta 1$  integrin signaling is strongly influenced by the underlying substrate elasticity. Finally, the third aim of this thesis investigates a chemical strategy that allows for dynamically tunable presentation of biochemical ligands in 4D. We hypothesize that an addition-fragmentation-chain transfer capable allyl sulfide functional group will allow for reversible exchange of thiol containing biomacromolecules under cytocompatible reaction conditions and that this chemistry may prove beneficial in investigating more complex questions about temporal and sequential signaling on hMSC osteogenic differentiation.

To test the above hypotheses, the specific objectives of this thesis research are as follows:

**Aim I. Study the role of phosphate functional groups in mediating hMSC attachment and understand the mechanisms underlying osteogenic differentiation of hMSCs on phosphate functionalized PEG hydrogels in the absence of osteogenic induction cues.**

Towards understanding the interaction of hMSCs with phosphate functionalized PEG hydrogels, experiments are designed to verify the nature of interaction of hMSCs with covalently bound phosphate functional groups, directly or indirectly, via sequestering serum proteins in the culture medium. Further, the total amount of adsorbed serum proteins will be quantified to determine the effect of phosphate functional group concentration in sequestering serum proteins. Adhesion blocking and integrin blocking experiments will be investigated to determine the importance of specific ECM proteins in mediating the adhesion of hMSCs to the gels. Phosphorylation of focal adhesion kinase is a focal point for the signaling pathways initiated by integrins upon binding to ECM proteins. Hence, towards understanding the role of the ECM proteins in driving osteogenic differentiation of hMSCs cultured on phosphate containing gels, ALP activity measurement and gene expression studies will be characterized in the presence of small chemical inhibitor to focal adhesion kinase (FAK). Successful completion of this objective will layout a putative mechanism of the signaling pathways underlying osteogenic differentiation of hMSCs on phosphate functionalized PEG hydrogels.

**Aim II. Synthesize PEG-peptide hydrogels that prime  $\alpha 5$  integrin and study the role of substrate elasticity on  $\alpha 5\beta 1$  induced osteogenic differentiation in hMSCs.**

This objective explores the use of peptide-PEG hydrogels as culture platforms that can signal specific integrins to study the role of integrin signaling and mechanical signals, such as substrate elasticity, on osteogenic differentiation of hMSCs. Specifically, a peptide motif  $\text{cyl(RRETAWA)}$  that has been shown to bind  $\alpha 5$  integrin with high specificity<sup>2</sup> will be synthesized and tagged with a thiol containing cysteine for functionalization into PEG hydrogels. Bioactivity of the peptide will be verified by measuring ALP activity upon dosing hMSCs solubly with the synthesized peptides. Thiol-ene polymerization reactions will be utilized to synthesize PEG hydrogels functionalized with pendant  $\text{cyl(RRETAWA)}$  groups. The biochemical functionalization and biophysical properties of the hydrogel will be tailored independently by changing the material formulations to control ligand dose and substrate elasticity (as characterized rheometrically). To de-convolute the role of substrate stiffness and ligand density on hMSC adhesion, cell attachment density, cell adhesion area, aspect ratio and focal adhesion area of attached hMSCs will be characterized as a function of the underlying gel properties. Further, the interplay of substrate stiffness and ligand density on  $\alpha 5\beta 1$  integrin induced osteogenic differentiation of hMSCs will be studied by monitoring ALP activity and osteogenic gene expression in hMSCs. Successful completion of these studies will help to understand the role of matrix elasticity on  $\alpha 5\beta 1$  signaling in hMSCs.

**Aim III. Synthesize and characterize allyl sulfide functionalized hydrogels and demonstrate photocoupling and photoexchange of biochemical ligands reversibly.**

*In vivo*, the hMSC bone marrow niche is far from static, and ECM cues are generally presented in a dynamically regulated manner. Hence, to conduct more biologically relevant experiments to assess the role of ECM cues on hMSC biology, culture platforms that can recapitulate the dynamic presentation of signaling cues would be particularly advantageous. With this in mind, a chemical strategy based on addition-fragmentation chain transfer capable allyl sulfide functional group will be used to create PEG hydrogels that enable the reversible presentation of biochemical ligands important for osteogenesis of hMSCs. Towards the development of such programmable hydrogels, PEG hydrogel will be functionalized homogeneously with addition-fragmentation-chain transferable, allyl sulfide, functional groups.<sup>3-5</sup> To achieve spatial and temporal control over the presentation of biological ligands, we will utilize photo-lithography to pattern cysteine-containing peptides. The characteristic fragmentation of allyl sulfide functional group upon attack by thiyl radicals<sup>3,4</sup> in the hydrogels will be exploited to pattern peptide epitopes via thiol-ene photoconjugation. Here, a thiol containing cysteine conjugated RGDS peptide found on the ECM protein fibronectin will be used as a model biomimetic peptide epitope to demonstrate the patterning. By patterning in fluorescently labeled peptides, the degree of network biofunctionalization will be characterized and compared to the fluorescence of patterns obtained with known standard concentrations. Further, two-photon lithography will be used to demonstrate exchange of thiol containing peptide epitopes in spatially defined regions in three-dimensions. Both Alexa Fluor 555 and Alexa Fluor 488 conjugated CRGDS peptides will be used as model peptides to

demonstrate and characterize the exchange reactions. The dependence of the extent of exchange of peptides on the two-photon laser power and pixel dwell time will be characterized as before by comparing the fluorescence of the resultant patterns with known standard concentrations. The resulting knowledge will be exploited to construct opposing gradients of two distinct functional groups with only one exchange reaction. Successful completion of this objective will lay the framework for dynamically tailoring the biochemical environment of the hMSCs for understanding and assessing the role of ECM cues in a biologically relevant fashion.

## **2.1 References:**

1. Tibbitt, M. W. & Anseth, K. S. Hydrogels as extracellular matrix mimics for 3D cell culture. *Biotechnol. Bioeng.* **103**, 655–663 (2009).
2. Koivunen, E., Wang, B. & Ruoslahti, E. Isolation of a highly specific ligand for the alpha 5 beta 1 integrin from a phage display library. *J. Cell Biol.* **124**, 373–380 (1994).
3. Scott, T. F., Schneider, A. D., Cook, W. D. & Bowman, C. N. Photoinduced Plasticity in Cross-Linked Polymers. *Science* **308**, 1615–1617 (2005).
4. Kloxin, C. J., Scott, T. F. & Bowman, C. N. Stress relaxation via addition-fragmentation chain transfer in a thiol-ene photopolymerization. *Macromolecules* **42**, 2551–2556 (2009).
5. Kloxin, C. J., Scott, T. F., Park, H. Y. & Bowman, C. N. Mechanophotopatterning on a Photoresponsive Elastomer. *Advanced Materials* **23**, 1977–1981 (2011).

## CHAPTER 3

### **Extra-cellular matrix protein adsorption to phosphate-functionalized hydrogels from serum promotes osteogenic differentiation of human mesenchymal stem cells (hMSCs)**

*As appearing in Acta Biomaterialia*

---

#### **3.1 Abstract**

One of the primary goals for tissue engineering is to induce new tissue formation by stimulating specific cell function. Human mesenchymal stem cells (hMSCs) are a particularly important cell type that has been widely studied for differentiation down the osteogenic (bone) lineage, and we recently found that simple phosphate functional groups incorporated into poly(ethylene glycol) hydrogels could induce osteogenesis without using differentiation medium by unknown mechanisms. Here, we aimed to determine whether direct or indirect cell/materials interactions were responsible for directing hMSCs down the osteogenic lineage on phosphate ( $\text{PO}_4$ ) functionalized poly(ethylene glycol) (PEG) hydrogels. Our results indicated that serum components adsorbed onto  $\text{PO}_4$ -PEG hydrogels from media in a pre-soaking step were sufficient for attachment and spreading of hMSCs, even when seeded in serum-free conditions. Blocking antibodies for collagen and fibronectin (targeted to the hydrogel), as well as  $\beta 1$  and  $\beta 3$  integrin blocking antibodies (targeted to the cells), each reduced attachment of hMSCs to  $\text{PO}_4$ -PEG hydrogels, suggesting that integrin-mediated interactions between cells and adsorbed matrix components facilitate attachment and spreading. Outside-in signaling, and not merely shape change, was found to be required for osteogenesis, as alkaline



phosphatase (ALP) activity and expression of CBFA1, osteopontin and collagen-1 (coll-1) were each significantly down regulated upon inhibition of focal adhesion kinase (FAK) phosphorylation even though focal adhesion structure or cell shape were unchanged. Our results demonstrate that complex function (i.e., osteogenic differentiation) can be controlled using simple functionalization strategies, such as incorporation of  $\text{PO}_4$ , but that the role of these materials may be due to more complex influences than has previously been appreciated.

### **3.2. Introduction**

Human mesenchymal stem cells derived from bone marrow have been shown to be capable of differentiating down osteogenic, adipogenic and chondrogenic lineages<sup>1</sup>. Traditionally, differentiation of these cells has been achieved by adding soluble cues to the culture medium. The roles and mechanisms of various media additives in inducing differentiation of hMSCs have been extensively studied. For example, dexamethasone, bone morphogenetic protein (BMP),  $\beta$ -glycerol phosphate have been shown to up-regulate expression of osteogenic related genes in hMSCs<sup>1-5</sup>. To complement these approaches, there is growing interest in the biomaterial research community to use synthetic biomaterials as culture platforms for hMSCs and for applications in tissue regeneration. Their design has been inspired by previous work to capture and present molecular interactions that induce specific functions of hMSCs.

Specifically, synthetic scaffolds have been extensively used as culture platforms to introduce both biochemical and biophysical signals to control and promote osteogenic differentiation of hMSCs. Inorganic materials, such as tricalcium phosphate, hydroxyapatite, and bioglass, have all been widely used as coatings and bulk materials

and considered osteoconductive materials for bone regeneration applications<sup>6-10</sup>. The main limitation when using inorganic materials is the inability to control and tune the materials properties, especially degradability, as well as the limited ability to alter the chemistry to incorporate biochemical cues that promote bone formation<sup>9,10</sup>. As an alternative, materials based on organic polymers have become attractive as biomaterial scaffolds for bone tissue engineering. While their mechanical properties can be inferior compared to inorganic materials, polymers allow for tailoring of material properties and introduction of a wide range of chemistries that allow researchers to incorporate functionalities into the materials<sup>10</sup>.

In particular, poly(ethylene glycol) (PEG) based hydrogel scaffolds have been used by our group and others to present various biochemical signals to study and control osteogenic differentiation of hMSCs<sup>11,12</sup>. Because PEG minimizes non-specific protein interactions, the role and function of specific biochemical signals on hMSC function can be studied independent of non-specific protein adsorption from serum employed in cell culture. Researchers have employed PEG gels to present various biochemical cues, including peptides<sup>13</sup>, growth factors<sup>14</sup>, chemical functionalities<sup>15</sup>, enzymatic degradability<sup>16</sup>, and controlled material elasticity<sup>17,18</sup>, and study the role of integrin signaling, growth factor signaling, matrix degradability and matrix mechanics during osteogenic differentiation of hMSCs.

Complexity, cost and limited understanding of the most critical factors for inducing desired hMSC functions have prompted researchers to investigate alternative and simpler approaches for the design of synthetic biomaterials. For example, researchers have identified biomaterial formulations based on simple chemistries that influence critical cell

functions such as proliferation, differentiation etc. Several studies have investigated the influence of small chemical functional groups on proliferation and/or differentiation of hMSCs using self-assembled monolayers<sup>19-22</sup> and hydrogel systems<sup>15,23</sup>. For example, osteogenic and chondrogenic differentiation of hMSCs depends on the choice of small molecules used to functionalize surfaces, with thiol or amine functional groups promoting osteogenic differentiation and acid or hydroxyl functional groups promoting chondrogenic differentiation<sup>20,21</sup>. Of interest to this work, Benoit *et al.* demonstrated that phosphate functional groups induced osteogenic differentiation in hMSCs on 2D gels, as well as when encapsulated in 3D hydrogel environments<sup>15</sup>. Interestingly, osteogenic differentiation on this otherwise inert PEG hydrogel was achieved without the addition of any soluble osteoinductive factors to the media, indicating that osteogenic differentiation was specifically due to the presence of the small molecule phosphate functional group. Collectively, these studies demonstrate the potential for simple strategies to offer simpler, cheaper and more efficient design principles for cell carriers to promote hMSC differentiation. While these phenomenological observations are quite interesting and insightful, they provide very little mechanistic understanding of how these functionalized biomaterials guide cell behavior.

Here, we attempt to elucidate some aspects of the mechanism driving osteogenic differentiation of hMSCs on phosphate-functionalized PEG gels, as they were previously shown to induce osteogenic differentiation in hMSCs without the need for osteoinduction media<sup>15</sup>. Several studies have previously shown the importance of adsorbed extra cellular matrix (ECM) proteins in mediating cell interaction with biomaterials and that composition, as well as orientation, of the adsorbed ECM proteins is considered to be a

major determinant of cell material interactions with biomaterials<sup>24-29</sup>. Specifically, previous literature has shown that ECM proteins influence hMSC differentiation in *in vitro* cultures<sup>30-35</sup>. For example, collagen-1 (coll-1) and fibronectin (FN) when adsorbed onto TCPS were shown to promote mineralization and upregulate osteogenic genes, CBFA-1 and osteocalcin, in hMSCs<sup>30</sup>. Further, integrins that bind to these ECM proteins were demonstrated to play a key role in both promoting and inhibiting osteogenic differentiation of MSCs<sup>31</sup>. Previous studies also showed that interaction of  $\alpha 2\beta 1$  integrin with collagen-1 activated the transcription factor CBFA-1 and promoted matrix mineralization, and further, that blocking these interactions resulted in a marked decrease in matrix mineralization<sup>32,33</sup>. Blocking interaction of integrins  $\alpha 5\beta 1$ ,  $\alpha 3\beta 1$  with FN has been shown to inhibit upregulation of osteogenic genes, ALP activity and mineral formation in osteoprogenitor cultures<sup>35</sup>. Specifically, FN fragments with high specificity for binding to  $\alpha 5\beta 1$  integrins increased ALP activity and upregulated gene expression of ALP, CBFA-1 and osteocalcin in hMSCs<sup>35</sup>. Interestingly, the integrin  $\alpha v\beta 3$ , which also has binding sites on FN, was shown to have a negative effect on hMSC osteogenic differentiation. hMSCs when cultured on FN fragments with a high specificity for binding to  $\alpha v\beta 3$  integrins were shown to decrease gene expression of ALP, CBFA-1 and osteocalcin<sup>35</sup>.

Here, we aimed to determine if hMSCs were directly interacting with the phosphate functional groups on PEG hydrogel or indirectly with adsorbed ECM proteins present in serum. The role of focal adhesion kinase (FAK) signaling in inducing osteogenic differentiation on these gels was also investigated. Gaining a mechanistic understanding of how these gels cause phenotypic changes in hMSCs is an important

aspect to our overall understanding of matricellular signaling, as well as our ability to design improved materials for tissue engineering applications.

### **3.3. Material and Methods**

All materials were purchased from Sigma-Aldrich unless otherwise specified.

#### **3.3.1. Cell culture**

hMSCs were isolated from human bone marrow (Cambrex) and cultured in growth media (low glucose Dulbecco's Modified Eagle Medium (DMEM, Gibco) supplemented with 10% fetal bovine serum (Gibco), 1% Penicillin/Streptomycin (Gibco), and 0.2% Fungizone (GIBCO)). hMSCs at passage three were used in all the studies.

#### **3.3.2. Phosphate functionalized poly(ethylene glycol) polymer gels**

Gels were formed by polymerizing poly(ethylene glycol) dimethacrylate (PEGDMA) ( $M_n \sim 550$  Da) with 0.5 wt% of the photo-initiator, 2,2-dimethoxy-1,2-di(phenyl) acetophenone (Ciba-Giegy) by exposure to  $\sim 4 \text{ mWcm}^{-2}$  ultraviolet light for 10 min. Phosphate functional groups were incorporated into the gels by adding ethylene glycol methacrylate phosphate (EGMP) at a concentration of 50mM (or otherwise mentioned) to the macromer-initiator solution before polymerization. Gels were swollen in phosphate buffer saline (PBS, 1x, GIBCO) for at least 24 h. Circular disks (10 mm diameter, 120  $\mu\text{m}$  thick) were cut from the gel using biopsy punches and transferred to tissue culture plates. For cell culture experiments gels were sterilized in 70% ethanol and washed thoroughly in PBS before seeding.

### **3.3.3. Quantification of protein adsorption**

Phosphate functionalized gels were incubated in 10% serum containing media for overnight and washed with PBS (0.5 ml in each well of a 24 well plate, 3x) to remove weakly adsorbed proteins. Adsorbed proteins were eluted in sodium dodecyl sulfate (SDS) buffer for 2 h and concentrated using Zeba desalting columns (7k MWCO, Pierce). Protein levels were quantified by a  $\mu$ BCA assay (Pierce) according to manufacturer's instructions.

### **3.3.4. Focal adhesion staining and calculating cell shape parameters**

Focal adhesion staining was performed on hMSCs attached to the gels ( $5 \times 10^3$  cells/cm<sup>2</sup> seeding density) using a focal adhesion staining kit (FAK100, EMD Millipore) according to manufacturer's instructions. Cell density was chosen to avoid excessive cell-cell contacts after hMSC attachment to gels. Cells were counterstained with 4,6-diamidino-2-phenylindole (DAPI, Invitrogen, 300nM) for nuclei and stored in PBS at 4C until imaged with a Zeiss confocal microscope.

hMSC shape parameters were quantified by immunostaining with rhodamine phalloidin (Molecular Probes, R415, 1:200 dilution). Samples were imaged using a confocal microscope (Zeiss, LSM 710), and the RGB images were converted into binary images and analyzed by an in-built 'analyze particles' macro in ImageJ that automatically generates an average area per cell and aspect ratio. Ten images per condition were analyzed.

### 3.3.5. Adhesion blocking and integrin blocking experiments

Phosphate gels were incubated in growth media overnight to allow for serum proteins to adsorb. Gels were washed with PBS to remove weakly attached proteins and incubated with antibody solutions containing antibodies against fibronectin (Abcam, ab2413, 1:200), collagen-1 (Abcam, ab34710, 1:1000) or IgG (Isotype control, Sigma, M5284) in PBS for 1 h. Gels were then washed three times for 10 min each with PBS to remove loosely attached antibodies. hMSCs were then seeded onto gels in serum free media (low glucose Dulbecco's Modified Eagle Medium (DMEM, Gibco) supplemented with 1% Penicillin/Streptomycin (Gibco), and 0.2% Fungizone (GIBCO)) at a density of  $5 \times 10^3$  cells/cm<sup>2</sup> and allowed to attach for 12 h. Gels were washed in PBS to remove loosely attached cells and stained with calcein AM (Invitrogen) for live cells as per manufacturer's protocols. hMSCs were imaged using an epifluorescence microscope and live cells were counted manually using ImageJ software.

For integrin blocking experiments, hMSCs were incubated with antibody solutions containing antibodies against  $\beta 1$  (Abcam, ab52971, 1:50 dilution),  $\beta 3$  (Abcam, ab47584, 1:50 dilution) integrins or IgG (Isotype control, Sigma, M5284) in serum-free media for 30 min and seeded onto serum pre-incubated gels in serum free media at  $5 \times 10^3$  cells/cm<sup>2</sup> density. Integrin blocked hMSCs were allowed to attach to the gels for 12 h, washed with PBS and stained with calcein AM. Stained hMSCs were imaged using an epifluorescence microscope and the number of attached cells were counted using ImageJ software.

### **3.3.6. Role of focal adhesion kinase (FAK) in osteogenesis of hMSCs on phosphate gels**

To examine integrin signaling dependent osteogenic differentiation of hMSCs on phosphate gels, cells were cultured in the presence (at  $3\mu\text{M}$ ) and absence of a small chemical inhibitor for pFAK, PF-573228 (Tocris Biosciences). For the inhibition experiments, hMSCs were seeded onto phosphate gels or tissue culture polystyrene (TCPS) and cultured in growth or osteogenic media (high glucose Dulbecco's Modified Eagle Medium (DMEM, Gibco) supplemented with 10% fetal bovine serum (Gibco), 1% Penicillin/Streptomycin (Gibco), and 0.2% Fungizone (GIBCO), 10mM  $\beta$ -glycerol phosphate (Sigma), 50  $\mu\text{g/ml}$  ascorbic acid (Sigma), and 100 nM dexamethasone (Sigma)) at a density of  $5 \times 10^3$  cells/cm<sup>2</sup>.

### **3.3.7. Alkaline phosphatase (ALP) production of hMSCs cultured on phosphate gels**

ALP production was measured using an assay based on the change in absorbance of *o*-nitrophenol (ALP substrate, Invitrogen) as it is enzymatically cleaved by ALP. Cells were removed from culture, washed in PBS and lysed in 50  $\mu\text{l}$  RIPA buffer (Invitrogen) for 15 min with gentle shaking. The sample solutions were diluted with 50  $\mu\text{l}$  of PBS. 50  $\mu\text{l}$  of the sample solution was then mixed with 50  $\mu\text{l}$  of ALP substrate, and the absorbance of the solution at 405 nm was measured at 1-minute intervals ten times with a plate reader (Victor<sup>2</sup>, Perkin Elmer). ALP activity levels were calculated as the slope of the increase in absorbance at 405 nm with time. In parallel, gels were stained with calcein AM (Invitrogen) to stain live cells. Ten images per sample were analyzed for cell number using a cell counter plug-in in ImageJ. ALP activity levels were normalized using the total cell numbers on the gel.



### **3.3.8. Gene expression of hMSCs cultured on phosphate gels**

Gene expression of hMSCs cultured on phosphate gels was analyzed using reverse-transcription polymerase chain reaction (RT-PCR). At day 14 of culture, gels were removed from culture and washed three times in PBS. RNA was isolated using TRI reagent (Sigma) and standard manufacturer's protocols. The resulting RNA pellet was re-suspended in nuclease free water and treated with DNase (Bio-Rad) to digest any residual genomic DNA. The obtained RNA was precipitated in isopropanol after washing with phenol-chloroform, re-suspended in 20  $\mu$ l nuclease free water, and quantified by measuring absorbance at 280 nm with a NanoDrop ND-1000 spectrophotometer (Thermo Scientific). Samples with a 280 nm to 260 nm absorbance ratios greater than 1.85 were considered pure and were used for the reverse transcription step.

Reverse transcription was performed using the iScript cDNA Synthesis Kit (Bio-rad). A total of 15 ng RNA was used for the single-stranded cDNA synthesis. The reverse transcription reaction tube was incubated at 25 C for 5 min, at 42 C for 30 min, and terminated at 85 C for 5 min. PCR was conducted using the iCycler Real-Time PCR machine (Bio-Rad). Primers and probes were obtained from Bio-Rad. Table 1 shows the primer sequences used in this study. The following PCR parameters were utilized: 95 C for 90 s followed by 45 cycles of 95 C for 30 s and 55 C for 60 s. Threshold cycle ( $C_T$ ) analysis was used to quantify PCR products, normalized to GAPDH and relative to expression of hMSCs at day 1 cultured on TCPS in growth media.

**Table 3.1:** Primers used for RT-PCR studies

Primer	Nucleotide Sequence (5'-3')
COLL-1a	GGGCAAGACAGTGATTGAATACA GGATGGAGGGAGTTTACAGGAA
CBFA1	GGTATGTCCGCCACCACTC TGACGAAGTGCCATAGTAGAGATA
GAPDH	GCAAGAGCACAAGAGGAAGAG AAGGGGTCTACATGGCAACT
OPN	ATTCTGGGAGGGCTTGGTTG TCTGGTCCCGACGATGCT

### 3.3.9. Statistical Analysis

Data collected throughout this study are represented as mean  $\pm$  standard error of three different samples (or otherwise mentioned). For effect of serum on hMSC attachment, shape and for gene expression studies, data sets were compared using two-way ANOVA analysis with Tukey tests for comparison. For effect of PO<sub>4</sub> concentration on serum protein adsorption and integrin or adhesion blocking studies, data sets were compared using one-way ANOVA analysis with Tukey tests for comparison. In all studies, p-values less than 0.05 were considered as significant.

### 3.4. Results

#### 3.4.1 Serum proteins facilitate hMSC attachment and spreading on PO<sub>4</sub>-PEG hydrogels.

In order to determine the importance of serum in mediating cell/matrix interactions, we first investigated hMSC attachment to phosphate functionalized gels compared to control PEG gels in the presence and absence of serum, with results presented in Figure 3.1. While attachment was limited in serum free media for both gel formulations (Figure 3.1A, grey bars), PO<sub>4</sub>-PEG gels promoted significantly higher hMSC attachment ( $\sim 550$  cells/cm<sup>2</sup>, Figure 3.1A, black bars), spreading ( $\sim 10^4$   $\mu\text{m}^2$ , Figure 3.1B, solid black bars), in the presence of serum compared to control PEG hydrogels. Aspect ratio of hMSCs on PO<sub>4</sub>-PEG gels was similar to control PEG gels in the presence of serum ( $\sim 2$ , Figure 3.1B, textured bars). Next, we investigated whether the influence of serum was due to soluble or sequestered proteins. Phosphate functionalized hydrogels were incubated in media containing serum for overnight, washed thoroughly to remove weakly attached serum components, and then seeded with hMSCs in serum free media. As shown in Figure 3.2 (See Experimental section for details), phosphate functionalized hydrogels promoted higher protein adsorption ( $\sim 500$  ng/cm<sup>2</sup>) compared to control PEG control hydrogels ( $\sim 100$  ng/cm<sup>2</sup>) independent of phosphate concentration (Figure 3.2). Our results indicated that hMSCs attached to pre-treated PO<sub>4</sub>-PEG in serum-free conditions similarly to cells seeded in serum (Figure 3.1A, white bar textured,  $\sim 525$  cells/cm<sup>2</sup>) while very few cells attached to control gels. Based on these results, we conclude that adsorbed serum components were mediating attachment and spreading of hMSCs on PO<sub>4</sub>-PEG hydrogels.

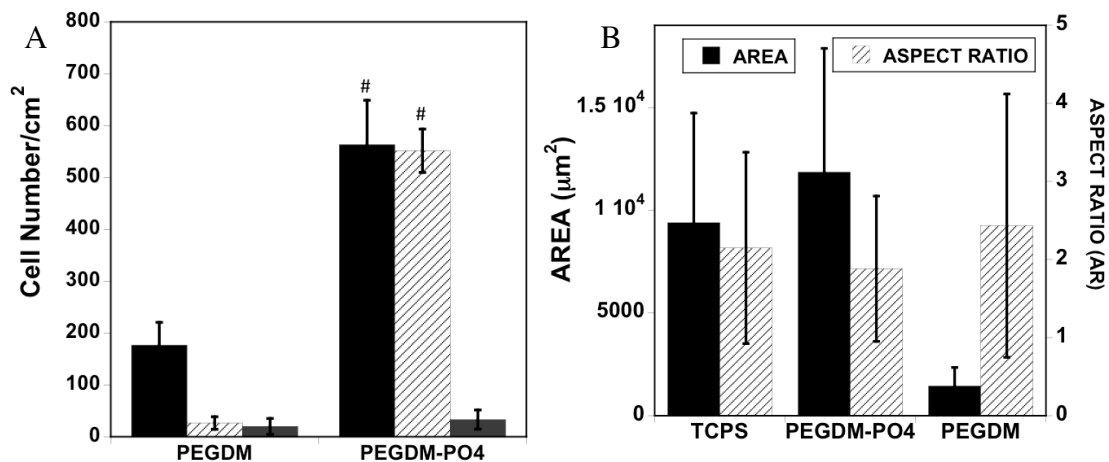


**Figure 3.1. Serum components mediate hMSC attachment and spreading on PO<sub>4</sub>-PEG gels ([PO<sub>4</sub> = 50mM])** (A) Effect of seeding conditions on hMSC adhesion to gels. Average number of cells per area attached to PEGDM and PO<sub>4</sub>-PEG gels when seeded in serum containing media (black bar), pre-incubated with serum containing media and seeded in serum free media (white bar, textured), and seeded in serum free media (grey bar). (# indicates significant difference compared to that on control gels (PEGDM); p<0.05, Data represents averages of N=3 different experiments with n = 3 replicates during each experiments). (B). Cell shape parameters; average cell area (filled black bars) and average aspect ratio (striped bars) when cultured for 24 h on different gels as indicated. Cell shape parameters of hMSCs on TCPS were also included for comparison. Phosphate functional groups promote cell spreading similar to cells cultured on tissue culture polystyrene (TCPS) when seeded in growth media. Error bars represent standard deviations for N=150-250 cells.

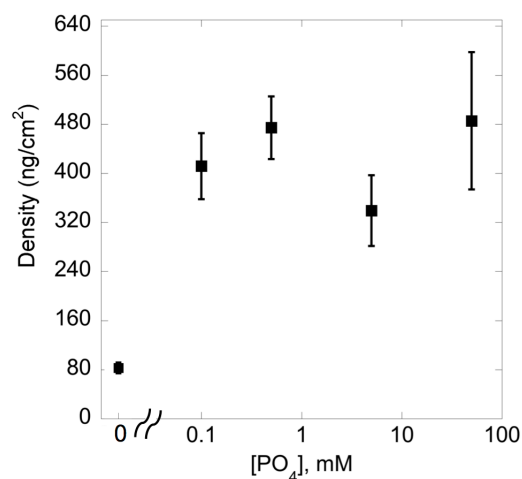


**Figure 3.2. Effect of [PO<sub>4</sub>] concentration on total protein adsorbed from serum.** Total protein adsorbed was significantly higher on phosphate gels compared to the control ([PO<sub>4</sub>] = 0 mM) gels. Increasing the concentration of [PO<sub>4</sub>] in the gels did not result in any significant increase in protein adsorption. Total protein adsorbed on TCPS under similar conditions is 0.5 μg/cm<sup>2</sup> (#, indicates significant difference compared to the control ([PO<sub>4</sub>] = 0 mM) gel; Data represent averages of N=3 different experiments with 4 replicates in each experiment. p<0.05).

### 3.4.2 hMSC attachment is mediated by ECM protein-integrin interactions

The ECM plays a role in influencing cell function by interacting with integrins, which can lead to “outside-in” signaling. Previous studies have indicated that collagen I (Coll-1) and fibronectin (FN) enhanced osteogenic differentiation in hMSCs. Interaction of hMSCs with Coll-1 and FN with specific integrins has been previously shown to control ALP activity, gene expression of CBFA1 and bone sialoprotein<sup>26,27</sup>. Here, we investigated potential roles for Coll-1 and FN in mediating hMSC attachment to PO<sub>4</sub>-PEG hydrogels, with results illustrated in Figure 3.3. To determine possible roles for Coll-1 and FN in mediating hMSC attachment to PO<sub>4</sub>-PEG hydrogels, we blocked cell adhesive sites present on fibronectin and collagen-1 using specific antibodies. As shown in Figure 3.3, cell attachment was significantly reduced when either matrix component was blocked

using antibodies, suggesting that both Coll-1 and FN were present on PO<sub>4</sub>-PEG hydrogels and that each provided binding sites for hMSCs.

Both  $\beta$ 1- and  $\beta$ 3- integrins have been shown to have binding ligands on Coll-1 and FN. Also, these integrins have been previously shown to regulate hMSC osteogenic differentiation<sup>31</sup>. We investigated the role of integrin binding for hMSCs on phosphate-functionalized hydrogels using blocking antibodies against  $\beta$ 1 and  $\beta$ 3 integrins. hMSCs were incubated with antibodies against  $\beta$ 1 and  $\beta$ 3 integrins in serum free medium and then seeded onto serum media pre-soaked phosphate functionalized gels (still in the presence of serum free medium). As shown in Figure 3.4A, hMSC attachment was reduced to about 60% and 50% upon blocking  $\beta$ 1 and  $\beta$ 3 integrins, respectively, while blocking both did not lead to additional statistically significant inhibition. These results indicate that both  $\beta$ 1 and  $\beta$ 3 integrins facilitate hMSC attachment to phosphate-functionalized hydrogels.

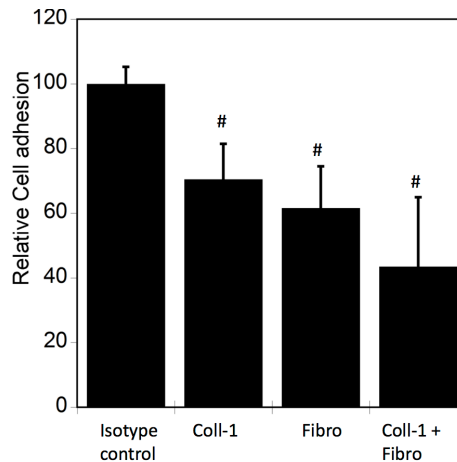


**Figure 3.3. ECM proteins are differentially adsorbed on to PO<sub>4</sub>-PEG gels ([PO<sub>4</sub> = 50mM]).** Blocking cell adhesion sites corresponding to specific ECM proteins (Fibro = Fibronectin, Coll-1 = Collagen-1) adsorbed onto the PO<sub>4</sub>-PEG gel influences cell attachment. Average number of cells that remained attached to PO<sub>4</sub>-PEG gels upon blocking were counted and reported as a percentage compared to control. # indicates significant difference compared to control  $p \leq 0.05$ . (Data represent averages of N=3 different experiments with 3 replicates in each experiment.)

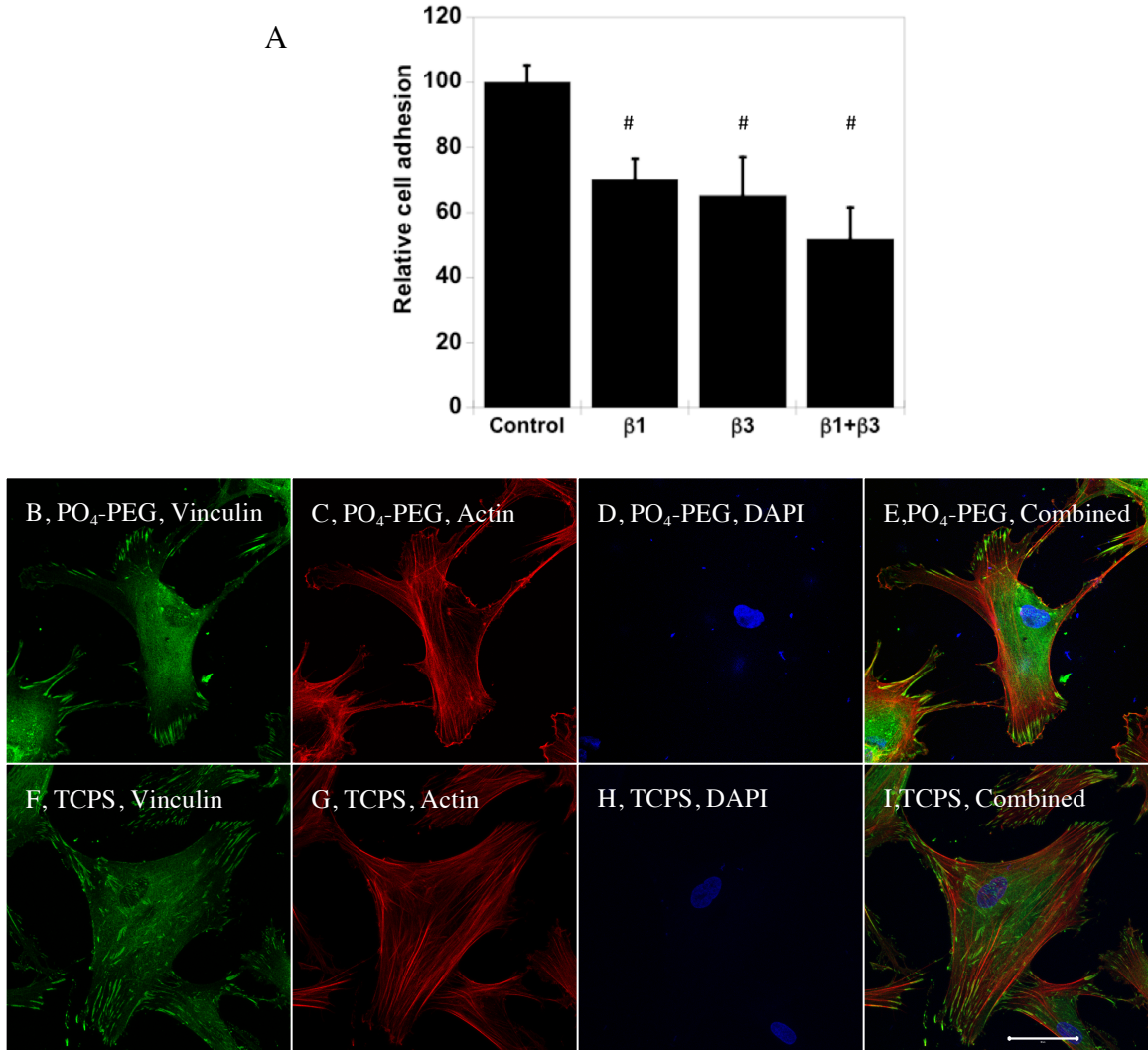
### **3.4.3 Focal Adhesion Kinase (FAK) signaling is required for PO<sub>4</sub>-PEG hydrogel induced osteogenesis.**

FAK induction of the MAP kinase pathway has been shown to be a critical component in osteogenesis due to activation of CBFA-1 transcription factors.<sup>27</sup> Upon integrin binding and clustering, focal adhesions facilitate the recruitment and phosphorylation of FAK, which subsequently induces a cascade of downstream signaling events that ultimately control cell fate, including osteogenic differentiation of hMSCs when stimulated in conjunction with other signals found in osteogenic supplements.<sup>30</sup> Our results indicated that hMSC attachment to PO<sub>4</sub>-PEG hydrogels involved integrin binding to adsorbed ECM proteins. Figure 3.4B-I shows representative images of vinculin (Figure 3.4B,F) and actin (Figure 3.4C,G) staining of hMSCs on PO<sub>4</sub>-PEG gels in growth media (Figure 3.4B-E) and on TCPS in OS media (Figure 3.4F-I). hMSCs seeded on PO<sub>4</sub>-PEG hydrogels expressed vinculin, as well-defined fibrillar structures (10-20 μm) that were consistent with focal complexes and well developed actin stress fibers. Qualitatively, the number of fibrillar structures of vinculin and amount of actin stress fibers in hMSCs was lower on PO<sub>4</sub>-PEG gels compared to that on TCPS, indicating that the interaction of hMSCs with the adsorbed protein layer is different in both conditions. We therefore hypothesized that PO<sub>4</sub>-PEG hydrogels induced osteogenic differentiation of hMSCs through integrin recruitment of focal complexes and subsequent FAK signaling.

To verify the involvement of FAK signaling in osteogenesis for hMSCs on PO<sub>4</sub>-PEG gels, we measured the expression of osteogenic markers for cells treated with the small chemical inhibitor PF-573228, which prevents downstream signaling by interrupting phosphorylation of FAK at Tyr<sup>397</sup>.<sup>37</sup> hMSCs were cultured on phosphate

functionalized gels in growth media or TCPS with OS supplements over a period of 14 days in the absence or presence of PF-573228. The effect of pFAK inhibition on fold change in cell numbers on PO<sub>4</sub>-PEG gels in growth media and on TCPS in OS media are shown in Figure 3.5A. The concentration of pFAK inhibitor used did not significantly affect the proliferation of hMSCs on both PO<sub>4</sub>-PEG and TCPS throughout the time scale of the study. ALP activity (Figure 3.5B), an early osteogenic marker, at days 1, 7, and 14, or gene expression levels of Coll-1A, CBFA1, osteopontin (OPN) (Figure 3.6) at day 14 of hMSCs were studied. ALP activity of hMSCs cultured on phosphate functionalized gels and TCPS was increased by 2.5 and 4 fold by day 7, respectively, compared to day 1. Inhibition of phosphorylation of FAK abrogated the increase in ALP activity of hMSCs cultured on both phosphate functionalized gels and TCPS at day 7 and day 14. At day 7, hydrogels.

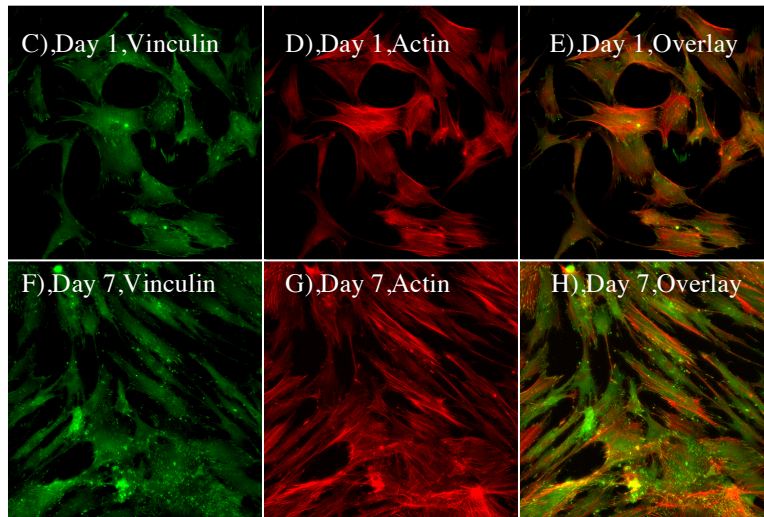
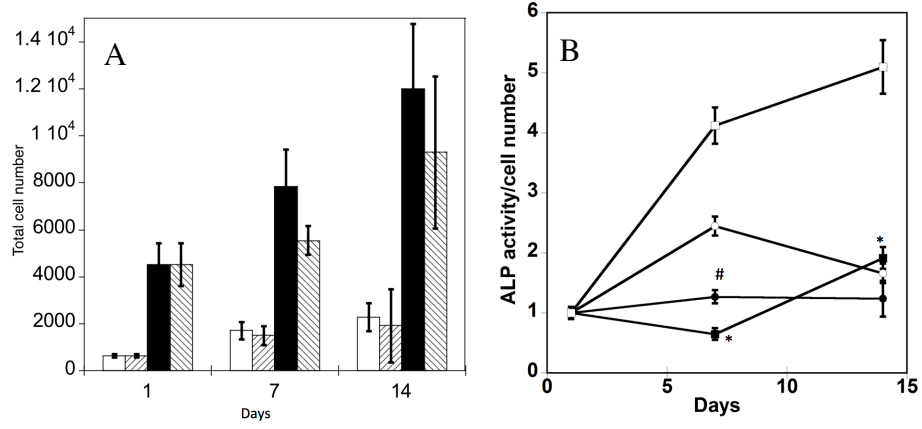




**Figure 3.4. hMSC interaction with the PO<sub>4</sub>-PEG gels ([PO<sub>4</sub>] = 50mM) is mediated through  $\beta 1$  and  $\beta 3$  integrins.** (A) Integrin blocking studies. Cells were incubated with  $\beta 1$ ,  $\beta 3$ ,  $\beta 1 + \beta 3$  or control (IgG) antibodies for 30 min and seeded onto phosphate gels. Average number of cells attached were counted and reported as a percentage compared to control. Data represent averages of N=3 different experiments with 3 replicates in each experiment. (B-I). Immunostaining for vinculin (green, B, F), actin (red, C, G), nuclei (blue, D, H) and overlay (E, I) of hMSCs seeded on PO<sub>4</sub>-PEG gels (B-E) and on TCPS (F-I) shows the presence of well-developed focal adhesion plaques. (Scale bar = 50 $\mu$ m). # indicates significant difference compared to control,  $p \leq 0.05$ .

ALP was increased for both TCP and PO<sub>4</sub>-PEG hydrogels, an effect that was abrogated by treatment with FAK inhibitor. While TCP had elevated expression of ALP at day 14

that was prevented by FAK inhibitor, there was no difference observed for PO<sub>4</sub>-PEG hydrogels



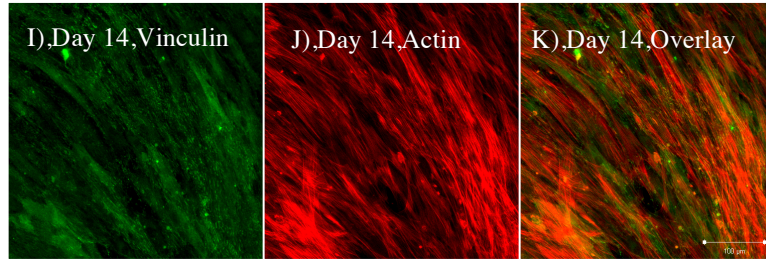


**Figure 3.5. Effect of inhibition of FAK phosphorylation on ALP activity of hMSCs.** (A) Total cell number of hMSCs on  $\text{PO}_4$ -PEG gels ( $[\text{PO}_4] = 50\text{mM}$ ) in growth media with ( $45^\circ$  striped bar) and without (white bar) pFAK inhibitor. Total cell number of hMSCs on TCPS in OS media with ( $135^\circ$  striped bar) and without (black bar) pFAK inhibitor. (B) ALP activity profiles of hMSCs cultured on  $\text{PO}_4$ -PEG gels ( $[\text{PO}_4] = 50\text{mM}$ ) in growth media with (filled circles) or without (open circles) PF-573228 normalized to cell number. Positive control cultures of hMSCs on TCPS with osteogenic supplements (OS) and with (filled squares) or without (open squares) PF-573228 are also shown. # indicates significant difference compared to hMSC cultures on  $\text{PO}_4$ -PEG gel without pFAK inhibitor, (\*) indicates significant difference compared to hMSC cultures on TCPS with OS. Data represent averages of normalized ALP activity of  $N=3$  different experiments with  $n=3$  replicates (C-K). Addition of pFAK inhibitor, PF-573228, doesn't affect the formation of focal adhesion plaques. Immunostained images for vinculin (green, C,F,I), actin (red, D,G,J), overlay (E,H,K) of hMSCs at day1 (C-E), day 7 (F-H), day 14 (I-K) cultured on  $\text{PO}_4$ -PEG constructs in the presence of FAK inhibitor. Vinculin staining shows the presence of well-developed focal adhesion plaques upon inhibiting phosphorylation of FAK. (Scale bar=  $100\mu\text{m}$ )

As with ALP activity, FAK inhibited several genes associated with osteogenesis. Specifically, gene expression of OPN, Coll-1 and CBFA1 were increased by 18, 3, and 17 fold respectively on phosphate functionalized gels cultured in growth media and by 9, 1.7, 10 fold respectively on TCPS cultured with OS supplements by day 14, consistent with osteogenic differentiation. However, when treated with FAK inhibitor, expression was reduced significantly compared to controls for all the genes studied. Coll-1 expression was reduced to 1.5 fold, while CBFA1 and OPN expression reduced to 6 and 4 fold relative to control, respectively. Similarly, FAK inhibition reduced expression of each of these genes on TCPS in the presence of OS media. The effect of pFAK inhibition was not due to changes in shape or focal complex formation, as spreading and focal

adhesion expression was similar with or without FAK inhibitor (Figure 3.5C-K). Therefore, we conclude that FAK signaling is required for osteogenic differentiation for hMSCs seeded on PO<sub>4</sub>-PEG hydrogels, and we again note that osteogenic supplements are not required to mediate this signaling.

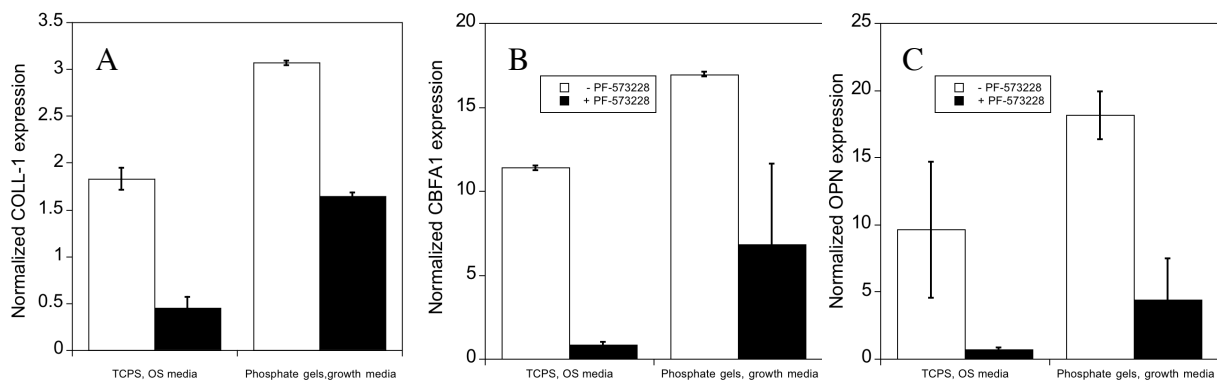


**Figure 3.6.** Effect of inhibition of phosphorylation of FAK on expression of osteogenic related genes in hMSCs. hMSCs cultured on PO<sub>4</sub>-PEG gels ([PO<sub>4</sub>] = 50mM) in growth media on TCPS in OS media in the presence (black bars) or absence (white bars) of FAK inhibitor (PF-573228). All data are normalized to GAPDH gene and further normalized to a corresponding TCPS, growth media control. Data are shown for OS genes, a) Collagen-1 (COLL-1), b) CBFA1, c) Osteopontin (OPN). # indicates significant difference compared to cultures that did not receive pFAK inhibitor p<=0.05. Data represent fold increase averaged over N=3 biological replicates with n=2 technical replicates of each.

### 3.5. DISCUSSION

Biomaterial strategies aimed at harnessing stem cells for regenerative medicine applications typically provide cells with biologically relevant signals to guide cell function, such as differentiation down tissue-specific lineages.<sup>38</sup> Discovery-based approaches have become increasingly prevalent for screening chemical and biological functionality for desired influences on cell function, often without any prior knowledge

of potential outcomes.<sup>39-43</sup> While many strategies are aimed towards designing peptide mimics or attaching other biomolecules to mimic physiological signaling mechanisms,<sup>38,</sup>  
<sup>44</sup> approaches that minimize complexity have also been pursued.<sup>15,23,40,41</sup>

Recently, Benoit *et al.* demonstrated that small chemical functional groups induced differentiation of hMSCs down several lineages without the use of differentiation media.<sup>15</sup> Several functional groups were chosen to mimic chemical characteristics of microenvironments associated with common hMSC lineages and screened at different concentrations using a 2D array-based approach, and it was discovered that osteogenic differentiation was induced by PO<sub>4</sub> groups while adipogenesis was induced by t-butyl groups. Results were then validated in 3D to demonstrate that the chemical functional groups, and not cell shape, were the guiding influence for differentiation. The 3D results were crucial for demonstrating the specific role of the functionalized hydrogels, since cell shape has been shown to be an important factor for directing hMSC differentiation, with osteogenic differentiation being preferential for spread morphologies while rounded morphologies often favors adipogenic differentiation, even when exposed to the same soluble components in the media.<sup>45,46</sup> Benoit *et al.*<sup>15</sup> have shown that PO<sub>4</sub>-PEG gels promoted a spread morphology and t-butyl functional groups promoted a rounded morphology, consistent with the previous studies on the effects of cell shape on hMSC differentiation pathway. However, while it was definitively shown that the functionalized hydrogels specifically induced hMSC differentiation, it was not determined if the mechanism was due to direct interactions with the functional groups or proteins preferentially adsorbed or presented by the different chemical environments. Therefore, we aimed to gain a better understanding of how small chemical functional groups were

able to direct specific differentiation of hMSCs down the osteogenic lineage in an effort to guide more rational choices for future biomaterials designs.

First, we aimed to determine whether attachment and spreading of hMSCs on PO<sub>4</sub>-PEG hydrogels was due to direct interactions with phosphate groups or due to adsorbed serum proteins. Our results indicated that hMSCs did not attach to PO<sub>4</sub>-PEG hydrogels when seeded in serum free medium. However, hMSC attachment and spreading on gels that were *pre-incubated* in serum containing media prior to seeding with cells in serum free media was similar to seeding in serum. As a control, very low hMSC attachment was observed on blank PEG gels (i.e., unfunctionalized) for serum-free conditions under all treatments. Since attachment occurred on PO<sub>4</sub>-PEG hydrogels incubated in serum media prior to seeding under serum-free conditions, soluble components were not required to mediate attachment. Thus, our combined results demonstrated that adsorbed serum components, and not phosphate groups alone, mediated hMSC attachment to PEG-PO<sub>4</sub> hydrogels. Interestingly, the cell seeding efficiency on PO<sub>4</sub>-PEG gels (~600 cells/cm<sup>2</sup> when seeded at 5000 cells/cm<sup>2</sup>) is lower compared to that usually observed on TCPS (90-95%). We note that this cell lower density is often observed when seeding cells on PEG hydrogels, and a potential complication is that one might enrich for a particular subpopulation of hMSCs that are more adherent to these gels. Since hMSCs are a heterogeneous population,<sup>47,48</sup> this subset might be more predisposed to undergo osteogenic differentiation in growth media. It is difficult to de-convolute the effects of preferential selection of an hMSC population from the effects of the phosphate groups on osteogenic differentiation, but this is a point worthy of further investigation.

Next, we have quantified the amount of serum proteins adsorbed onto PO<sub>4</sub>-PEG gels. Our results show that presence of PO<sub>4</sub> functionalities promote protein adsorption significantly compared to the control PEG gel. Although the exact cause of this protein adsorption is not clear from this study, incorporation of charged PO<sub>4</sub> functional groups could result in altered zeta potential around the PEG gel compared to the control gels resulting in strong protein adsorption. This hypothesis is supported by finding of a recent study by Meder *et al.*,<sup>49</sup> in which alumina particles functionalized with PO<sub>4</sub> functional groups resulted in negative zeta potential and preferentially adsorbed positively charged proteins. These results suggest that electrostatic forces play an important role in determining the protein adsorption to these particles. Interestingly, PO<sub>4</sub> concentration did not have any effect on level of protein adsorption to PO<sub>4</sub>-PEG gels. This observation could be explained by considering the network structure of polymers formed by chain polymerization of PEGDM monomers. Here, PO<sub>4</sub> functionalities are incorporated only in the kinetic chains and results in a network structure with dense regions of PO<sub>4</sub> functionalities connected by long PEG chains.<sup>50</sup> This is also supported by our observation that the swelling ratio of the gels is also unchanged with increasing PO<sub>4</sub> concentration (data not shown). The amount of protein adsorbed onto TCPS (which is used to expand hMSCs) is significantly higher than PO<sub>4</sub>-PEG gels. This suggests that the PO<sub>4</sub>-PEG gels could preferentially adsorb specific ECM proteins (compared to proteins adsorbed on TCPS) that signal hMSCs to differentiate down the osteogenic pathway.

Several studies have shown that the identity and structural orientation of adsorbed proteins are strongly dependent on the biophysical and biochemical aspects of the biomaterial,<sup>24,28,51-54</sup> leading to different influences on cell behavior even when the same

protein is present.<sup>28,29,51,55</sup> For example, Keselowsky *et al.*<sup>28,29</sup> showed that substrate chemistry controlled the presentation of adhesion sites present on adsorbed fibronectin and hence influenced the differentiation of osteoblasts. Other studies have shown that interaction of hMSCs with ECM proteins, Coll-1 and FN, influenced the matrix mineralization, expression of osteogenic genes and ALP activity of *in vitro* hMSC cultures.<sup>26,27,41,45,46</sup> For example, Salasznyk *et al.*<sup>30</sup> demonstrated that hMSCs cultured on Coll-1 up-regulated ALP activity and secretion of osteopontin without any need for osteogenic supplements. Since, Coll-1 and FN were each present on PO<sub>4</sub>-PEG hydrogels, suggesting a similar possible role for these ECM components here. Previously, published results on TCPS also show that coll-1 and FN can upregulate expression of osteogenic signal in hMSCs. To complement the results presented here, further studies exploring how osteogenic differentiation is affected by blocking adhesion sites of coll-1 and FN might provide insight as to the role of these proteins in osteogenic differentiation of hMSCs on PO<sub>4</sub>-PEG gels.

Osteogenesis is influenced by the ECM due to attachment that is mediated by integrins, with  $\beta$ 1- and  $\beta$ 3-integrins having each been shown to be important regulating osteogenic differentiation of hMSCs.<sup>31</sup> Interaction of hMSCs with Coll-1 occurs via  $\beta$ 1 integrins and has been shown to be critical for their osteogenic differentiation when cultured on Coll-1. Also, hMSC interaction with FN via  $\alpha$ 5 $\beta$ 1 integrins has been shown to enhance osteogenic related genes CBFA1, bone sialoprotein and ALP. hMSC adhesion to FN functionalized surfaces mediated by  $\beta$ 3 integrins has been shown to negatively influence growth and differentiation of hMSCs.<sup>31,35</sup> We demonstrated that hMSC attachment was decreased on PO<sub>4</sub>-PEG hydrogels when either  $\beta$ 1- or  $\beta$ 3-integrins were



blocked with functional antibodies, demonstrating that  $\beta$ 1- and  $\beta$ 3-integrins can each mediate attachment and spreading.

Outside-in signaling through integrin binding is due to the recruitment of focal complexes, which are required for phosphorylation of FAK.<sup>58</sup> Phosphorylated FAK then triggers downstream signaling through the MAP kinase pathway, which ultimately controls expression of osteogenic transcription factors that are crucial for guiding hMSC differentiation down the osteogenic lineage.<sup>30,36</sup> Inhibition of FAK led to significant down-regulation of each of the osteogenic markers studied, which included alkaline phosphatase activity and gene expression for CBFA1, osteopontin, and Coll-1A. The influence of FAK inhibition was not due to changes in cell shape or focal adhesions, as hMSCs showed similar morphology on PO<sub>4</sub>-PEG gels and continued to express vinculin in a fibrillar organization similar to non-inhibited controls. Substrate elasticity has been previously shown to play an important role during osteogenic differentiation of hMSCs.<sup>17,18,59</sup> Previous studies have also shown that phosphorylation of FAK is dependent on the underlying substrate elasticity.<sup>60,61</sup> For example, Khatiwala *et al.*<sup>60</sup> have shown that levels of phosphorylation (Tyr<sup>397</sup>) of FAK increased with increasing stiffness when pre-osteoblast cells are cultured on poly(acrylamide) substrates. Although not studied in this work, it is possible that substrate elasticity also affects the osteogenic differentiation of hMSCs on PO<sub>4</sub>-functionalized hydrogels. Thus, we conclude that the influence of PO<sub>4</sub>-PEG hydrogels on differentiation of hMSCs down the osteogenic lineage requires FAK signaling and that shape or cell attachment alone is not sufficient for inducing this effect.

Previously, Benoit *et al.*<sup>15</sup> showed (1) PO<sub>4</sub>-PEG hydrogels induced osteogenesis, while other functional groups with similar charges did not induce similar effects, (2) Incorporation of PO<sub>4</sub> functionality was at a low enough concentration to prevent changes in gel hydrophobicity, (3) Shape was not responsible for differentiation, as similar results were obtained for rounded cells in 3D environments.<sup>15</sup> Here, we provided further insight into the mechanism by providing evidence that PO<sub>4</sub>-PEG hydrogels induce differentiation of hMSCs down the osteogenic lineage through specific outside-in signaling induced by interactions with serum proteins adsorbed onto the PO<sub>4</sub>-containing matrix. This mechanism is supported by several pieces of evidence that we presented here: (1) Adsorbed serum proteins are required for attachment and spreading, (2) Attachment is partially mediated by  $\beta$ 1- and  $\beta$ 3-integrins, (3) Cells seeded on PO<sub>4</sub>-PEG hydrogels form well-defined focal complexes, (4) FAK signaling is required for osteogenic differentiation independent of cell shape. Our results are particularly important for researchers pursuing strategies aimed at simplifying biomaterials design since the influence of small molecules may not be easily predicted. While combinatorial approaches to screen for small molecules are often predicated on little knowledge of how materials may lead to changes in cell function, our results suggest that the dominating influence is likely due to differences in how proteins adsorb to these materials. Therefore, an exciting potential direction for these combinatorial approaches may be to identify specific influences on cell function, and how these materials adsorb and present proteins that are important for these changes. Ultimately, a better understanding of how biomaterials interact with proteins in the soluble environment will be important for both

guiding cell function and avoiding potential side effects associated with *in vivo* application.

### **3.6. Conclusions**

In this work we investigated the role of hydrogel chemistry on osteogenic differentiation of hMSCs. We demonstrate that the presence of phosphate functional groups promoted adsorption of ECM proteins, including fibronectin and collagen-1, while hMSC attachment was partially mediated via  $\beta 1$  and  $\beta 3$  integrins. Adsorbed ECM proteins directed hMSCs down the osteogenic lineage despite the absence of osteogenic supplements, as demonstrated by elevated alkaline phosphatase production and up-regulation of classic osteogenic markers. Combined with our previous study,<sup>15</sup> we demonstrated that attachment and cell shape alone were insufficient for promoting osteogenesis of hMSCs, but that FAK signaling was necessary for the influence of  $\text{PO}_4$ -PEG hydrogels on differentiation. This study provides evidence that adsorbed serum proteins can play a crucial role for the influence of synthetic biomaterials in guiding cell function, including PEG hydrogels which are designed to prevent non-specific adsorption. While the specific result reported here ( $\text{PO}_4$ -PEG hydrogel induction of osteogenic differentiation for hMSCs) is directly applicable to bone tissue engineering, our work is more generally important due to the broader implications associated with the mechanisms by which functionalized hydrogels guide cell function.

### **3.7 Acknowledgements**

We wish to thank Dr. Sarah Anderson for helpful discussions in designing the experiments. The authors gratefully acknowledge financial support from National Institute of Health (R01, DE016523) and the Howard Hughes Medical Institute.

### 3.8 References:

1. Pittenger MF, Mackay AM, Beck SC, Jaiswal RK, Douglas R, Mosca JD, et al. Multilineage potential of adult human mesenchymal stem cells. *Science*. 1999; 284:143-7.
2. Jaiswal N, Haynesworth SE, Caplan AI, Bruder SP. Osteogenic differentiation of purified, culture-expanded human mesenchymal stem cells in vitro. *J Cell Biochem*. 1997; 64:295-312.
3. Friedman MS, Long MW, Hankenson KD. Osteogenic differentiation of human mesenchymal stem cells is regulated by bone morphogenetic protein-6. *J Cell Biochem*. 2006; 98:538-54.
4. Cheng SL, Yang JW, Rifas L, Zhang SF, Avioli LV. Differentiation of human bone marrow osteogenic stromal cells in vitro: induction of the osteoblast phenotype by dexamethasone. *Endocrinology*. 1994; 134:277-86.
5. Aubin JE. Advances in the osteoblast lineage. *Biochemistry and cell biology = Biochimie et biologie cellulaire*. 1998; 76:899-910.
6. Dorozhkin SV. Bioceramics of calcium orthophosphates. *Biomaterials*. 2010. 31(7):1465–85.
7. Oh S, Oh N, Appleford M, Ong JL. Bioceramics for tissue engineering applications – A review. *Am. J. Biochem. & Biotechnol*. 2006. 2 (2): 49-56.
8. LeGeros RZ. Calcium Phosphate-based osteoinductive materials. *Chem Rev*. 2008, 108, 4742-4753.
9. Rezwan K, Chen QZ, Blaker JJ, Boccaccini AR. Biodegradable and bioactive porous polymer/inorganic composite scaffolds for bone tissue engineering. 2006, 27(18), 3413-3431.
10. Holland TA, Mikos AG. Review: Biodegradable polymeric scaffolds. Improvements in bone tissue engineering through controlled drug delivery. *Adv Biochem Engin/Biotechnol*. 2006, 102: 161-185.
11. Lin CC, Anseth KS. PEG hydrogels for the controlled release of biomolecules in regenerative medicine. 2009. 26(3), 631-643.
12. Zhu J. Bioactive modification of poly(ethylene glycol) hydrogels for tissue engineering. *Biomaterials*. 2010. 31(17), 4639-4656.

13. Yang F, Williams CG, Wang DA, Lee H, Manson PN, Elisseff J. The effect of incorporating RGD adhesive peptide in polyethylene glycol diacrylate hydrogel on osteogenesis of bone marrow stromal cells. *Biomaterials*. 2005. 26(30), 5991-81.
14. He X, Ma J, Jabbari E. Effect of grafting RGD and BMP-2 protein-derived peptides to a hydrogel substrate on osteogenic differentiation of marrow stromal cells. *Langmuir*. 2008. 24:12508:12516.
15. Benoit DS, Schwartz MP, Durney AR, Anseth KS. Small functional groups for controlled differentiation of hydrogel-encapsulated human mesenchymal stem cells. *Nat Mater*. 2008; 7:816-23.
16. Lutolf MP, Weber FE, Schmoekel HG, Schense JC, Kohler T, Muller T *et al*. Repair of bone defects using synthetic mimetics of collagenous extracellular matrices. *Nat Biotechnol*. 2003. 21: 513-518.
17. Khatiwala CB, Kim PD, Peyton SR, Putnam AJ. ECM compliance regulates osteogenesis by influencing MAPK signaling downstream of RhoA and ROCK. *J Bone Miner Res*. 2009. 24(5):886-98.
18. Parekh SH, Chatterjee K, Lin-Gibson S, Moore NM, Cicerone MT, Young MF, Simon CG Jr. Modulus-driven differentiation of marrow stromal cells in 3D scaffolds that is independent of myosin-based cytoskeleton tension. *Biomaterials*. 2011. 32(9):2256-64.
19. Curran JM, Chen R, Hunt JA. Controlling the phenotype and function of mesenchymal stem cells in vitro by adhesion to silane-modified clean glass surfaces. *Biomaterials*. 2005; 26:7057-67.
20. Curran JM, Chen R, Hunt JA. The guidance of human mesenchymal stem cell differentiation in vitro by controlled modifications to the cell substrate. *Biomaterials*. 2006; 27:4783-93.
21. Curran JM, Chen R, Hunt JA. Using silane modified surfaces to control the differentiation pathways of human mesenchymal stem cells. *Tissue Engineering*. 2006; 12:1015
22. Phillips JE, Petrie TA, Creighton FP, Garcia AJ. Human mesenchymal stem cell differentiation on self-assembled monolayers presenting different surface chemistries. *Acta Biomater*. 2010; 6:12-20.
23. Nuttelman CR, Tripodi MC, Anseth KS. Synthetic hydrogel niches that promote hMSC viability. *Matrix Biology*. 2005; 24:208-18.

24. Allen LT, Tosetto M, Miller IS, O'Connor DP, Penney SC, Lynch I, et al. Surface-induced changes in protein adsorption and implications for cellular phenotypic responses to surface interaction. *Biomaterials*. 2006; 27:3096-108.
25. Shen M, Horbett TA. The effects of surface chemistry and adsorbed proteins on monocyte/macrophage adhesion to chemically modified polystyrene surfaces. *J Biomed Mater Res*. 2001; 57:336-45.
26. Steele JG, Dalton BA, Johnson G, Underwood PA. Adsorption of fibronectin and vitronectin onto Primaria and tissue culture polystyrene and relationship to the mechanism of initial attachment of human vein endothelial cells and BHK-21 fibroblasts. *Biomaterials*. 1995; 16:1057-67.
27. Iuliano DJ, Saavedra SS, Truskey GA. Effect of the conformation and orientation of adsorbed fibronectin on endothelial cell spreading and the strength of adhesion. *J Biomed Mater Res*. 1993; 27:1103-13.
28. Keselowsky BG, Collard DM, Garcia AJ. Surface chemistry modulates fibronectin conformation and directs integrin binding and specificity to control cell adhesion. *J Biomed Mater Res A*. 2003; 66:247-59.
29. Keselowsky BG, Collard DM, Garcia AJ. Integrin binding specificity regulates biomaterial surface chemistry effects on cell differentiation. *Proc Natl Acad Sci U S A*. 2005; 102:5953-7.
30. Salaszyk RM, Klees RF, Williams WA, Boskey A, Plopper GE. Focal adhesion kinase signaling pathways regulate the osteogenic differentiation of human mesenchymal stem cells. *Experimental Cell Research*. 2007; 313:22-37.
31. Shekaran A, Garcia AJ. Extracellular matrix-mimetic adhesive biomaterials for bone repair. *J Biomed Mater Res A*. 2011; 96:261-72.
32. Mizuno M, Fujisawa R, Kuboki Y. Type I collagen-induced osteoblastic differentiation of bone-marrow cells mediated by collagen- alpha 2 beta 1 integrin interaction. *J Cell Physiol* 2000;184: 207–213.
33. Mizuno M, Kuboki Y. Osteoblast-related gene expression of bone marrow cells during the osteoblastic differentiation induced by type I collagen. *J Biochem* 2001;129:133–138.
34. Moursi AM, Globus RK, Damsky CH. Interactions between integrin receptors and fibronectin are required for calvarial osteoblast differentiation in vitro. *J Cell Sci* 1997;110(Pt 18):2187–2196.

35. Martino MM, Mochizuki M, Rothenfluh DA, Rempel SA, Hubbell JA, Barker TH. Controlling integrin specificity and stem cell differentiation in 2D and 3D environments through regulation of fibronectin domain stability. *Biomaterials*. 2009; 30:1089-97.
36. Salaszyk RM, Klees RF, Hughlock MK, Plopper GE. ERK signaling pathways regulate the osteogenic differentiation of human mesenchymal stem cells on collagen I and vitronectin. *Cell Communication and Adhesion*. 2004; 11:137-53.
37. Slack-Davis JK, Martin KH, Tilghman RW, Iwanicki M, Ung EJ, Autry C, et al. Cellular characterization of a novel focal adhesion kinase inhibitor. *J Biol Chem*. 2007; 282:14845-52.
38. Lutolf MP, Hubbell JA. Synthetic biomaterials as instructive extracellular microenvironments for morphogenesis in tissue engineering. *Nature biotechnology*. 2005; 23:47-55.
39. Davies MC, Alexander MR, Hook AL, Yang J, Mei Y, Taylor M, et al. High throughput surface characterization: A review of a new tool for screening prospective biomedical material arrays. *Journal of drug targeting*. 2010; 18:741-51.
40. Anderson DG, Levenberg S, Langer R. Nanoliter-scale synthesis of arrayed biomaterials and application to human embryonic stem cells. *Nat Biotech*. 2004; 22:863-6.
41. Flaim CJ, Teng D, Chien S, Bhatia SN. Combinatorial signaling microenvironments for studying stem cell fate. *Stem Cells Dev*. 2008; 17:29-39.
42. Peters A, Brey DM, Burdick JA. High-throughput and combinatorial technologies for tissue engineering applications. *Tissue engineering Part B, Reviews*. 2009; 15:225-39.
43. Simon CG, Jr., Lin-Gibson S. Combinatorial and high-throughput screening of biomaterials. *Adv Mater*. 2011; 23:369-87.
44. Place ES, Evans ND, Stevens MM. Complexity in biomaterials for tissue engineering. *Nat Mater*. 2009; 8:457-70.
45. McBeath R, Pirone DM, Nelson CM, Bhadriraju K, Chen CS. Cell Shape, Cytoskeletal Tension, and RhoA Regulate Stem Cell Lineage Commitment. *Developmental Cell*. 2004; 6:483-95.

46. Treiser MD, Yang EH, Gordonov S, Cohen DM, Androulakis IP, Kohn J, et al. Cytoskeleton-based forecasting of stem cell lineage fates. *Proceedings of the National Academy of Sciences*. 2010; 107:610-5.
47. Vogel W, Grünebach F, Messam CA, Kanz L, Brugger W, Bühring HJ. Heterogeneity among human bone marrow-derived mesenchymal stem cells and neural progenitor cells. *Haematologica*. 2003. 88(2), 126-33.
48. Javazon EH, Beggs KJ, Flake AW. Mesenchymal stem cells: paradoxes of passaging. *Exp Hematol*. 2004. 32(5): 414-25.
49. Meder F, Daberkow T, Treccani L, Wilhelm M, Schowalter M, Rosenauer A, Madler L, Rezwani K. Protein adsorption on colloidal alumina particles functionalized with amino, carboxyl, sulfonate and phosphate groups. *Acta Biomater*. 2012. 8 (3): 1221-1229.
50. Lin-Gibson S, Jones RL, Washburn NR, Horkay F. Structure-Property relationships of photopolymerizable poly(ethylene glycol) dimethacrylate hydrogels. *Macromolecules*. 2005, 38: 2897-2902.
51. Guerra NB, Gonzalez-Garcia C, Llopis V, Rodriguez-Hernandez JC, Moratal D, Rico P, et al. Subtle variations in polymer chemistry modulate substrate stiffness and fibronectin activity. *Soft Matter*. 2010; 6.
52. Rowlands AS, George PA, Cooper-White JJ. Directing osteogenic and myogenic differentiation of MSCs: interplay of stiffness and adhesive ligand presentation. *Am J Physiol Cell Physiol*. 2008; 295:C1037-44.
53. Elliott JT, Woodward JT, Umarji A, Mei Y, Tona A. The effect of surface chemistry on the formation of thin films of native fibrillar collagen. *Biomaterials*. 2007; 28:576-85.
54. Sherratt MJ, Bax DV, Chaudhry SS, Hodson N, Lu JR, Saravanapavan P, et al. Substrate chemistry influences the morphology and biological function of adsorbed extracellular matrix assemblies. *Biomaterials*. 2005; 26:7192-206.
55. Keselowsky BG, Collard DM, Garcia AJ. Surface chemistry modulates focal adhesion composition and signaling through changes in integrin binding. *Biomaterials*. 2004; 25:5947-54.
56. Popov C, Radic T, Haasters F, Prall WC, Aszodi A, Gullberg D, et al. Integrins  $\alpha 2\beta 1$  and  $\alpha 11\beta 1$  regulate the survival of mesenchymal stem cells on collagen I. *Cell Death and Dis*. 2011; 2:e186.



57. Lund AW, Stegemann JP, Plopper GE. Inhibition of ERK promotes collagen gel compaction and fibrillogenesis to amplify the osteogenesis of human mesenchymal stem cells in three-dimensional collagen I culture. *Stem Cells Dev.* 2009;18:331-41.
58. Boudreau NJ, Jones PL. Extracellular matrix and integrin signalling: the shape of things to come. *Biochem J.* 1999; 339:481-8.
59. Engler AJ, Sen S, Sweeney HL, Discher DE. Matrix elasticity directs stem cell lineage specification. *Cell.* 2006; 126(4):677-89.
60. Khatiwala CB, Peyton SR, Putnam AJ. Intrinsic mechanical properties of the extracellular matrix affect the behavior of pre-osteoblastic MC3T3-E1 cells. *Am J Physiol Cell Physiol.* 2006; 290:C1640-50.
61. Friedland JC, Lee MH, Boettinger D. Mechanically activated integrin switch controls  $\alpha 5\beta 1$  function. *Science.* 2009; 323: 642-644.

## CHAPTER 4

### **$\alpha 5$ integrin priming hydrogels to study the interplay of substrate elasticity and ligand concentration on osteogenic differentiation of hMSCs via $\alpha 5\beta 1$ integrin signaling**

---

#### **4.1 Introduction**

*In vitro* osteogenic differentiation program of hMSCs is achieved by dosing with soluble cues such as dexamethasone,  $\beta$ -glycerol phosphate etc. and by insoluble cues presented by ECM *in vivo*. Significant progress has been made in understanding the role of the soluble cues and the signaling pathways initiated upon their uptake or binding to cell receptors. For example, upon dosing with dexamethasone, hMSCs upregulate integrin expression<sup>1-3</sup> and signal expression of CBFA1 driving osteogenic differentiation in hMSCs. There is growing interest to study and understand the role of insoluble cues on the osteogenic differentiation program of hMSCs. Integrin signaling is one of the important signaling mechanisms originating from ECM and several studies have implicated their role in maintaining the survival,<sup>4</sup> differentiation<sup>2,5</sup> and migration<sup>6,7</sup> in hMSCs. For example,  $\alpha 5\beta 1$  integrin has been shown to play an important role in hMSC migration, osteogenic differentiation while upregulating  $\alpha V\beta 3$  integrin negatively regulates their osteogenic differentiation. Integrins initiate intracellular biochemical pathways upon binding to their ligands and the dynamics of their signaling is highly dependent on the biophysical properties of the underlying substrate that directly affect their binding and engagement. Also, several studies have demonstrated that the

biophysical properties directly influence differentiation program of hMSCs via ROCK/Rho pathways that converge to upregulate expression of several genes.<sup>8,9</sup> For example, hMSCs cultured on poly(acrylamide) hydrogels with high substrate elasticity upregulated expression of osteogenic related gene CBFA1 via Rho/ROCK dependent pathways without the need for any soluble cues.<sup>8</sup> Integrins act as pivot points through which cells sense the mechanical properties of the underlying substrate and hence it is crucial to study the interplay of substrate elasticity on integrin signaling in hMSCs.

Hydrogels have emerged as an important class of biomaterials for use as *in vitro* culture platforms to conduct systematic studies to decipher the biological role of insoluble cues as their chemistry provides avenues to tune biophysical properties and biochemical functionalization. Towards this end, PEG hydrogels formed via thiol-ene photopolymerizations offer several advantages as they form nearly ideal uniform network structure and allow facile covalent functionalization of any cysteine containing biochemical cues. Their elastic modulus can be readily tuned by varying the monomer formulation allowing researchers to achieve independent control of the material elasticity and the biochemical signal. Similar hydrogels have been used to present adhesive ligands such as small peptide motifs,<sup>10</sup> tether dexamethasone<sup>11</sup> to serve as bioactive culture platforms as well as delivery platforms for controlling the fate of hMSCs.

Osteogenic capacity of hMSCs is highly regulated by several integrins.<sup>2,5,12,13</sup> Studies done by blocking integrin function via antibodies or siRNA knockdown have demonstrated that  $\alpha 5\beta 1$ ,<sup>2,5</sup>  $\alpha 2\beta 1$ ,<sup>4</sup>  $\alpha 3\beta 1$ <sup>12</sup> integrins promote osteogenesis while  $\alpha V\beta 3$ <sup>5,14</sup> integrin lowers ALP activity and reduces matrix mineralization. In this study, we are interested in understanding the role of  $\alpha 5\beta 1$  integrin in promoting osteogenesis in

hMSCs. Recent studies by Hamidouche *et al.*<sup>2,3</sup> have demonstrated that dexamethasone induced osteogenic differentiation in hMSCs is mediated via  $\alpha 5\beta 1$  integrin as evidenced by abrogation of the ALP activity and osteogenic gene expression upon silencing  $\alpha 5\beta 1$  integrin expression with siRNA. Also, hMSCs underwent osteogenesis upon forced induction of  $\alpha 5\beta 1$  integrin without the need for dexamethasone indicating the importance of  $\alpha 5\beta 1$  integrin signaling pathway in osteogenic differentiation in hMSCs. Further, fibronectin fragments which allowed for specific interaction with  $\alpha 5\beta 1$  integrin upregulated ALP activity and osteogenic gene expression demonstrating that signaling  $\alpha 5\beta 1$  integrin specifically promotes osteogenic capacity in hMSCs.<sup>5</sup> Owing to the importance of  $\alpha 5\beta 1$  integrin signaling during osteogenic differentiation of hMSCs, we sought to further understand the interplay of  $\alpha 5\beta 1$  integrin signaling and substrate elasticity on osteogenic differentiation of hMSCs. To realize this goal, we utilize a peptide-functionalized PEG hydrogels that allows binding and priming of  $\alpha 5\beta 1$  integrin that allows to conduct systematic studies to better understand the role of  $\alpha 5\beta 1$  integrin signaling on osteogenic differentiation of hMSCs.

The non-natural cyclic peptide sequence, Cys-Arg-Arg-Glu-Thr-Ala-Trp-Ala-Cys (CRRETAWAC) has been shown to bind  $\alpha 5\beta 1$  integrin with very high affinity and specificity ( $IC_{50}$  for  $\alpha 5\beta 1$  integrin binding is  $0.01\mu M$  and for  $\alpha V\beta 3$  integrin is  $>1000\mu M$ ).<sup>15</sup> Epitope mapping studies have revealed that the high specificity and affinity is due to the interaction of Arg-Arg-Glu motif with  $\beta 1$  integrin subunit and the strong hydrophobic interaction of Trp residue with the  $\alpha 5$  subunit.<sup>16-18</sup> The resulting conformational changes of  $\alpha 5\beta 1$  integrin upon binding to the peptide activates the

intracellular domain of the integrin further triggering downstream signaling events originating from the integrin.<sup>19</sup>

In the present study we report synthesis of cyl(RRETAWA) functionalized PEG hydrogels via thiol-ene photopolymerizations that allows attachment of hMSCs specifically via  $\alpha 5$  integrin and study the interplay of level  $\alpha 5$  integrin priming and substrate elasticity in driving osteogenic differentiation in hMSCs. Our results demonstrate that substrate stiffness and ligand concentration plays a significant role on the interaction of hMSCs with the peptide-functionalized gels. Stiffer substrates allowed hMSCs to interact with the peptides much more robustly evident by their ability to form well developed focal adhesions even at lower peptide concentrations while softer substrates required higher ligand concentration to form stable focal adhesions. Our results also suggest that priming of  $\alpha 5$  integrin alone is not sufficient and higher substrate elasticity is required for inducing osteogenic differentiation in hMSCs.

## **4.2 Materials and Methods**

All materials are purchased from Sigma unless otherwise mentioned

### **4.2.1 Cell culture**

hMSCs were isolated from bone marrow (Lonza) and cultured in growth media (low glucose Dulbecco's Modified Eagle Medium (DMEM, Gibco) supplemented with 10% fetal bovine serum (Gibco), 1% Penicillin/Streptomycin (Gibco), and 0.2% Fungizone (Gibco)). hMSCs at passage three were used in all the studies.

#### 4.2.2 Synthesis of cyl(RRETAWA) and CRDGS:

Peptide sequences (Ac-CAhxK(Alloc)RRETAWAE(ODmab) , H-CRDGS-NH<sub>2</sub>, H-CRGDS-NH<sub>2</sub>) were synthesized through standard Fmoc solid-phase synthesis method using 2-(1H-benzotriazole-1-yl)-1,1,3,3-tetramethyluronium hexafluorophosphate/N-hydroxybenzotriazole (HBTU/HOBt) activation using Tribute solid-phase peptide synthesizer. The N-terminus amine of the H-CAhxK(Alloc)RRETAWAE(ODmab) was acetyl capped (resulting in Ac-CAhxK(Alloc)RRETAWAE(ODmab) peptide sequence) and on-resin cyclization was performed described in Section 4.3.5. Peptides H-CRDGS-NH<sub>2</sub> and H-CRGDS-NH<sub>2</sub> was cleaved from resin with trifluoroacetic acid/triisopropyl silane/water/phenol (94:2.5:2.5:1) mixture and precipitated and washed (2x) in cold ethyl ether. Precipitated peptide was desiccated for overnight and used without any further purification.

Peptide sequence, Ac-CAhxK(Alloc)RRETAWAE(ODmab), was treated with 2% hydrazine in DMF (3x) to cleave ODmab protecting group. Resin was then thoroughly washed in DMF. Resin was then washed in DCM and allowed to swell for overnight. The Alloc deprotection was carried out by treating resin with a solution of 0.1 eqv. Tetrakis(triphenylphosphine)palladium(0) (Pd(PPh<sub>3</sub>)<sub>4</sub>, Sigma) and 24 eqv. phenyl silane (C<sub>6</sub>H<sub>8</sub>Si, Sigma) in DCM for 10 min and washed in DCM (4x). The Alloc deprotection step was repeated three times to ensure complete deprotection. Alloc deprotection of amines was verified by positive Kaiser test. The resin was washed and swelled in DMF for overnight. On resin cyclization of the peptide was conducted in 1 eq. of HBTU in DMF for overnight. Negative Kaiser test was used to monitor the disappearance of amines due to cyclization of the peptide. Peptide was cleaved from resin with

trifluoroacetic acid/triisopropyl silane/water/phenol (94:2.5:2.5:1) mixture and precipitated and washed (2x) in cold ethyl ether. Precipitated peptide was desiccated for overnight and purified using HPLC, lyophilized and stored at -20 C until further use. The required HPLC fraction was identified using matrix assisted laser desorption/ionization (MALDI).

#### **4.2.3 Synthesis of PEG-Norbornene (PEG-N):**

Multiarm poly(ethylene glycol) (8 arm  $M_n = 10000$  Da and 4 arm  $M_n = 20000$  Da) norbornene was synthesized as described previously. Briefly, poly(ethylene glycol) amine (JenKem, USA) was dissolved in DCM and reacted with 2 eq. norbornene carboxylic acid at 50 C for overnight in the presence of 0.5 eq. 4-dimethylaminopyridine (DMAP) and 1eq. N,N'-Diisopropylcarbodiimide (DIC). The reaction mixture was then precipitated slowly in cold ethyl ether dropwise. The product was desiccated for overnight and dialysed against water using 2000 Da molecular weight cutoff membrane for 24 h. The product was lyophilized and stored at -20 C until further use. Proton NMR was used to verify successful functionalization and >90% of hydroxyl groups were found to be functionalized with norbornene.

#### **4.2.4. Rheological characterization of peptide hydrogels**

Gels were formed between two glass slides separated by 1 mm gasket under conditions described in Section 4.3.2 and allowed to swell in PBS for 48 h. 8 mm cylindrical disks were then cut out and their shear modulus was measured by conducting frequency sweep from 1-100 rad/s at 3% strain rate using Rheometer. Strain rate chosen was in the linear visco-elastic regime. The results are reported as average measurements

of three independent gels. Young's modulus ( $E$ ) of gels was then calculated from the shear modulus ( $G$ ) using the following equation from rubber elasticity theory,

$$E = 2(1 + \nu)G \quad (1)$$

Where,  $\nu$  is the Poisson's ratio and is taken to be 0.5 for an incompressible material.

#### **4.2.5 Preparation of thiolated glass coverslips**

Heat treated glass cover slips were dipped in a solution of mercaptopropyltriethoxy silane in ethanol for 5-10 min. Coated glass cover slips were then cleaned with ethanol and water (2x) to remove any excess silane and dried in air. Air dried cover slips were then baked at 80 C for atleast 1 h and stored at 4 C until further use.

#### **4.2.6 Preparation of peptide functionalized hydrogels for cell culture:**

For the preparation of stiff hydrogels, eight-armed PEG-N (MW: 10,000), PEG-diSH (MW: 2000) and 1mM of pendant monothiol peptides were dissolved in sterile PBS to yield a final monomer mixture of 80 mM [ene], 79 mM [linker thiol] and 1 mM [monothiol peptide]. For preparation of soft hydrogel, four-armed PEG-N (MW: 20000), PEG-diSH (MW: 2000) and 1 mM pendant monothiol peptides were dissolved in sterile PBS to yield a final monomer mixture of 16 mM [ene], 15 mM [linkerthiol] and 1mM [monothiol peptides]. To these monomer mixtures, photo-initiator lithium phenyl-2,4,6-trimethylbenzoylphosphinate (LAP) was added at a final concentration of 0.05 wt%. The 1mM pendant monothiol peptide mixture consisted of either 0.1 mM of cyl(RRETAWA) and 0.9 mM CRDGS or 1mM of cyl(RRETAWA).

120  $\mu$ m thick hydrogels were formed on thiolated glass coverslips by exposing the monomer mixture to  $\sim 10$  mW/cm<sup>2</sup>, 365 nm light for 5 min. Gels were swelled in PBS for atleast 48 h before and sterilized under UV for 12 h before cell seeding.



#### **4.2.7 Integrin blocking experiments**

hMSCs were incubated with antibody solutions containing antibodies against  $\alpha 5$  (Abcam),  $\alpha V\beta 3$  (Abcam) integrins or IgG (Isotype control, Sigma, M5284) in serum-free media for 30 min and seeded onto 1 mM cyl(RRETAWA) stiff gels (see section 4.4.3 for description of stiff gels) in serum free media at  $5 \times 10^3$  cells/cm<sup>2</sup> density. Integrin blocked hMSCs were allowed to attach to the gels for 12 h, washed with PBS to removed loosely attached cells and stained with calcein AM for live cells. Stained hMSCs were imaged using an epifluorescence microscope and the number of attached cells were counted using ImageJ software.

#### **4.2.8 Focal adhesion staining and determination of cell area, aspect ratio and focal adhesion area**

Focal adhesion staining was performed on hMSCs attached to the gels ( $5 \times 10^3$  cells/cm<sup>2</sup> seeding density) using rhodamine phalloidin (Life Technologies) for f-actin and mouse anti-vinculin antibody (Abcam). Cell density was chosen to avoid excessive cell-cell contacts after hMSC attachment to gels. Cells were counterstained with 4,6-diamidino-2-phenylindole (DAPI, Invitrogen, 300nM) for nuclei and stored in PBS at 4C until imaged with a Zeiss confocal microscope.

hMSC shape parameters were quantified by immunostaining with rhodamine phalloidin (Molecular Probes, R415, 1:200 dilution). Samples were imaged using a confocal microscope (Zeiss, LSM 710), and the RGB images were converted into binary images and analyzed by an in-built ‘analyze particles’ macro in ImageJ that automatically generates an average area per cell and aspect ratio. A total of nine images per condition were analyzed.

Focal adhesion area was quantified by analysis of images obtained immunostaining for vinculin as described above. Immunostained samples were imaged under similar settings using 40x objective of Zeiss 710 confocal microscope. Obtained images were processed using ImageJ for background normalization using FFT bandpass filter and converted to binary images and morphometric analysis of focal adhesions were conducted by analyze particles plugin. A total of nine images per condition were analyzed and the average focal adhesion area is reported.

#### **4.2.9 Alkaline phosphatase (ALP) production of hMSCs on peptide functionalized gels**

ALP production was measured using an assay based on the change in absorbance of *o*-nitrophenol (ALP substrate, Invitrogen) as it is enzymatically cleaved by ALP. Cells were removed from culture, washed in PBS and lysed in 50  $\mu$ l RIPA buffer (Invitrogen) for 15 min with gentle shaking. The sample solutions were diluted with 50  $\mu$ l of PBS. 50  $\mu$ l of the sample solution was then mixed with 50  $\mu$ l of ALP substrate, and the absorbance of the solution at 405 nm was measured at 1-minute intervals ten times with a plate reader (Biotek). ALP activity levels were calculated as the slope of the increase in absorbance at 405 nm with time. Lysed solution was used to measure total DNA content using Picogreen assay (Invitrogen). ALP activity levels were normalized to total DNA content ( $\mu$ g) and reported as relative to day 1 normalized ALP activity.

## 4.3 Results

### 4.3.1 Synthesis and characterization of $\alpha 5$ binding peptide

Kouvinen *et al.* have shown that cyclization of RRETAWA peptide results in significantly higher binding and priming of  $\alpha 5$  integrin.<sup>15</sup> The reported peptide sequence was modified to include side chain protected lysine(Alloc) and glutamic acid(ODmab) residues at N- and C- terminus respectively to allow for cyclization via lactam bridge formation between side chain amine of lysine and side chain carboxylic acid of glutamic acid. Thiol containing cysteine was also introduced at the N-terminus to tether the peptide into the network during the gel formation. Also, to allow for higher accessibility for the cells an alkyl spacer, amino-hexanoic acid (Ahx), was included resulting in the peptide sequence Cys-Ahx-Lys(Alloc)-Arg-Arg-Glu-Thr-Ala-Trp-Ala-Glu(ODmab). Cyclization of peptide was conducted as detailed in section 4.3.2 and verified via MALDI spectroscopy. Figure 4.1 details the synthesis scheme for synthesis of cyl(RRETAWA) peptide.

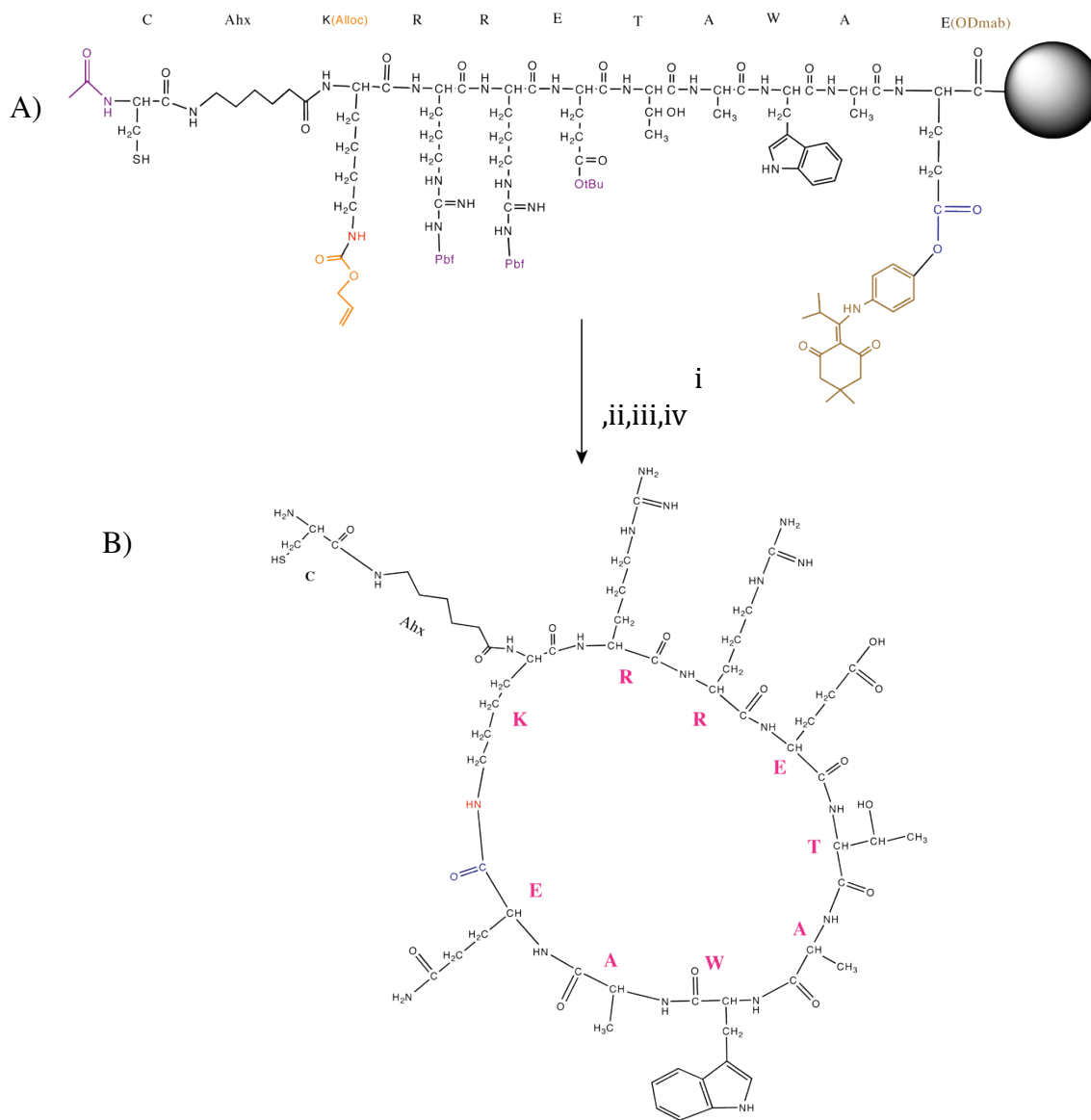


**Figure 4.1: Synthesis of cyl(RRETAWA) peptide (B) via lactam bridge formation.** On-resin cyclization of (A) CAhxK(Alloc)RRETAWAE(ODmab). (i-iv) Steps involving lactam bridge formation. i) Deprotection of ODmab in 2% Hydrazine in DMF, ii) Deprotection of Alloc in 0.1 eq Pd(PPh<sub>3</sub>), in DCM, iii) HOBt/ HBTU coupling to form the lactam bridge, iv) Peptide cleavage from resin in THF, TIPS, phenol.

### **4.3.2 Soluble delivery of Cyl(RRETAWA) induces osteogenic differentiation in hMSCs**

To assess the effect of cyl(RRETAWA) on osteogenic differentiation, the peptide was mixed with the growth media and delivered solubly to hMSCs cultured on tissue culture polystyrene (TCPS) at a dosage of 10 and 100  $\mu\text{g/ml}$ . Figure 4.2 shows that the normalized ALP activity of hMSCs was significantly up-regulated at day 7 and 14 compared to the control. Also, increasing the dosage 10 fold (i.e. from 10  $\mu\text{g/ml}$  to 100  $\mu\text{g/ml}$ ) significantly increased the ALP activity indicating that the effect was dosage dependent. ALP activity results demonstrate that priming  $\alpha 5$  integrin via the cyl(RRETAWA) peptide induced ALP production indicating osteogenic differentiation of hMSCs.

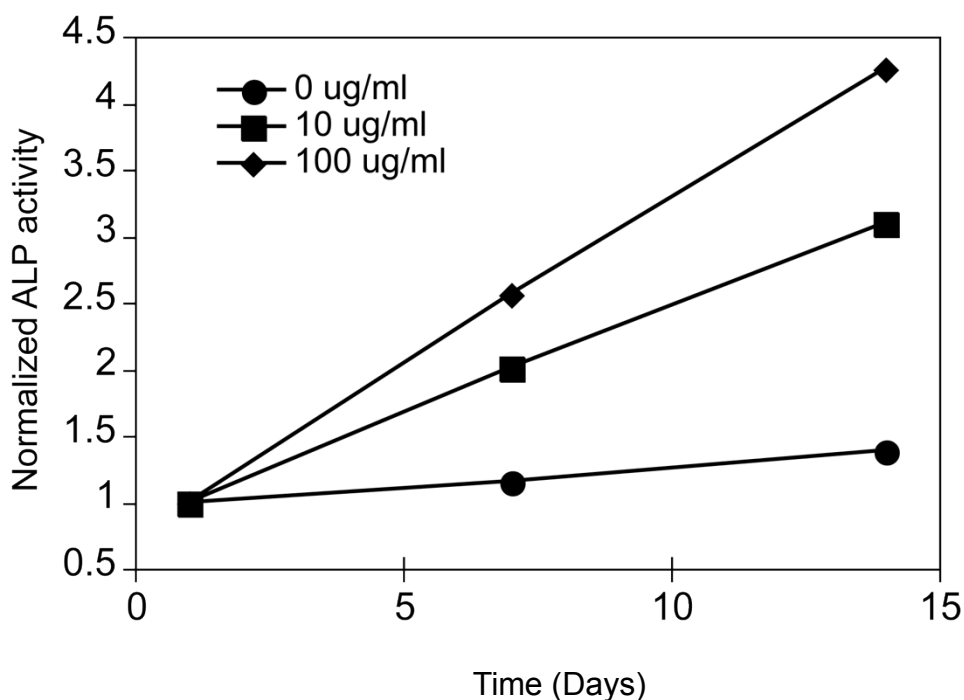


**Figure 4.2: Priming  $\alpha 5$  integrin induces osteogenic differentiation in hMSCs.** Figure shows the ALP activity of hMSCs at day 7 and 14 cultured on TCPS in growth media supplemented with 10  $\mu\text{g}/\text{ml}$  (●) or 100  $\mu\text{g}/\text{ml}$  (■) cyl(RRETAWA) peptide. Normalized ALP activity of hMSCs cultured on TCPS in osteogenic media (◆) without the peptide is also included as positive control. Normalized ALP activity was calculated by normalizing the measured ALP activity to that of day 1.

### 4.3.3 hMSCs bind to cyl(RRETAWA) gels via $\alpha 5$ integrin

Nature of hMSC binding to cyl(RRETAWA) functionalized gels was assessed by studying the effect of blocking the  $\alpha 5$  integrin on their attachment to 1 mM cyl(RRETAWA) gels. As shown in Figure 4.3A, the attachment of hMSCs to cyl(RRETAWA) gels was reduced to  $\sim 20\%$  of control upon blocking the  $\alpha 5$  integrin before seeding. To verify that hMSCs selectively utilize  $\alpha 5$  integrin in binding to these gels, hMSCs were blocked with  $\alpha V\beta 3$  integrin and their attachment to the

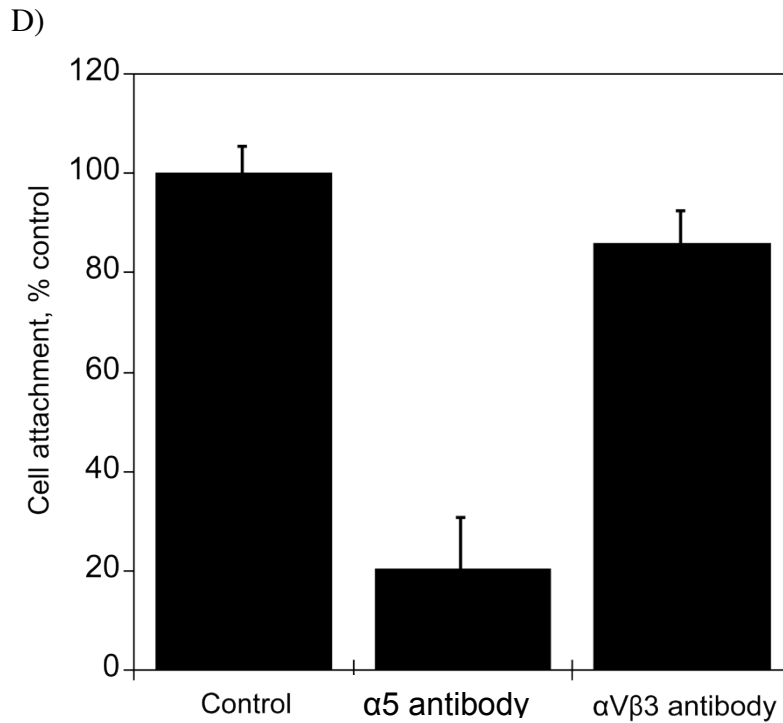
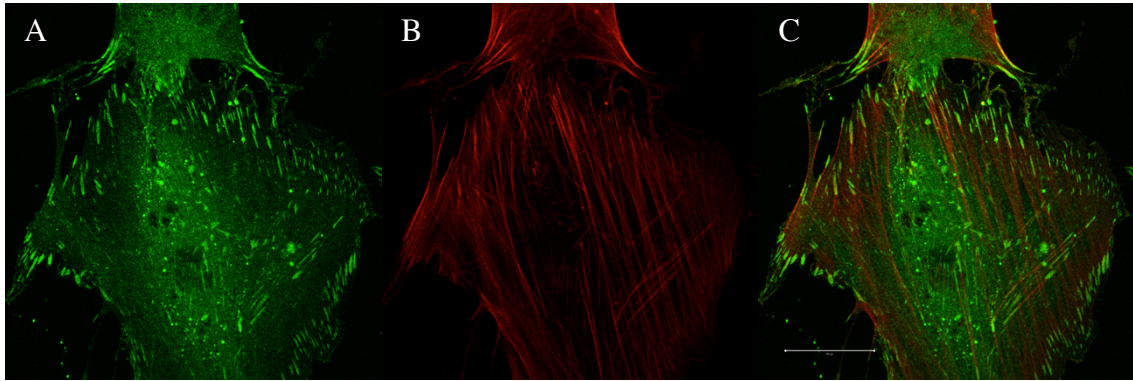


**Figure 4.3. Interaction of hMSCs to cyl(RRETAWA) occurs via  $\alpha 5$  integrin.** A-C: Immunostaining for  $\alpha 5$  integrin (green, A,C), f-actin (red, B,C) and combined (C) in hMSCs cultured on 1mM cyl(RRETAWA) PEG gels. Scale bar = 100  $\mu$ m. D) Effect of blocking  $\alpha 5$  integrin and  $\alpha V\beta 3$  on hMSC adhesion to  $\alpha 5$  integrin specific cyl(RRETAWA) gels. hMSCs were incubated with corresponding antibodies for 30 mins to allow for binding of the antibodies to integrins and seeded onto 1 mM cyl(RRETAWA) gels and number of hMSCs that remain attached were measured and reported as percentage compared to the control. Isotype antibody was used as a control antibody.

cyl(RRETAWA) gels was tested. As shown in Figure 4.3A, ~85% of the blocked hMSCs remained attached to the gels demonstrating that blocking  $\alpha V\beta 3$  integrin did not have a significant effect on hMSCs binding. Figure 4.3B-D shows immunostaining for  $\alpha 5$  (green) integrin and f-actin cytoskeleton (red) in hMSCs seeded onto cyl(RRETAWA) gels. Images clearly demonstrate localization of  $\alpha 5$  integrin as dash shaped structures at the tips of the actin fibers. These results taken together demonstrate that the hMSCs bind to the cyl(RRETAWA) gels selectively via  $\alpha 5$  integrin.

#### **4.3.4 Effect of substrate elasticity and peptide concentration on hMSC adhesion to cyl(RRETAWA) gels**

hMSCs have been shown to be sensitive to the substrate elasticity and several studies have implicated the role of mechanotransduction in determining the differentiation pathway of hMSCs. In this study, we are interested in studying the role of substrate elasticity and ligand concentration independently on hMSC fate on cyl(RRETAWA) functionalized gels. Monomer formulations were designed to form soft and stiff substrates that can be functionalized with 0.1 and 1 mM cyl(RRETAWA). Table 4.1 lists the monomer formulations used to form soft and stiff gels and their Young's modulus. Non-cell adhesive peptide, CRDGS (scrambled version of RGD), was included in the monomer formulations as listed in Table 2 to maintain the total thiol:ene functional group at 1:1. The Young's modulus of soft gels used in this study falls in the range that is not conducive for hMSC osteogenic differentiation, while the modulus of stiff gels was shown to be conducive for hMSCs osteogenic differentiation.



**Table 4.1:** Macromolecular monomer compositions for the preparation of cyl(RRETAWA) functionalized PEG gels used in the study to form soft and stiff gels and their corresponding modulus.

PEG-N MW	In-text description	[Ene] mM	Cyl(RRETAWA) mM	CRDGS mM	[Linker peptide thiol] mM	Young's Modulus, E, kPa
20 kDa, 4 arm	Soft	16	0.1	0.9	15	~2.5
20 kDa, 4 arm	Soft	16	1	0	15	~2.7
10 kDa, 8 arm	Stiff	80	0.1	0.9	79	~22
10 kDa, 8 arm	Stiff	80	0.1	0.9	79	~25

Initially, we assessed the effect of substrate elasticity and ligand concentration on hMSC adhesion by measuring the cell attachment density, cell shape parameters (area and aspect ratio) and focal adhesion formation. Figure 4.4A shows the hMSC attachment density to soft and stiff cyl(RRETAWA) gels as a function of peptide concentration. hMSC attachment was significantly higher on stiffer substrates as compared to the softer ones irrespective of the ligand concentration. Also, at both the substrate elasticities higher concentration allowed higher hMSCs attachment and interestingly the difference was highest on the stiff gels. Figure 4.4B,C shows the cell area and aspect ratio of attached hMSCs respectively. Significantly higher cell area and similar aspect ratio on stiff gels compared to soft gels demonstrates that higher stiffness allowed much higher spreading of hMSCs. At a ligand concentration of 1 mM, cell area was increased 4 fold from ~5000  $\mu\text{m}^2$  on soft to ~20000  $\mu\text{m}^2$  on stiff gels. Interestingly, increasing the ligand concentration on stiff gels significantly increased the cell spreading area without affecting the aspect ratio and only marginally on soft gels. To assess the nature of focal adhesions formed in hMSCs on these gels, immunostaining for vinculin and f-actin formation (red) was

conducted and resulting images are shown in Figure 4.5A-L. Images clearly demonstrate that, on stiffer gels, hMSCs form prominent focal adhesions and well developed actin cytoskeleton as compared to soft gels. On soft gels hMSCs formed prominent focal adhesions and developed actin fibers only at the 1 mM cyl(RRETAWA) while at lower concentration hMSC did not developed good cytoskeleton evident by evident by diffused vinculin (demonstrating no focal adhesion formation) and f-actin staining. On stiff gels, hMSCs formed well-developed actin fibers and prominent dash shaped focal adhesions on both 0.1 and 1 mM peptide concentrations. Qualitatively, there was no difference in actin fiber organization on stiff gels at both concentrations. Upon binding to their corresponding ligands, integrins present on the cell surface undergo clustering and form dash shaped focal adhesions which act as a scaffold for recruitment of several signaling proteins including focal adhesion kinase (FAK). Given the importance of FAK signaling in osteogenic differentiation of hMSCs demonstrated by previous studies and our results presented in chapter 3, we quantified the area of focal adhesions by immunostaining for vinculin in hMSCs on soft and stiff gels at 0.1 and 1 mM peptide concentrations. As shown in Figure 4.6, hMSCs developed larger focal adhesions on stiff gels compared to soft gels. On stiff gels, hMSCs developed ~3 fold larger focal adhesions at 1 mM as compared to 0.1 mM indicating that the interaction of hMSCs with the higher ligand concentration allowed for much larger focal adhesion formation. On soft gels, hMSCs developed small (compared to stiff gels) but prominent focal adhesions indicating that hMSCs can form focal adhesions but need higher ligand concentration to form stable focal adhesions on the softer substrate.

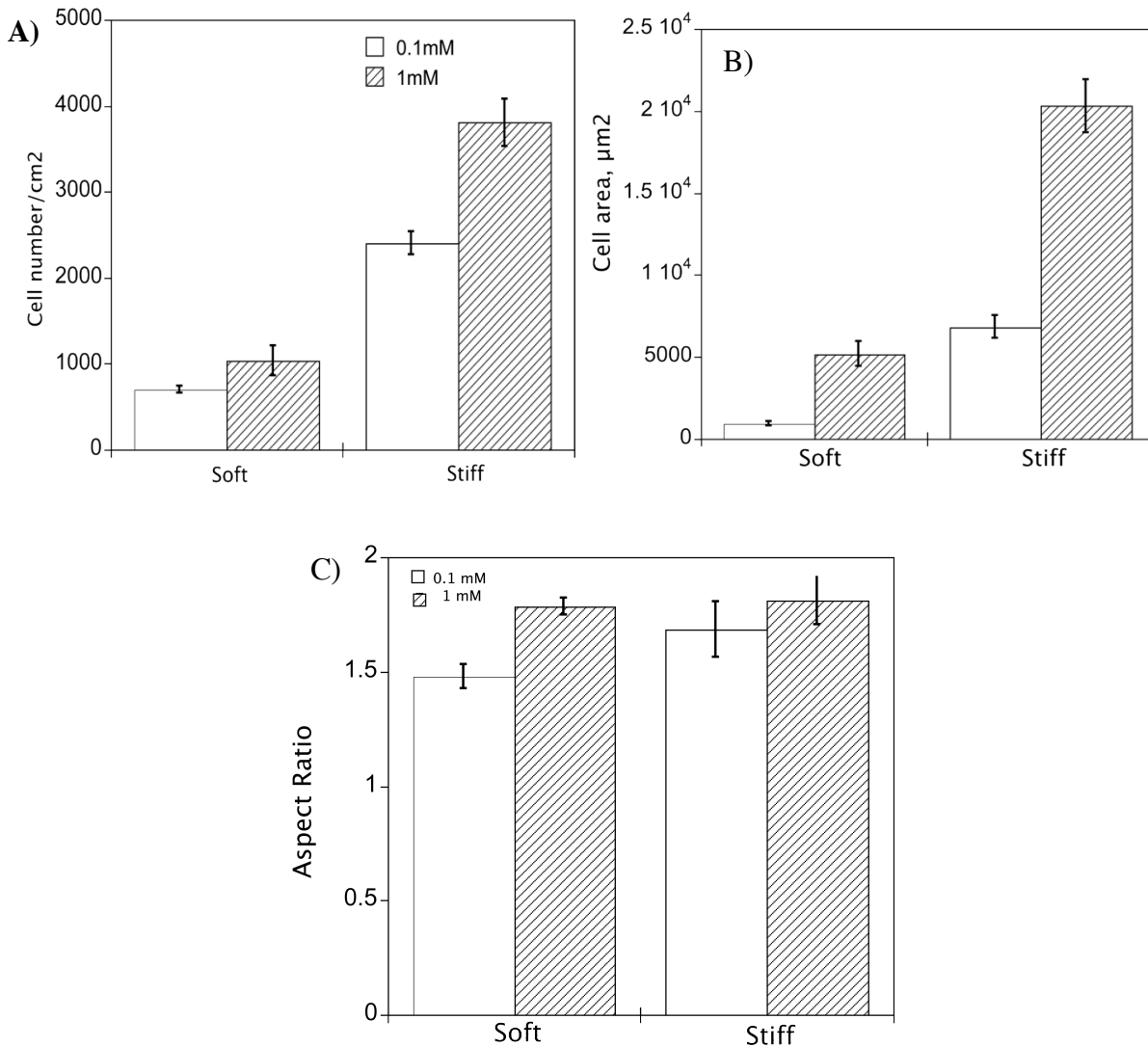


**Figure 4.4: Effect of substrate elasticity and ligand concentration on hMSC adhesion to cyl(RRETAWA) gels.** A) Cell adhesion density B) Cell area C) Aspect ratio of hMSCs on soft and stiff gels at 0.1 and 1 mM cyl(RRETAWA) concentration. hMSC attachment is dependent on both substrate elasticity and ligand concentration. Stiff gels supported significantly higher cell attachment at both the concentrations studied. Cell area and aspect area results demonstrate that hMSCs show well-spread morphology on stiffer substrates.

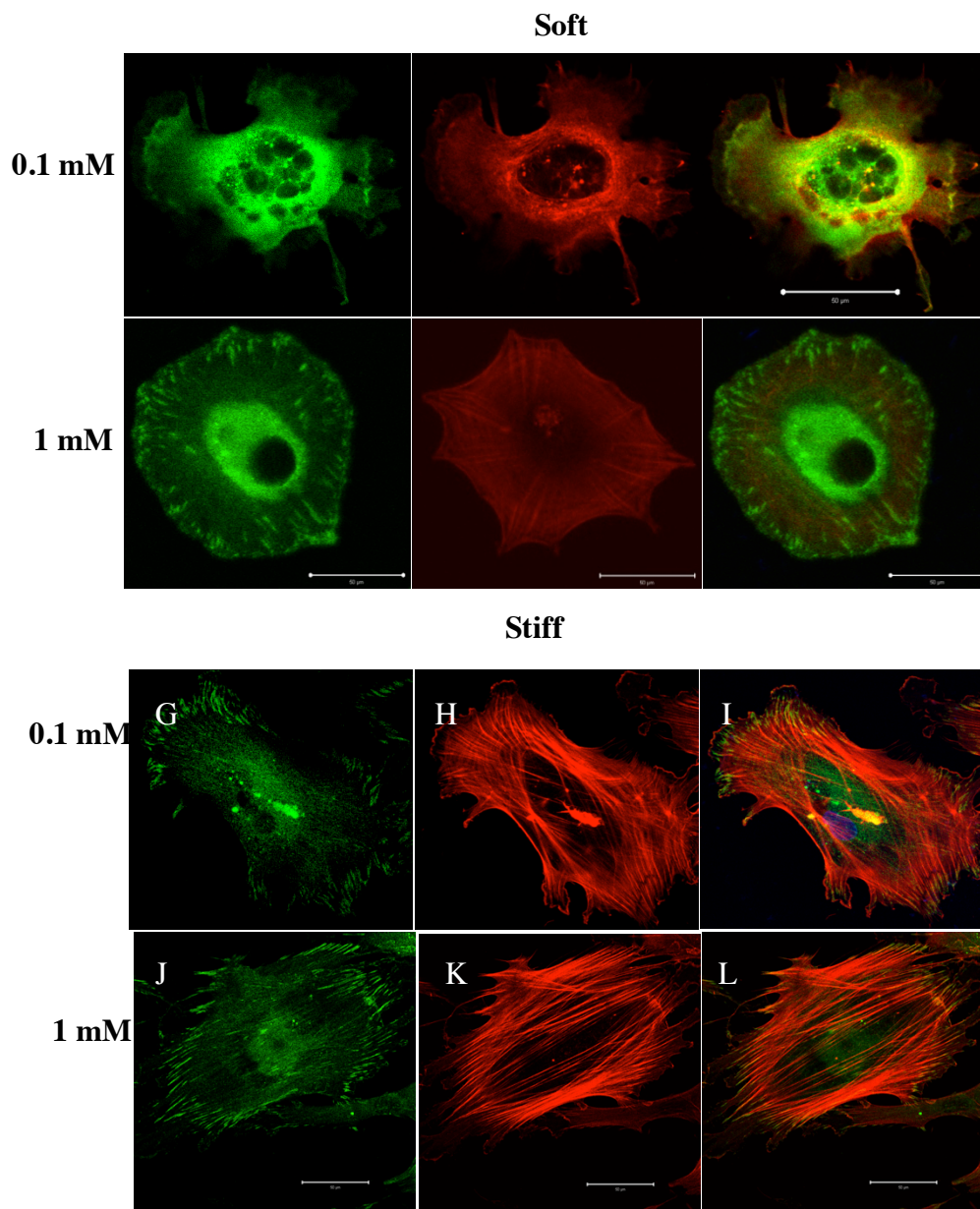


**Figure 4.5** A-L) Immunostaining for focal adhesions (vinculin, green A,D,G,J), f-actin (red, B,E,H,K) and combined (C,F,I,L) of hMSCs on soft (A-F) and stiff (G-L) gels at 0.1 mM (A-C, G-I) and 1 mM (D-F, J-L) cyl(RRETAWA) (ligand). hMSCs showed diffused f-actin and did not form any focal adhesions on soft gels at 0.1 mM ligand concentration and poor organization of f-actin and small focal adhesions at 1mM peptide concentration. hMSCs formed well developed f-actin organization on stiff gels at both the concentrations while highly prominent focal adhesions were only formed at 1mM peptide concentration. Scale bar = 50  $\mu$ m.

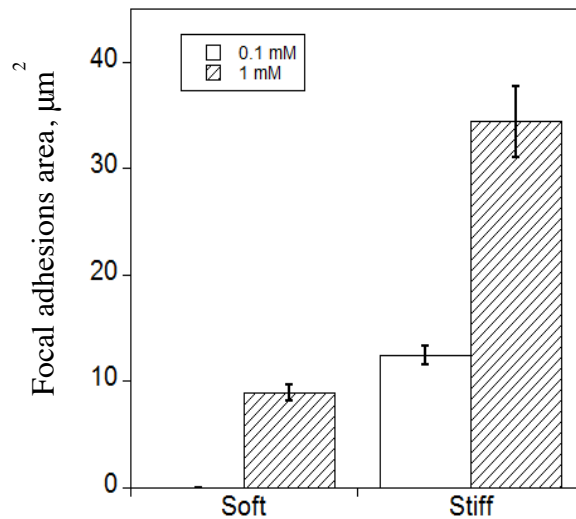


**Figure 4.6.** Effect of substrate elasticity and cyl(RRETAWA) (ligand) concentration on focal adhesion area. Average area of focal adhesions formed by hMSCs on soft and stiffer substrates at 0.1 and 1 mM ligand concentrations were measured using ImageJ as described in Methods section. hMSCs developed significantly larger focal adhesions on stiff gels at 1 mM compared to 0.1 mM ligand concentration. On softer substrates hMSCs formed small but significantly larger focal adhesions only at 1mM ligand concentrations.

#### 4.3.5 Osteogenic differentiation of hMSCs on cyl(RRETAWA) functionalized gels

To test the osteogenic differentiation of hMSCs on cyl(RRETAWA) functionalized gels, we measured ALP activity of hMSCs on stiff and soft gels at 0.1 and 1 mM peptide concentration. Figure 4.7 shows the normalized ALP activity of hMSCs relative to day 1 on these gels in growth media. ALP activity of hMSCs on TCPS grown in growth media and osteogenic media is also included as negative and positive control, respectively. The ALP activity of hMSCs at day 7 and 14 grown on soft gels was found to be similar to negative control irrespective of the ligand concentration indicating that osteogenesis was not induced in hMSCs on softer gels. hMSCs cultured on stiff gels significantly upregulated ALP activity to ~ 4 at day 7 and to ~3.5 at day 14 on 1 mM cyl(RRETAWA) gels. Interestingly, ALP activity on 0.1 mM stiff gels was increased

only slightly to around ~2.5 by day 7 and day 14 significantly higher than the negative control. Our results indicate that substrate stiffness plays a significant role in upregulation of ALP activity induced by  $\alpha 5\beta 1$  signaling in hMSCs.

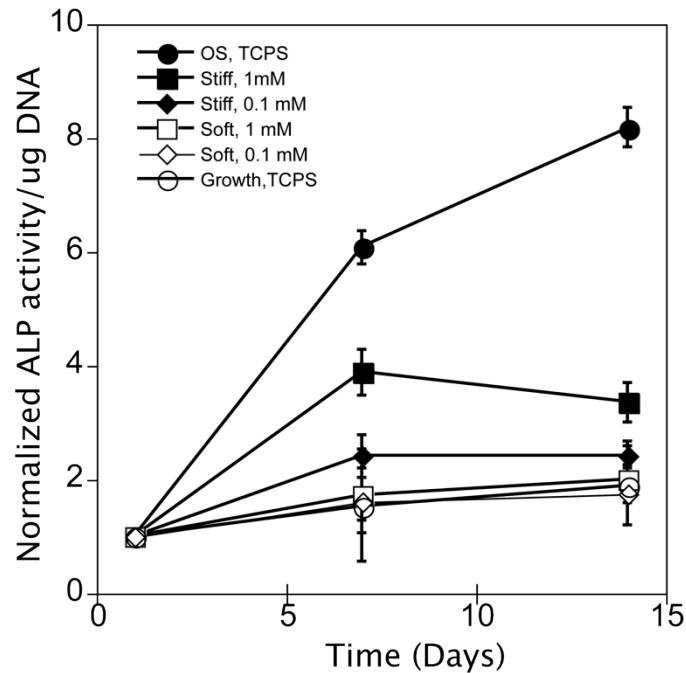


**Figure 4.7. Osteogenic differentiation of hMSCs on cyl(RRETAWA) functionalized PEG gels.** A) ALP activity of hMSCs cultured on stiff (■, ◆) and soft (□, ◇) gels at 1mM (squares) and 0.1 mM (triangles). ALP activity was significantly increased only in hMSCs cultured on stiff substrates. Higher cyl(RRETAWA) concentration induced higher ALP activity in hMSCs on stiff substrates.

#### 4.4 Discussion

$\alpha 5\beta 1$  is an important fibronectin specific integrin that has been previously shown to be important for hMSC osteogenic differentiation.<sup>2,5</sup> Expression of  $\alpha 5\beta 1$  is upregulated in dexamethasone induced hMSCs and also several pathways that converge to upregulate osteogenic related genes have been shown to be dependent on the integrin activation.<sup>2</sup> Previous studies have shown that  $\alpha 5\beta 1$  bind synergistically to both RGD peptide motif

and the PHSRN motif found in fibronectin.<sup>20</sup> Interestingly, other fibronectin binding integrins such as  $\alpha V\beta 3$  do not require this synergistic interaction with PHSRN. Hence, stimulation of  $\alpha 5\beta 1$  integrin cannot be accomplished via RGD peptide motifs alone, although RGD peptide supports hMSC attachment. To overcome this problem, researchers have previously used engineered fibronectin fragments that retain the domain conformation to bind and activate  $\alpha 5\beta 1$ .<sup>5</sup> Use of these fragments poses significant challenges to systematically study the interplay substrate elasticity and the level of integrin binding as often non-covalent coating efficiency of these fragments on culture substrates is highly dependent on chemical composition, elasticity of the underlying substrate thus coupling the substrate elasticity and ligand concentration.<sup>21-23</sup> In this study, we utilize small peptide motif that that has been previously shown to be capable of priming  $\alpha 5\beta 1$  integrin to study the role of substrate elasticity and ligand concentration independently.

Non-natural peptide motif RRETAWA was used as ligand to bind  $\alpha 5\beta 1$ , as it has been previously found to bind and prime  $\alpha 5$  integrin with high specificity.<sup>15</sup> In this study, we synthesized a cyl(RRETAWA) peptide that can be easily incorporated into PEG hydrogels. First we tested the effect of priming of  $\alpha 5\beta 1$  integrin on osteogenic differentiation of hMSCs by delivering in soluble form. Dosing hMSCs with 10 and 100  $\mu\text{g}/\text{ml}$  of cyl(RRETAWA) increased ALP activity significantly at day 7 and 14 indicating that hMSCs underwent osteogenic differentiation. Ultimately we are interested in studying the interplay of substrate elasticity and ligand concentration on  $\alpha 5\beta 1$  induced osteogenic differentiation of hMSCs. Hence, we covalently tether the peptide to PEG hydrogels to form cyl(RRETAWA) gels. Thiol-ene photopolymerizations has been

recently established as robust scheme for the synthesis of peptide functionalized step-growth PEG hydrogel. This synthesis scheme allows for facile functionalization of PEG hydrogels with cysteine containing biochemical moieties without any requirement of post-synthetic modification. Using this scheme our group has reported PEG gels whose biochemical functionalization and elasticity can be independently tuned via controlling the ratio of reactive functionalities (i.e. [thiol]:[ene] ratio) as well as PEG macromere molecular weight. Rubber elasticity theory predicts that the gel modulus is inversely correlated with cross-linking density. Hence, as PEG molecular weight is increased the distance between the crosslinks is effectively increased which results in decrease of bulk gel modulus. In this study, we use PEG 8 arm 10kDa and PEG 4 arm 20kDa macromere to form hydrogels resulting in  $\sim 25$  kPa and  $\sim 2$  kPa hydrogels respectively. These hydrogels were formed under stoichiometric conditions and functionalized with either 0.1 mM or 1 mM of cyl(RRETAWA) peptide. To maintain the on-stoichiometry conditions, scrambled CRDGS peptide was included in the monomer formulations. hMSCs do not interact with CRDGS peptide motif and hence should not compete or interfere with the binding of cyl(RRETAWA) peptide.

Binding of hMSCs to these gels was verified via blocking experiments. Blocking of  $\alpha 5$  integrin with antibodies resulted in  $\sim 80\%$  reduction of hMSC attachment to cyl(RRETAWA) gels suggesting that majority of adhesion to these gels occurs via  $\alpha 5$  integrin. To further verify that this binding is specific we monitored attachment levels upon blocking  $\alpha V\beta 3$  integrin on hMSCs. Blocking  $\alpha V\beta 3$  integrin resulted in only slight reduction of hMSC attachment demonstrating the specificity of binding to these via  $\alpha 5\beta 1$  integrin. Immunostaining for  $\alpha 5$  integrin was done to visually verify the interaction of



hMSCs with the gels via  $\alpha 5$  integrin. As shown in Figure 4.3,  $\alpha 5$  staining largely localized to dash shaped structures present at the ends of actin fibers. This is expected as integrin binding to ligands results in formation of dash shaped focal adhesions which act as a scaffold from which actin monomers polymerize to form cell cytoskeleton. Qualitatively, we observe that the majority of actin fibers end with  $\alpha 5$  staining further supporting our blocking data that, hMSC bind to these gels primarily via  $\alpha 5\beta 1$  integrin.

Our ALP activity results indicate that osteogenic differentiation of hMSCs on  $\alpha 5\beta 1$  priming hydrogels was highly dependent on substrate stiffness. We hypothesize that engagement of  $\alpha 5\beta 1$  to form stable focal adhesions and upregulation of integrin signaling is achieved only on the stiffer substrates resulting in osteogenic differentiation of hMSCs. This is also supported by inability to form longer focal adhesions and largely diffuse actin cytoskeleton in hMSCs on softer gels while in contrast to stiff gels on which hMSCs formed longer focal adhesions and highly organized f-actin (Figure 4.5). Our hypothesis is also supported by previous study by Friedland *et al.*<sup>24</sup>, that demonstrated the role of substrate elasticity on conformational stability of  $\alpha 5\beta 1$  binding to its ligand. They found that the gel stiffness positively correlated with the number of  $\alpha 5\beta 1$  integrin bonds formed and FAK phosphorylation at Y397 residue. Y397 phosphorylation of FAK has been previously implicated in osteogenic differentiation of hMSCs. Since we observe longer focal adhesions on stiff gels, it is possible that the total FAK phosphorylation at Y397 could be higher resulting in the higher downstream signal. To further confirm our hypothesis future experiments are focused on studying the ALP activity and gene expression of osteogenic genes (Coll-1a, Osteopontin and CBFA1) in presence of small chemical pFAK inhibitors such as PF-573228.

## 4.5 References

1. Yun, S. P., Ryu, J. M. & Han, H. J. Involvement of  $\beta$ 1-integrin via PIP complex and FAK/paxillin in dexamethasone-induced human mesenchymal stem cells migration. *J. Cell. Physiol.* **226**, 683–692 (2011).
2. Hamidouche, Z. *et al.* Priming integrin  $\alpha$ 5 promotes human mesenchymal stromal cell osteoblast differentiation and osteogenesis. *Proc Natl Acad Sci U S A* **106**, 18587–18591 (2009).
3. Hamidouche, Z., Fromigué, O., Ringe, J., Häupl, T. & Marie, P. J. Crosstalks between integrin alpha 5 and IGF2/IGFBP2 signalling trigger human bone marrow-derived mesenchymal stromal osteogenic differentiation. *BMC Cell Biology* **11**, 44 (2010).
4. Popov, C. *et al.* Integrins  $\alpha$ 2 $\beta$ 1 and  $\alpha$ 11 $\beta$ 1 regulate the survival of mesenchymal stem cells on collagen I. *Cell Death Dis* **2**, e186 (2011).
5. Martino, M. M. *et al.* Controlling integrin specificity and stem cell differentiation in 2D and 3D environments through regulation of fibronectin domain stability. *Biomaterials* **30**, 1089–1097 (2009).
6. Veevers-Lowe, J., Ball, S. G., Shuttleworth, A. & Kielty, C. M. Mesenchymal stem cell migration is regulated by fibronectin through  $\alpha$ 5 $\beta$ 1-integrin-mediated activation of PDGFR- $\beta$  and potentiation of growth factor signals. *J. Cell. Sci.* **124**, 1288–1300 (2011).
7. Zou, C., Song, G., Luo, Q., Yuan, L. & Yang, L. Mesenchymal stem cells require integrin  $\beta$ 1 for directed migration induced by osteopontin in vitro. *In Vitro Cell.Dev.Biol.-Animal* **47**, 241–250 (2011).
8. Engler, A. J., Sen, S., Sweeney, H. L. & Discher, D. E. Matrix elasticity directs stem cell lineage specification. *Cell* **126**, 677–689 (2006).
9. Shih, Y.-R. V., Tseng, K.-F., Lai, H.-Y., Lin, C.-H. & Lee, O. K. Matrix stiffness regulation of integrin-mediated mechanotransduction during osteogenic differentiation of human mesenchymal stem cells. *J. Bone Miner. Res.* **26**, 730–738 (2011).
10. Anderson, S. B., Lin, C.-C., Kuntzler, D. V. & Anseth, K. S. The performance of human mesenchymal stem cells encapsulated in cell-degradable polymer-peptide hydrogels. *Biomaterials* **32**, 3564–3574 (2011).
11. McCall, J. D. & Anseth, K. S. Thiol–Ene Photopolymerizations Provide a Facile Method To Encapsulate Proteins and Maintain Their Bioactivity. *Biomacromolecules* **13**, 2410–2417 (2012).
12. Klees, R. F. *et al.* Laminin-5 induces osteogenic gene expression in human mesenchymal stem cells through an ERK-dependent pathway. *Mol. Biol. Cell* **16**, 881–890 (2005).

13. Salasznyk, R. M., Klees, R. F., Williams, W. A., Boskey, A. & Plopper, G. E. Focal adhesion kinase signaling pathways regulate the osteogenic differentiation of human mesenchymal stem cells. *Exp. Cell Res.* **313**, 22–37 (2007).
14. Cheng, S. L., Lai, C. F., Blystone, S. D. & Avioli, L. V. Bone mineralization and osteoblast differentiation are negatively modulated by integrin alpha(v)beta3. *J. Bone Miner. Res.* **16**, 277–288 (2001).
15. Koivunen, E., Wang, B. & Ruoslahti, E. Isolation of a highly specific ligand for the alpha 5 beta 1 integrin from a phage display library. *J. Cell Biol.* **124**, 373–380 (1994).
16. Mould, A. P., Burrows, L. & Humphries, M. J. Identification of amino acid residues that form part of the ligand-binding pocket of integrin alpha5 beta1. *J. Biol. Chem.* **273**, 25664–25672 (1998).
17. Humphries, J. D. *et al.* Molecular basis of ligand recognition by integrin alpha5beta 1. II. Specificity of arg-gly-Asp binding is determined by Trp157 OF THE alpha subunit. *J. Biol. Chem.* **275**, 20337–20345 (2000).
18. Mould, A. P., Askari, J. A. & Humphries, M. J. Molecular basis of ligand recognition by integrin alpha 5beta 1. I. Specificity of ligand binding is determined by amino acid sequences in the second and third NH2-terminal repeats of the alpha subunit. *J. Biol. Chem.* **275**, 20324–20336 (2000).
19. Clark, K. *et al.* A Specific  $\alpha 5\beta 1$  Integrin Conformation Promotes Directional Integrin Translocation and Fibronectin Matrix Formation. *J Cell Sci* **118**, 291–300 (2005).
20. Danen, E. H. *et al.* Requirement for the synergy site for cell adhesion to fibronectin depends on the activation state of integrin alpha 5 beta 1. *J. Biol. Chem.* **270**, 21612–21618 (1995).
21. Keselowsky, B. G., Collard, D. M. & García, A. J. Surface chemistry modulates fibronectin conformation and directs integrin binding and specificity to control cell adhesion. *J Biomed Mater Res A* **66**, 247–259 (2003).
22. Keselowsky, B. G., Collard, D. M. & García, A. J. Integrin binding specificity regulates biomaterial surface chemistry effects on cell differentiation. *PNAS* **102**, 5953–5957 (2005).
23. Guerra, N. B. *et al.* Subtle variations in polymer chemistry modulate substrate stiffness and fibronectin activity. *Soft Matter* **6**, 4748–4755 (2010).
24. Friedland, J. C., Lee, M. H. & Boettiger, D. Mechanically activated integrin switch controls alpha5beta1 function. *Science* **323**, 642–644 (2009).

## CHAPTER 5

### Photo-clickable living strategy for controlled reversible exchange of biochemical ligands

---

#### 5.1 Introduction

Synthetic hydrogels have been increasingly engineered to provide and recapitulate the complex and dynamic environment of extra-cellular matrix (ECM) surrounding the cells *in vivo*. Of significant interest is the design of chemical strategies not only to fabricate hydrogels that can function as cell culture platforms for both two-dimensional (2d) and three-dimensional (3d) cell culture systems, but also to incorporate biologically active features that mimic several critical aspects of the ECM<sup>1</sup>. Due to their hydrophilic nature, tunable mechanical properties, wide range of commercial availability and provision of tissue-like qualities, poly(ethylene glycol) (PEG) based hydrogels have received tremendous attention as a versatile biomaterial system. To compliment their biophysical properties, the bio-inertness of the PEG hydrogels renders opportunities to incorporate various biochemical cues and study their effects on host cells with minimal confounding non-specific interactions. Hence, there is a growing interest to functionalize PEG hydrogels with several biochemical cues, including peptides and proteins aimed at directing and controlling cellular functions such as adhesion, proliferation, differentiation, morphology etc.

Traditionally, these biochemical ligands have been modified with reactive functionalities that can be co-polymerized into the network during the hydrogel

formation. For example, peptides motifs that facilitate cell adhesion<sup>2-5</sup> (e.g., fibronectin derived RGD, PHSRN), cell directed degradability<sup>6-9</sup> (e.g., Matrix Metalloprotease (MMP) degradable GPQGIWGQ), growth factor sequestering<sup>10,11</sup> (e.g., FGF- $\beta$  binding KRTGQYKL) have been modified to contain thiol, acrylate or methacrylate functional groups and incorporate into PEG hydrogels via radical mediated polymerizations or Michael addition. While these strategies have allowed for synthesis of elegant ECM analogs, it is often more difficult to realize multidimensional control over presentation of these signals. Since the ECM is a dynamic environment, chemical strategies that allow sequential or reversible introduction of biological signals should enable new opportunities to tailor a cell's local microenvironment in a biologically relevant fashion.

One strategy of significant interest when designing dynamic biomaterials niches has been to introduce the biochemical cues post-synthesis of the hydrogel network. This allows for fabrication of ECM mimics with controlled bulk properties, while independently achieving well-defined and tunable presentation of the multiple biochemical cues to the cells. Specifically, bio-orthogonal click reactions have gained prominence owing to their efficiency, fidelity, facile incorporation of the functional groups into the widely used synthetic biomaterials, and their relatively mild reaction conditions.<sup>12</sup> In particular, light controlled click reactions are gaining prominence as they allow confinement of the reaction of interest only to defined locations where light is delivered. Photolithographic techniques use photomasks and collimated light to confine and pattern reactions in two-dimensions, while focused light (single or multiphoton) enables control of the reaction within a locally defined 'region of interest' (ROI) in three-dimensions. While these chemical approaches have been successfully applied to cell

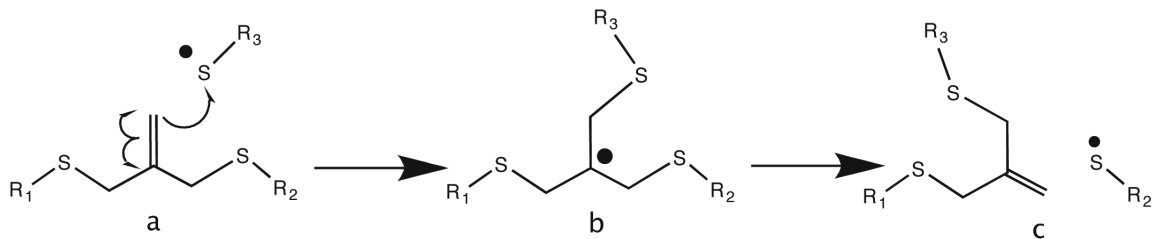
scaffolds to demonstrate localized control of cell spreading,<sup>13</sup> cell outgrowth,<sup>14</sup> control of stem cells fate,<sup>15</sup> and guided migration,<sup>16,17</sup> complementary strategies that simultaneously achieve the addition and removal of biochemical signals would be beneficial. Further, many of the strategies to create functional bioscaffolds rely on irreversible, thus ‘dead’, reactions and the sites for modifications are consumed permanently thus limiting the extent of multiple and sequential modifications. Hence, chemical strategies that regenerate reactive functional groups (i.e., reversible) would be powerful tools and complementary tools in material based strategies to study cellular processes.

Recently, a strategy that uses the equilibrium switching of unreactive 3-(hydroxymethyl)-2-naphthol and reactive o-2-naphthoquinone-3-methides (NQM) was used to demonstrate attachment, removal and reattachment of streptavidin to a thiol-derivitized glass slide.<sup>18</sup> This strategy used base catalyzed Michael addition to couple, [and 350 nm](#) UV light to cleave NQM functionalized chemical moieties on thiol-functionalized glass. Although this strategy, first of its kind, achieves reversibility in the addition and removal of NQM derivatized biochemical moieties, it requires the use of base and 350 nm or lower wavelength light thus limiting the use of this strategy in the presence of cells. Addition-Fragmentation-Chain transfer (AFCT) functional groups have emerged as unique paradigm that allow polymers to be formed possessing excellent stress relaxation characteristics and also allowing solution free physical patterns to be formed on a polymer substrates.<sup>19-21</sup> Key to the strategy is an AFCT capable allyl sulfide functional group. Inspired from concepts and strategies outlined above, we hypothesized that the allyl sulfide functional groups are excellent candidates to precisely and simultaneously control the introduction, exchange or removal of biochemical epitopes in the hydrogel

networks, while simultaneously regenerating the reactive functionality. This approach creates a pseudo-living biomaterial system for the introduction of biological epitopes using cytocompatible thiol-ene click reactions. Thiol-ene click reactions are increasingly used for biological applications due to their robustness, simplicity, and bioorthogonality to form hydrogel culture platforms,<sup>22-24</sup> as well as for patterning in biochemical cues in the presence of cells.<sup>13,22,25</sup> Towards achieve reversible photopatterning of biochemical ligand, here we report the synthesis of allyl sulfide functionalized hydrogel networks and characterize the reversible biochemical patterning using model bioactive peptide motif, RGD, found in ECM protein fibronectin.

## 5.2. Results and Discussion

The reversible exchange strategy reported in this study is inspired from the living nature of the chain transfer agent in RAFT based polymerizations.<sup>26</sup> Key to this reversible exchange of biochemical epitopes is addition fragmentation chain transfer (AFCT) capable allyl sulfide functional group that enables reversible addition and removal of thiol-containing compounds. Scheme 5.1 shows the reported mechanism demonstrating the  $\beta$ -scission of allyl sulfide. Upon attack of a thiyl radical on the double bond of allyl sulfide (Scheme 5.1a), the reaction results in a symmetric intermediate (Scheme 5.1b). This intermediate is unstable and undergoes  $\beta$ -scission resulting in addition of attacking species and regeneration of the new double bond (Scheme 5.1c). We refer to this aspect of regeneration of the double bond as ‘living’ in this system. The regenerated double bond is capable of further attack by another thiyl radical, thus allowing exchange of any thiol containing biochemical moieties of interest.



**Scheme 5.1.** Mechanism of addition fragmentation chain transfer of an allyl sulfide functional group upon attack by a thiyl radical.

### 5.2.1 Synthesis and biochemical patterning of *allyl sulfide* functionalized PEG hydrogel networks

Hydrogel containing allyl sulfide functional groups were synthesized by a Cu-catalyzed click reaction between 4-arm PEG tetra azide and di-functional alkyne crosslinkers that proceeds quantitatively via a rapid, non-radical mechanism to form step growth networks.<sup>25,27</sup> The monomers used to form the hydrogel networks are shown in Figure 5.1. Here, orthogonal Cu click reactions were chosen to synthesize the hydrogel networks to preserve the integrity of the double bond on the allyl sulfide functional group (i.e., the double bond is dormant during the formation of the hydrogel).



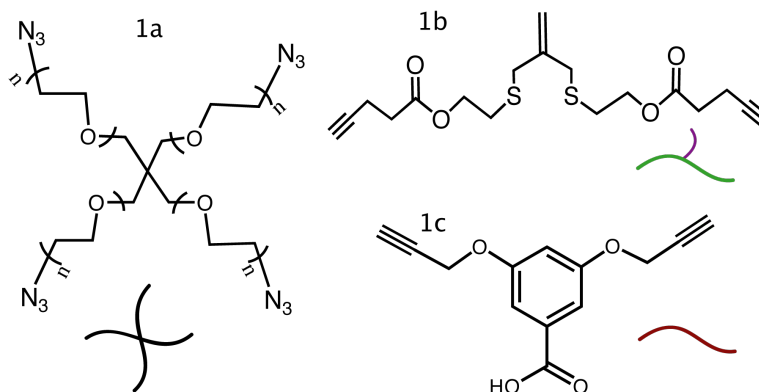


**Figure 5.1.** Structures of monomers used to form the hydrogel networks. 1a: 4-arm-poly(ethylene glycol)-tetra azide. 1b: 2-methylene-propane-1,3-bis(thioethyl 4-pentynoate). 1c: Benzoic acid-3,5-bis(4-pentynoate).

The patterning process was initiated by homolytic photolysis of a photoinitiator 2-hydroxy-1-[4-(2-hydroxyethoxy) phenyl]-2-methyl 1-propanone (I2959) at 365 nm (collimated light lamp) or at 720 nm (2-photon laser light) resulting in a production of thiyl radical that attacks the double bond on allyl sulfide. The  $\beta$ -scission of the allyl sulfide moiety, functionalized into the hydrogel networks, due to the photopatterning process was readily demonstrated upon irradiating specific regions of the hydrogel formed from 1a and 1b to 365 nm light in the presence of patterning agent and photoinitiator I2959 using a photomask (Figure 5.2A). Here, cysteine conjugated cell adhesive peptide derived from extra cellular matrix fibronectin, CRGDS, is used as patterning agent. Since 100% of the network crosslinks are functionalized with allyl sulfide moieties, the  $\beta$ -scission of the allyl sulphide functional group upon attack by a thiyl radical results in losing connectivity of the crosslinks to the surrounding unexposed network (Figure 5.2B). Figure 5.2B confirms that the exposure of optically thin hydrogels with this formulation in the presence of 20 mM RGDSC and 15 mM I2959 for 30 mins

results in physical degradation of hydrogel network. Bulk degradation of the hydrogel also confirms the behavior of the allyl sulphide functional group as shown in Scheme 5.1 in these hydrogels. We are ultimately interested in forming hydrogels that can be decorated reversibly with the biochemical moieties. Hence, we have synthesized hydrogels from 1a crosslinked with 1b and 1c, where crosslinker 1c is dormant to the biochemical patterning procedure (Figure 5.2C). The monomer formulations are adjusted to form networks containing 22% of crosslinks with the allyl sulfide functional group (corresponds to 6.4 mM of allyl sulfide functional group in the formed hydrogel) to prevent bulk degradation as in the case of Figure 5.2A. Flory-Stockmayer theory<sup>28</sup> predicts that for the chosen formulation conditions, ~43% of crosslinks needs to be broken to hit reverse gelation point, i.e. for transition from solid to liquid. The chosen formulation can only result in a maximum of 22% of the crosslinks cleaved if all the allyl sulfide functional groups were reacted and hence patterning in these gels does not result in bulk degradation of the network. To demonstrate that the reaction scheme allows for the attachment of a thiol containing compound to the network by photopatterning a RGDSC peptide using standard stereo-lithographic techniques. The RGDSC peptide was modified with 6-aminohexanoic acid to conjugate Alexa Fluor 555 (denoted as AF<sub>555</sub>AhxRGDSC) to visually confirm and study the addition of patterning agent to the allyl sulfide functional group. Here, patterning in the hydrogels is achieved by exposing gels swollen in solution containing photoinitiator, I2959 and AF<sub>555</sub>AhxRGDSC to U.V light at 365 nm using a photomask. Confinement of the reaction only to the exposed regions was confirmed by resultant fluorescent patterns only in the exposed regions as

shown in Figure 5.2D. The formed patterns clearly demonstrate high fidelity in pattern transfer over micrometer length scales.

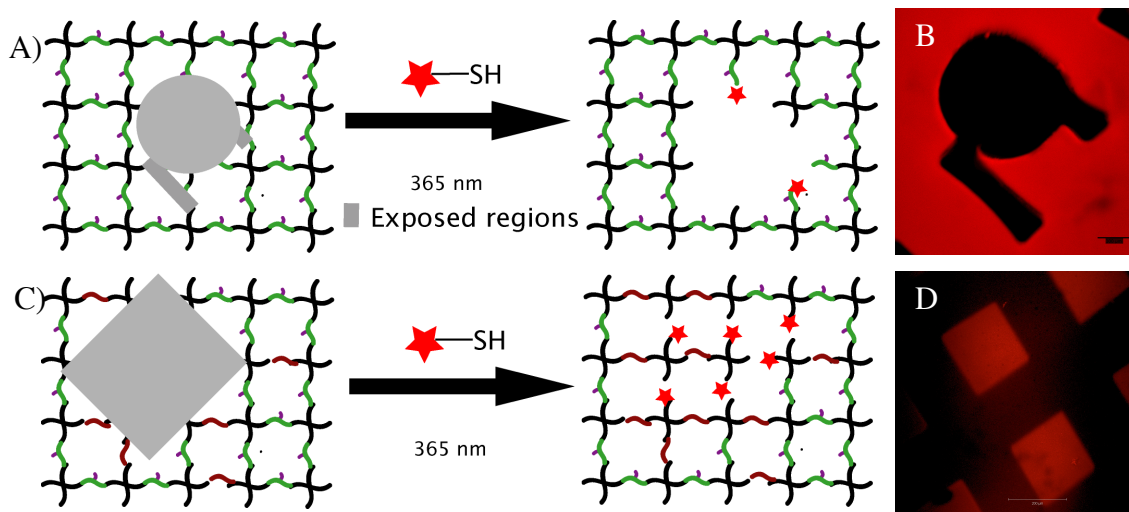


**Figure 5.2.** Biochemical patterning of allyl sulfide functionalized PEG hydrogels. A) Exposing specific regions of networks formed from 1a and 1b to 365 nm wavelength light results in mass loss in exposed regions due to the  $\beta$ -scission of allyl sulfide functional group resulting in degradation of the crosslinks. B) Image demonstrates the mass loss of hydrogel in the exposed regions. After patterning, the gel was swollen in AF555 solution and imaged under confocal microscope. Black regions represent the degraded regions of the hydrogel. C) Exposing specific regions of networks formed from 1a, 1b and 1c result in stable patterning of the biochemical ligand as opposed to degradation in (A). D) Confocal image of array of 100  $\mu\text{m}$  square patterns formed by exposing specific regions of the network to 365 nm light in the presence of patterning conditions. Scale bar = 50  $\mu\text{m}$ .

### 5.2.2 Kinetics of biochemical patterning in *allyl sulfide* functionalized PEG hydrogels networks:

To better understand the biochemical functionalization of the allyl sulfide hydrogel networks, we sought to characterize the kinetics of addition of a thiol containing compound to the hydrogel using standard stereolithographic techniques. The intermediate formed upon attack of a photo-initiated thiyl radical is symmetrical (Scheme 5.1), and hence the direction of the  $\beta$ -scission ultimately determines the addition of external thiol

containing compounds on to the functional group. The reaction mechanism of addition of a thiol containing compounds onto the allyl sulfide in the hydrogel is shown in Figure 5.3A. We studied the kinetics of addition of AF<sub>555</sub>AhxRGDSC on to the allyl sulfide functional group by regulating the time of exposure, intensity of light, and initiator concentration, which control the rate of radical generation.

The rate of reaction during thiol-ene polymerization is given by,<sup>29</sup>

$$R_p \propto [C = C][S \cdot]$$

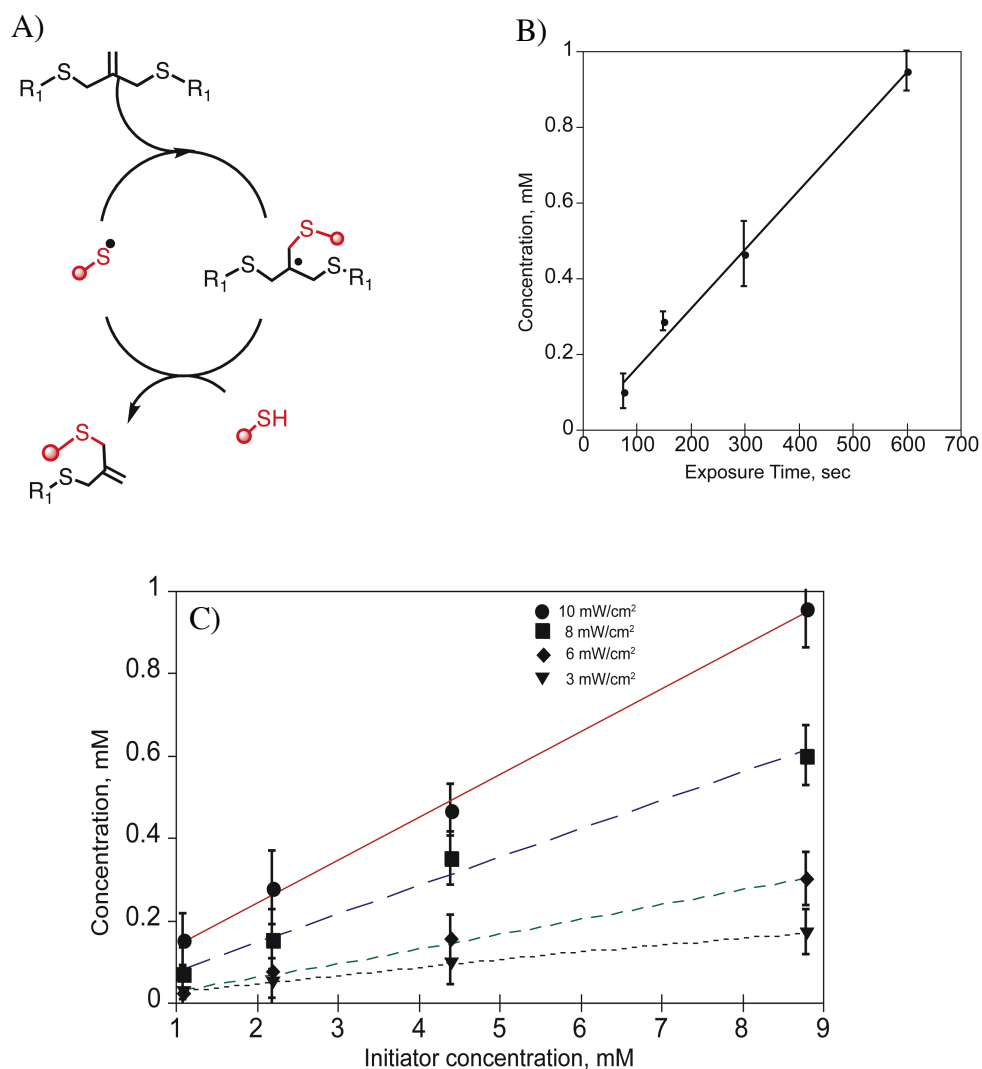
Here,  $[C = C]$  represent the alkene concentration on the allyl sulfide functional group and  $[S \cdot]$  represents the thiy radical concentration in the reaction. Due to the reaction scheme,  $[C = C]$  remains constant throughout the patterning reaction and hence the rate of reaction is directly proportional to thiy radical concentration  $[S \cdot]$ .

Figure 5.3B show the kinetics of the addition of AF<sub>555</sub>AhxCRGDS with exposure time. The amount of photo-coupled AF<sub>555</sub>AhxCRGDS varied linearly with time indicating a first order dependence of addition on time of exposure. We next studied the kinetics of AF<sub>555</sub>AhxCRGDS addition by varying the amount of initiator used to modify the gel at different light dosages. At a constant initiator concentration, the peptide concentration increased linearly with increase in the light dosage. At a constant dosage, the amount of peptide patterned also increased linearly with increasing initiator concentration, demonstrating that the rate of addition is first order dependent on both initiator concentration and light intensity. Previous studies by Kloxin *et al.*<sup>20</sup> have shown that the allyl sulfide double bond in glassy networks is consumed via termination only at very high concentrations of thiol compared to allyl sulfide (5:3 and 3:1 ratio of thiol to the allyl sulfide) in the network. Throughout this study, the thiol concentration was kept

lower than allyl sulfide concentration; the highest thiol:allyl sulfide ratio used was 1:1.2. Hence, we neglect any irreversible termination of the double bond on the allyl sulfide functionality. Assuming that the thiyl radical concentration depends on the rate of generation of initiator radicals and substituting for the thiyl radical concentration yields,

$$R_p \propto [I]_0 I_0 t$$

where  $[I]_0$  is the initial initiator concentration used,  $I_0$  is the light intensity and ' $t$ ' is time of light exposure (please see supplementary information for detailed calculation of thiyl radical concentration). This rate expression is in agreement with our kinetic experiments (Figure 5.3b,c). For example, at an initiator concentration of 2.2 mM, doubling the light dosage ( $=I_0 t$ ) roughly doubles the amount the peptide patterned into the hydrogel. At a particular light dosage, say 5 J/cm<sup>2</sup>, doubling the amount of initiator concentration, from 2.2 mM to 4.4 mM doubles the amount of peptide patterned into the gel. Thus, the amount of peptide patterned into the network is readily controlled and scales with light intensity and initiator concentration to the first power. The concentrations range of the patterned RGD peptide achieved in this study has been previously demonstrated to be relevant to control several cell functions.<sup>13,16,23,30,31</sup> For example, Salinas *et al.*,<sup>31</sup> has demonstrated matrix interaction via integrins and increased survival of human mesenchymal stem cells in PEG hydrogels functionalized with 1 mM RGD.



**Figure 5.3.** Kinetics of thiol-ene photopatterning of allyl sulfide functionalized PEG hydrogel networks. A) Reaction mechanism of addition of a thiol containing compound to the allyl sulfide functionalized hydrogel. B) Concentration of patterned peptide as a function of time of exposure shows that the rate of addition is directly proportional to the time of exposure. C) Concentration of patterned peptide as a function of initiator concentration at different light intensities used at 10 min exposure times. The figure shows linear dependence of rate of addition on both initiator concentration and light intensity.

### 5.2.3 Reversible exchange of biochemical moieties in *allyl sulfide* functionalized hydrogels:

Next, we demonstrate that the living alkene functionality of the allyl sulfide functional groups allows for sequential exchange of new biochemical moieties by using Alex fluor 555 and Alex fluor 488 conjugated AhxRGDSC peptide (AF<sub>555</sub>AhxRGDSC and AF<sub>488</sub>AhxRGDSC respectively). We track the addition and exchange reactions by measuring fluorescence of the peptides using confocal microscopy. 2-photon photo-patterning was used to demonstrate and characterize the exchange of thiol containing compounds on allyl sulfide containing hydrogels as it allows to control the exposed regions in three dimensions. The mechanism and schematic process for the exchange of patterning molecules in these hydrogel networks are shown in Figure 5.4a,b, respectively. Figure 5.4C-E shows a 250  $\mu\text{m}$  long cube patterned using 10 mM of AF<sub>555</sub>AhxCRGDS, 4.4 mM I2959 at a laser scan speed 4 which corresponds to  $\sim 9.41 \mu\text{sec}/\mu\text{m}^2$  pixel dwell time. To demonstrate the exchange, we repeated the patterning process by the swelling the patterned gel with 10 mM AF<sub>488</sub>AhxRGDSC and 4.4 mM I2959. The buffalo shaped region inside the square red pattern was exposed to 720 nm focused laser light to allow for the exchange reaction. Photo-exchange of the old peptide (AF<sub>555</sub>AhxRGDSC) with the new one (AF<sub>488</sub>AhxRGDSC) was confirmed by fluorescent images showing the disappearance of AF<sub>555</sub> fluorescence and appearance of AF<sub>488</sub> fluorescence in the exposed regions (Figure 5.4F-H).

No change in AF<sub>555</sub> fluorescence in the unexposed regions of the red square pattern (Figure 5.4F) confirmed the confinement of the photo-exchange only to the exposed regions. The living nature of the double bond allows performing further

exchange reactions multiple times, theoretically infinitely, but is limited by irreversible termination of the intermediate. To demonstrate this nature, we have performed second exchange step using a non-fluorescent AhxRGDSC peptide. User defined letters (CU) inside the green buffalo logo, obtained after the first exchange step, were exposed to laser light under similar conditions as the first exchange step (Figure 5.4I-K). Successful exchange of the patterned AF<sub>488</sub>AhxRGDSC peptide with the non-fluorescent peptide was confirmed by disappearance of green fluorescence in the exposed regions (Figure 5.4J). As expected, AF<sub>555</sub> and AF<sub>488</sub> fluorescence around the exposed regions after the second exchange step was not affected due to the exchange process (Figure I-K). Figure 5.4C-K clearly demonstrates the ‘living’ nature of alkene functionality on allyl sulfide functional group that allowed for the reversible exchange of the peptides. Since the exchange step allows for complete exchange of the initially coupled moieties, exchange reactions could be extended to remove the desired biochemical signals presented to the cells. Hence, the living characteristic of this hydrogel system allows, depending on the strategy, to achieve photo-coupling, photo-removal and photo-exchange of biochemical ligands with spatial and temporal control.



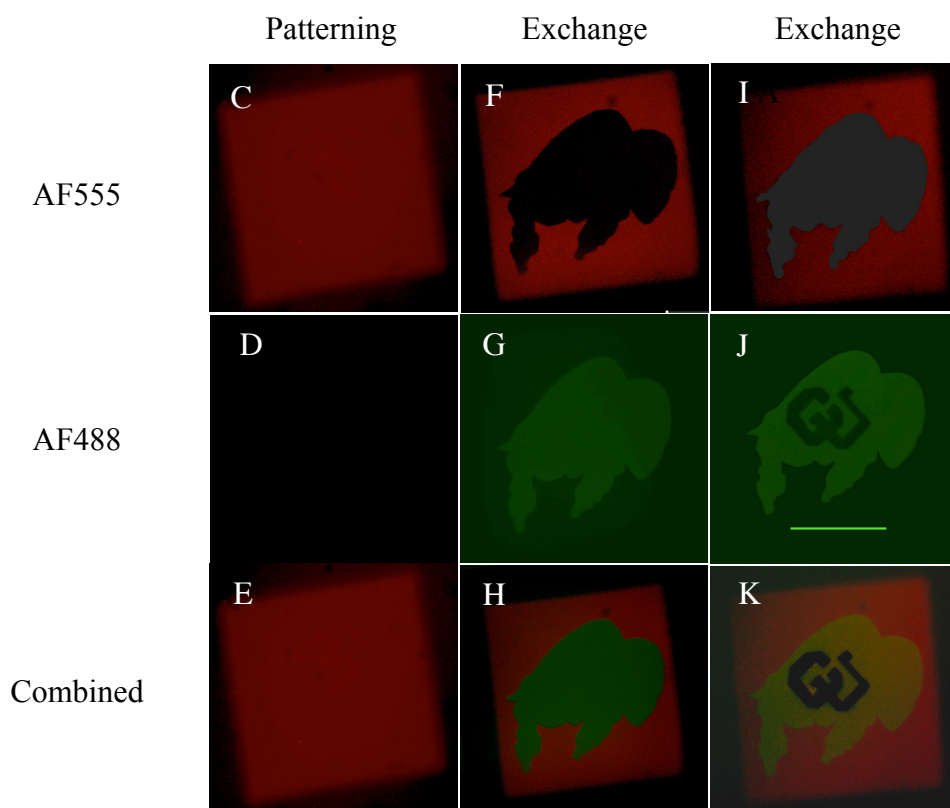
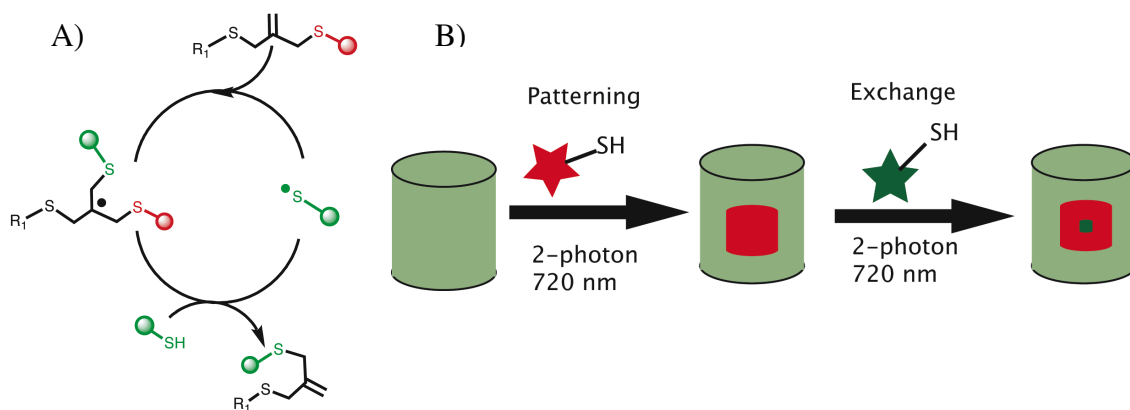


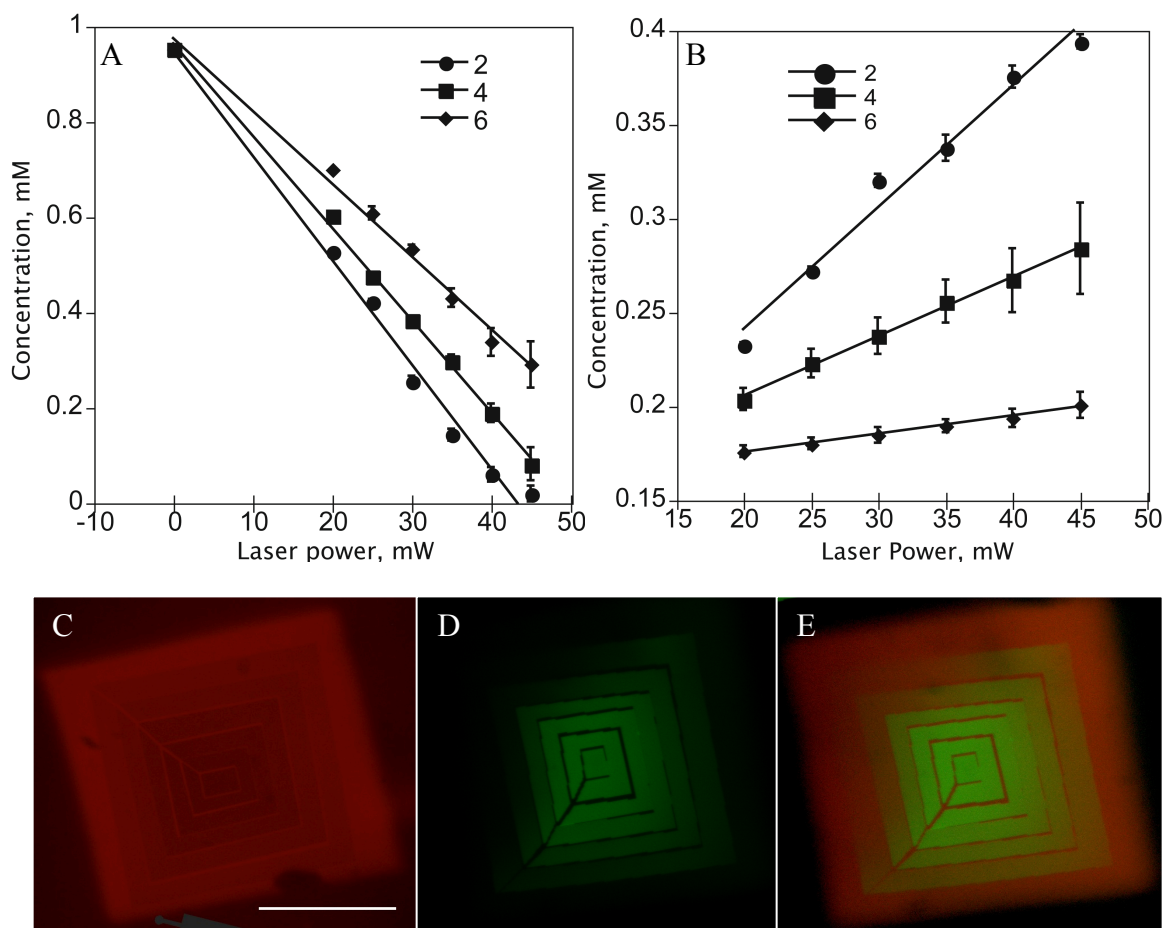
**Figure 5.4. Photoclick living strategy allows reversible exchange of biochemical ligands.** A) Mechanism of replacement of a thiol-containing compound on allyl sulphide functional group. B) Schematic of replacement of biochemical ligand. C-K) Demonstration of reversible exchange of thiol containing peptides. (C-E) 250 $\mu$ m square pattern of AF<sub>555</sub>AhxRGDSC. (F-H) Buffalo logo was formed by replacing AF<sub>555</sub>AhxRGDSC with AF<sub>488</sub>AhxRGDSC resulting in appearance of green fluorescence and disappearance of red fluorescence only in the exposed regions. (I-K) Demonstration of further replacement on living allyl sulfide: Letters ‘CU’ inside the buffalo logo were exposed to 720 nm light to photo-exchange with non-fluorescent AhxRGDSC peptide. Photo-exchange of peptides was confirmed by removal of green fluorescent (J) only at the exposed regions. Scale bar = 100  $\mu$ m.

#### **5.2.4 Kinetics of the exchange of biochemical moieties in *allyl sulfide* functionalized hydrogels:**

The extent of the exchange reaction depends on the production of initiator radicals responsible for initiating the thiol-ene reaction. We characterized the exchange process by regulating the laser power and scan speed, which determines the pixel dwell time of laser light and monitored the amount of initially patterned peptide that remains attached after the exchange process. Figure 5.5A shows the amount of AF<sub>555</sub>AhxRGDSC peptide remaining after the exchange reaction in the presence of 10 mM AF<sub>488</sub>AhxRGDSC peptide and 8.8 mM I2959 with increasing laser intensity at different laser scan speeds of the laser. At a given pixel dwell time, an increase in laser intensity results in higher dosage per pixel, and hence, higher concentration of radicals produced resulting in the lower concentration of AF<sub>555</sub>RGDSC peptide as shown in Figure 5.5A. Increasing the pixel dwell time at any delivered laser intensity also results in higher dosage to the reaction volume, and hence, lower concentration of AF<sub>555</sub>RGDSC peptide as shown in Figure 5.5A. Dependence of the amount of the peptide exchanged on light intensity was found to be linear in laser power at all the pixel dwell times studied. Figure 5.5B shows the dependence of addition of the AF<sub>488</sub>AhxRGDSC peptide to the network after the exchange reaction on laser power at different pixel dwell time. As expected, at a given pixel dwell time, the amount of peptide attached to the network increased with increasing the laser power, scaling linearly as was observed with Figure 5.5A. Also, at a given laser intensity, increasing the pixel dwell time increases the amount of peptide attached to the network at all laser power studied consistent with the results of Figure 5.5A. Our results

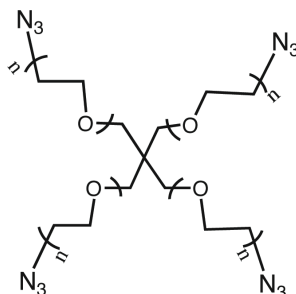
demonstrate complete control over the amount of the peptide exchanged by regulating the light delivered to the reaction volumes.

The ‘living’ aspect of this strategy offers unique opportunities to construct opposing patterns of two different biomacromolecules. As an example, we demonstrate synthesis of rectangular opposing gradients using the two AF<sub>555</sub> and AF<sub>488</sub> conjugated RGDSC peptides used above. Figure 5.5C-E shows the resultant rectangular radial gradient formed from exchanging reactions between AF<sub>555</sub>RGDSC and AF<sub>488</sub>RGDSC at a laser scan speed of 2. Specific polygon regions on a 250 μm long cube pattern were exposed to radially decreasing (measured from center to outside) laser power resulting in opposing patterns as shown in Figure 5.5C,D. The concentrations of the resultant AF<sub>555</sub>RGDSC and AF<sub>488</sub>RGDSC peptides are shown in Figure 5.5A,B respectively. Images clearly demonstrate the flexibility in constructing opposing gradient patterns by controlling the parameters of confocal microscopy. The patterning process occurs at typically used imaging speeds and the whole exchange reactions occurs on the order of seconds to minutes. Also, since the patterning strategy used in this work for the exchange reactions constructs ROIs using Zeiss software to form the patterns, advanced patterning procedures reported by Culver *et al.*<sup>32</sup> can be directly implemented to construct numerous relevant biomimetic patterns.



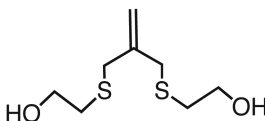
### 5.3. Materials and Methods

#### 5.3.1 Synthesis of 1a (PEG-tetra azide):



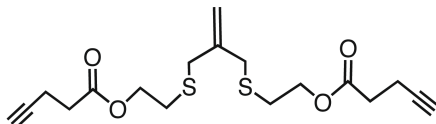
Vacuum dried 4 arm Poly(ethylene glycol) ( $M_n \sim 5000$  Da) was reacted with 8x equivalents methane sulfonyl chloride in DCM for overnight. The solution was precipitated in ice-cold ethyl ether and desiccated for 2 days. The mesylated PEG was dialyzed in water for 1 day and lyophilized. The mesylated PEG was then reacted with 8x equivalents sodium azide in DMF under argon at 80 C for overnight. The reaction mixture was precipitated in ice-cold ethyl ether and desiccated for 2 days. Dessicated PEG was dissolved in water and dialyzed against water for 2 days using 2kDa cutoff dialysis membrane (Sigma) and lyophilized.

#### 5.3.2 Synthesis of 1b:



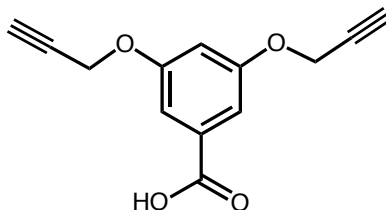
3-chloro 2-Chloromethyl-1-propene was reacted with 3 equivalents of mercapto-ethanol in DMF in the presence of cesium carbonate. The reaction was carried out at 60 C for overnight and then extracted in ethyl ether and water. The organic layer was concentrated and purified via column chromatography in ethyl acetate and hexane

(60:40). The synthesis of this precursor was verified by  $^1\text{H-NMR}$  spectra (300MHz,  $\text{CDCl}_3$ ):  $\delta$  5.01 (s, 2H), 3.69 (t,  $J = 6\text{Hz}$ , 4H), 3.29 (s, 4H), 2.61 (t,  $J = 6\text{Hz}$ , 4H).



The resultant compound was reacted with pentynoic acid in the presence of 1x equivalent DIC and 0.4 equivalent DMAP in dichloromethane for overnight at room temperature. The product was extracted in ethyl ether and water mixture and purified with column chromatography (ethyl acetate:hexane = 1:9). Synthesis of 1b was verified by  $^1\text{H-NMR}$  spectra (300MHz,  $\text{CDCl}_3$ ):  $\delta$  5.04 (s, 2H), 4.22 (t,  $J = 6\text{Hz}$ , 4H), 3.31 (s, 4H), 2.65 (t,  $J_1 = 6\text{Hz}$ , 4H), 2.59-2.46 (m, 8H), 1.98 (t,  $J_1 = 3\text{Hz}$ , 2H).

### 5.3.3 Synthesis of 1c:



This compound was synthesized by reacting 4,5-dihydroxy-1-benzoic acid (Sigma) with propargyl bromide (Sigma) in the presence of cesium carbonate in DMF. The product was extracted with ethyl ether and water and purified in column chromatography using ethyl acetate and hexane (75:25). Synthesis of 1c is verified by  $^1\text{H-NMR}$  spectra (300 MHz,  $\text{CDCl}_3$ ):  $\delta$  10.62 (s, 1H), 7.8 (d,  $J = 3\text{ Hz}$ , 1H), 7.24 (dd,  $J_1 = 3\text{Hz}$ ,  $J_2 = 6\text{Hz}$ , 1H), 7.14 (d,  $J = 6\text{Hz}$ , 1H), 4.93 (d,  $J = 3\text{Hz}$ , 2H), 4.74 (d, 2H), 2.67 (t, 1H), 2.56 (t, 1H).

### 5.3.4 Synthesis of peptides:

Peptide sequences (regular: H-CAhxRGDS-NH<sub>2</sub>, scrambled: H-CAhxRDGS-NH<sub>2</sub>) were synthesized (Protein technologies; Inc. Tribute Peptide synthesizer) through standard Fmoc solid-phase synthesis method using 2-(1H-benzotriazole-1-yl)-1,1,3,3-tetramethyluronium hexafluorophosphate/N-hydroxybenzotriazole (HBTU/HOBt) activation. Peptide was cleaved from resin with trifluoroacetic acid/triisopropyl silane/water/phenol (94:2.5:2.5:1) mixture and precipitated and washed (2x) in cold ethyl ether.

### 5.3.5 Synthesis of fluorescently labeled peptides:

Fluorescently activated esters [Alexa Fluor 555 carboxylic acid succinimidyl ester (1mg, Invitrogen), Alexa Fluor 488 carboxylic acid succinimidyl ester (1mg, Invitrogen)] were dissolved in NMP with catalytic amount of DIEA and stirred with resins attached to H-CAhxRGDS-NH<sub>2</sub> for 2 h at room temperature. Fluorescently tagged peptides were cleaved from resin with trifluoroacetic acid/triisopropyl silane/water/phenol (94:2.5:2.5:1) mixture, precipitated and washed (2x) in cold ethyl ether. The products denoted as AF<sub>555</sub>-AhxRGDSC-NH<sub>2</sub> and AF<sub>488</sub>-AhxRGDSC-NH<sub>2</sub> were used with no further purification.

### 5.3.6 Hydrogel synthesis:

50 µl of crosslinked hydrogel disks were formed by reacting four-arm 5000 PEG tetra-azide and corresponding crosslinkers in DMSO in the presence of copper (0.5 equivalents to alkyne) and base (DIPEA) at room temperature for 30 min. Monomer concentrations adjusted for 8 wt% PEG tetraazide in the final macromer mixture for 1:1.2 ratio of alkyne to azide functionality. Gels were washed in saturated solution of

ammonium chloride to remove the copper (5x for 30 min each time). Gels were swelled in PBS for atleast overnight before further use.

### **5.3.7 Biochemical patterning:**

Hydrogels were swollen in PBS containing Irgacure 2949 (I2949, Ciba) and 10 mM patterning reagent (AF<sub>555</sub>-CAhxRGDS-NH<sub>2</sub> or AF<sub>488</sub>-CAhxRGDS-NH<sub>2</sub>) for 2 h. Using conventional photolithographic techniques, gels were exposed to collimated UV light (365 nm wavelength) for various times and various light intensities as indicated. After the patterning is complete, gels were washed in PBS for 2 h to diffuse out the unreacted components. Patterning concentrations were determined using confocal microscopy by comparing the average fluorescence intensity averaged over a 400  $\mu\text{m}^3$  volume 100  $\mu\text{m}$  below gel surface against a standard curve relating fluorescence intensity to that of gels swollen in known concentrations of the patterning agent. 2-photon patterning experiments were conducted using 710 Zeiss LSM confocal microscope with 20x water objective at 720 nm using laser (details). 520x520 resolution regions of interest (ROIs) were constructed using the Zeiss imaging software and 1  $\mu\text{m}$  thick sections in z-direction were exposed to the laser.



## 5.4 References:

1. Zhu, J. Bioactive Modification of Poly(ethylene glycol) Hydrogels for Tissue Engineering. *Biomaterials* **31**, 4639–4656 (2010).
2. Fittkau, M. H. *et al.* The selective modulation of endothelial cell mobility on RGD peptide containing surfaces by YIGSR peptides. *Biomaterials* **26**, 167–174 (2005).
3. Schmidt, D. R. & Kao, W. J. Monocyte activation in response to polyethylene glycol hydrogels grafted with RGD and PHSRN separated by interpositional spacers of various lengths. *J Biomed Mater Res A* **83**, 617–625 (2007).
4. Burdick, J. A. & Anseth, K. S. Photoencapsulation of osteoblasts in injectable RGD-modified PEG hydrogels for bone tissue engineering. *Biomaterials* **23**, 4315–4323 (2002).
5. Liu Tsang, V. *et al.* Fabrication of 3D hepatic tissues by additive photopatterning of cellular hydrogels. *FASEB J.* **21**, 790–801 (2007).
6. Lutolf, M. P. *et al.* Synthetic matrix metalloproteinase-sensitive hydrogels for the conduction of tissue regeneration: Engineering cell-invasion characteristics. *PNAS* **100**, 5413–5418 (2003).
7. Lutolf, M. P. & Hubbell, J. A. Synthetic biomaterials as instructive extracellular microenvironments for morphogenesis in tissue engineering. *Nature Biotechnology* **23**, 47–55 (2005).
8. Lee, S.-H., Moon, J. J., Miller, J. S. & West, J. L. Poly(ethylene glycol) hydrogels conjugated with a collagenase-sensitive fluorogenic substrate to visualize collagenase activity during three-dimensional cell migration. *Biomaterials* **28**, 3163–3170 (2007).
9. Aimetti, A. A., Machen, A. J. & Anseth, K. S. Poly(ethylene glycol) hydrogels formed by thiol-ene photopolymerization for enzyme-responsive protein delivery. *Biomaterials* **30**, 6048–6054 (2009).
10. Lin, C.-C. & Anseth, K. S. Controlling Affinity Binding with Peptide-Functionalized Poly(ethylene glycol) Hydrogels. *Adv Funct Mater* **19**, 2325 (2009).
11. Impellitteri, N. A., Toepke, M. W., Lan Levengood, S. K. & Murphy, W. L. Specific VEGF sequestering and release using peptide-functionalized hydrogel microspheres. *Biomaterials* **33**, 3475–3484 (2012).
12. Nimmo, C. M. & Shoichet, M. S. Regenerative Biomaterials that ‘Click’: Simple, Aqueous-Based Protocols for Hydrogel Synthesis, Surface Immobilization, and 3D Patterning. *Bioconjugate Chem.* **22**, 2199–2209 (2011).

13. DeForest, C. A., Polizzotti, B. D. & Anseth, K. S. Sequential click reactions for synthesizing and patterning three-dimensional cell microenvironments. *Nature Materials* **8**, 659–664 (2009).
14. Seidlits, S. K., Schmidt, C. E. & Shear, J. B. High-Resolution Patterning of Hydrogels in Three Dimensions using Direct-Write Photofabrication for Cell Guidance. *Advanced Functional Materials* **19**, 3543–3551 (2009).
15. Khetan, S. & Burdick, J. A. Patterning network structure to spatially control cellular remodeling and stem cell fate within 3-dimensional hydrogels. *Biomaterials* **31**, 8228–8234 (2010).
16. Hahn, M. S., Miller, J. S. & West, J. L. Three-Dimensional Biochemical and Biomechanical Patterning of Hydrogels for Guiding Cell Behavior. *Advanced Materials* **18**, 2679–2684 (2006).
17. Aizawa, Y., Wylie, R. & Shoichet, M. Endothelial Cell Guidance in 3D Patterned Scaffolds. *Advanced Materials* **22**, 4831–4835 (2010).
18. Arumugam, S. & Popik, V. V. Attach, Remove, or Replace: Reversible Surface Functionalization Using Thiol–Quinone Methide Photoclick Chemistry. *J. Am. Chem. Soc.* **134**, 8408–8411 (2012).
19. Scott, T. F., Schneider, A. D., Cook, W. D. & Bowman, C. N. Photoinduced Plasticity in Cross-Linked Polymers. *Science* **308**, 1615–1617 (2005).
20. Kloxin, C. J., Scott, T. F. & Bowman, C. N. Stress relaxation via addition-fragmentation chain transfer in a thiol-ene photopolymerization. *Macromolecules* **42**, 2551–2556 (2009).
21. Kloxin, C. J., Scott, T. F., Park, H. Y. & Bowman, C. N. Mechanophotopatterning on a Photoresponsive Elastomer. *Advanced Materials* **23**, 1977–1981 (2011).
22. Fairbanks, B. D. *et al.* A Versatile Synthetic Extracellular Matrix Mimic via Thiol-Norbornene Photopolymerization. *Advanced Materials* **21**, 5005–5010 (2009).
23. Anderson, S. B., Lin, C.-C., Kuntzler, D. V. & Anseth, K. S. The performance of human mesenchymal stem cells encapsulated in cell-degradable polymer-peptide hydrogels. *Biomaterials* **32**, 3564–3574 (2011).
24. Lin, C.-C., Raza, A. & Shih, H. PEG hydrogels formed by thiol-ene photo-click chemistry and their effect on the formation and recovery of insulin-secreting cell spheroids. *Biomaterials* **32**, 9685–9695 (2011).
25. Polizzotti, B. D., Fairbanks, B. D. & Anseth, K. S. Three-dimensional biochemical patterning of click-based composite hydrogels via thiolene photopolymerization. *Biomacromolecules* **9**, 1084–1087 (2008).

26. Chiefari, J. *et al.* Living Free-Radical Polymerization by Reversible Addition–Fragmentation Chain Transfer: The RAFT Process. *Macromolecules* **31**, 5559–5562 (1998).
27. Malkoch, M. *et al.* Synthesis of well-defined hydrogel networks using Click chemistry. *Chem. Commun.* 2774–2776 (2006).doi:10.1039/B603438A
28. Stockmayer, W. H. Theory of Molecular Size Distribution and Gel Formation in Branched Polymers II. General Cross Linking. *The Journal of Chemical Physics* **12**, 125–131 (1944).
29. Cramer, N. B., Davies, T., O’Brien, A. K. & Bowman, C. N. Mechanism and Modeling of a Thiol–Ene Photopolymerization. *Macromolecules* **36**, 4631–4636 (2003).
30. DeForest, C. A. & Anseth, K. S. Photoreversible Patterning of Biomolecules within Click-Based Hydrogels. *Angewandte Chemie International Edition* **51**, 1816–1819 (2012).
31. Salinas, C. N. & Anseth, K. S. The influence of the RGD peptide motif and its contextual presentation in PEG gels on human mesenchymal stem cell viability. *J Tissue Eng Regen Med* **2**, 296–304 (2008).
32. Culver, J. C. *et al.* Three-Dimensional Biomimetic Patterning in Hydrogels to Guide Cellular Organization. *Advanced Materials* **24**, 2344–2348 (2012).
33. Asmussen, S., Arenas, G., Cook, W. D. & Vallo, C. Photoinitiation rate profiles during polymerization of a dimethacrylate-based resin photoinitiated with camphorquinone/amine. Influence of initiator photobleaching rate. *European Polymer Journal* **45**, 515–522 (2009).

## 5.5 Supplementary Information:

### 5.5.1 Derivation of Rate of addition to allyl sulphide containing networks:

Rate of reaction during thiol-ene photo-coupling is given by:

$$R_p \propto [C = C][S \cdot] \quad (1)$$

The initiator concentration,  $[I]$ , during the photo-initiation is given by<sup>33</sup>,

$$\frac{[I]}{[I]_0} = \frac{1}{\varepsilon[I]_0L} \ln[1 - (1 - e^{\varepsilon[I]_0L})e^{-\varepsilon\Phi I_0t}] \quad (2)$$

where,  $L$  = thickness of the sample (= 1 cm for the present study),  $[I]_0$  = initiator concentration at  $t = 0$  sec and  $\Phi$  = quantum yield of photo-initiator consumption (0.05 for I2959),  $\varepsilon$  = wavelength dependent absorption co-efficient (15.42 for I2959 at 365 nm), and  $I_0$  = irradiance at the base of the sample.

For the time scales considered in this study ( $\leq 600$  sec), the equation can be expanded using Taylor series and simplified to,

$$\frac{[I]}{[I]_0} = \frac{(e^{\varepsilon[I]_0L} - 1)}{\varepsilon[I]_0L} (1 - \varepsilon\Phi I_0t) \quad (3)$$

For the conditions employed for patterning in this study, the initial factor on R.H.S the of above equation  $\sim 1$  resulting in,

$$\frac{[I]}{[I]_0} = (1 - \varepsilon\Phi I_0t) \quad (4)$$

The total number of radicals produced during the patterning is then given by,

$$[I]_0 - [I] = \varepsilon\Phi[I]_0I_0t \quad (5)$$

To first approximation, the above equation represents the thiyl radical concentration generated during the photo-coupling reaction. By substituting for thiyl radical concentration in Eq. 1 we get,

$$R_p \propto [I]_0I_0t \quad (6)$$

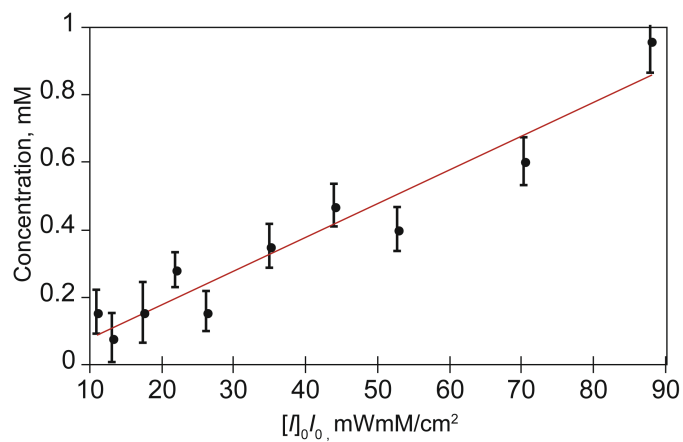


**Figure S5.1.** Amount of AF<sub>555</sub>AhxRGDSC photopatterned into the network as a function of  $[I]_0I_0$ . All the data points collapse onto a straight line validating Equation 6.

## CHAPTER 6

### CONCLUSIONS AND RECOMMENDATIONS

---

Cell functions such as proliferation, differentiation and migration are greatly influenced by wide variety of cues present in the surrounding extra-cellular matrix (ECM). This highly complex, bi-directional interaction of cells with the ECM is difficult to assay within a cell's native environment, due to myriad of constantly changing confounding factors that are difficult to isolate systematically. However, information on the role of this outside-in signaling is very important in understand how to regulate fundamental biological functions and also to design appropriate biomaterial platforms for applications in tissue engineering and regenerative medicine. Towards this goal, the main objective of this thesis was to design appropriate biomaterials platforms to study and understand how osteoprogenitor cells, human mesenchymal stem cells (hMSCs), receive and exchange information with their external, ECM environment. A synthetic poly(ethylene glycol) (PEG) hydrogel platform was chosen as the base scaffold chemistry, due to its hydrophilicity and non-fouling characteristics that allow one to form materials with tunable material properties and systematically introduce biological ligands to test their effect on hMSC functions. By altering the PEG chemistry, we synthesized programmable hydrogel substrates that enabled us to study the effect of the biochemical and biophysical environment on the differentiation program of hMSCs with the ultimate goal of understanding how biomaterial niches might be programmed to promote osteogenic differentiation and bone regeneration with hMSCs.

In Chapter 3, we focused on phosphate functionalized PEG hydrogels, formed via chain growth polymerization, to gain knowledge about how this small molecule chemistry found in the mineral phase of bone might influence osteogenic differentiation of hMSCs. *In vivo*, phosphate functional groups are abundantly found in bone ECM and have been previously shown to induce osteogenic differentiation in hMSCs.<sup>1</sup> Although, the mechanism of how this chemical functional group influenced the genetic program in hMSCs was unknown. Towards gaining a better mechanistic understanding, we examined the nature of hMSC interaction with phosphate functionalized PEG gels, and the role of integrin signaling in influencing osteogenic differentiation in hMSCs. Our results demonstrated that hMSCs interact indirectly with the phosphate functional groups via adsorbed ECM proteins. Integrin signaling via focal adhesion kinase (FAK) was determined to be responsible for up-regulation of alkaline phosphatase activity (ALP) and osteogenic related genes (i.e. CBFA1, Osteopontin and Coll-Ia) in hMSCs.

Building from this work, a natural direction would be to explore the interplay between substrate elasticity and integrin signaling and their potential synergistic effects on hMSC differentiation versus self-renewal. Since phosphate functional groups were found to be osteoinductive (i.e., promotes osteogenic differentiation) in the absence of growth factors or media additives, examining topographical effects on hMSC differentiation would be another natural extension of the research presented in this thesis. Topographical features such as micrometer-range ridges and wells of varying feature size and aspect ratio can be formed by incorporating photodegradable moiety<sup>2</sup> into the phosphate functionalized PEG gel and differential response of osteogenic genes of hMSC can be assessed. Morphological responses of hMSCs to such topographies have been

recently studied and characterized on such topographies using the photodegradable PEG hydrogels<sup>3</sup> and similar methods can be easily adopted here. Collectively, such information could prove useful for the design of improved in vitro culture systems for hMSC and/or enabling of the engineering of relevant cell carrier materials for applications in tissue engineering of bone.

Chapter 4 then presents the synthesis of  $\alpha 5$  integrin priming hydrogels and characterizes the interplay between  $\alpha 5$  integrin signaling and substrate elasticity on hMSC osteogenic differentiation. Building on previous literature that demonstrated  $\alpha 5$  was involved in downstream signaling events in dexamethasone induced osteogenic differentiation of hMSCs,<sup>4</sup> we utilized ideal two-dimensional peptide-functionalized PEG substrates to understand the role of substrate elasticity on this pathway. Our results established that integrin binding and signaling (determined by focal adhesion area) are greatly influenced by substrate elasticity. Interestingly, a positive correlation was observed between focal adhesion area, f-actin organization and osteogenic differentiation of hMSCs on these gels that allowed hMSCs form highly organized actin cytoskeleton. A significantly higher focal adhesion area resulted in increased ALP activity and osteogenic gene expression in hMSCs cultured on stiff substrates in the absence of osteogenic cues. To fully understand the interplay of the substrate elasticity and integrin signaling on hMSC differentiation, further studies should focus on examining the signaling pathways involved. These pathways might include FAK, Rho/ROCK, PI3K dependent pathways which were implicated by previous studies in substrate directed differentiation program in hMSCs.<sup>5-8</sup>



More recently, YAP (Yes-associated protein) and TAZ (transcriptional coactivator with PDZ-binding motif) have also been identified as nuclear relays of mechanical signals such as rigidity and cell shape in hMSCs.<sup>9</sup> Examining the role of  $\alpha 5$  integrin signaling on the regulation of the YAP and TAZ could be a promising new direction of research building on the results of this chapter. Finally, the cyl(RRETAWA) gels developed in this thesis, along with the PEG crosslinking chemistries, provide opportunities to tailor the biophysical properties of the gel and presentation of biochemical cues systematically and, hence, are well suited to conduct studies that examine the individual and synergistic role of these matrix cues on intracellular signaling dynamics.

Towards developing programmable hydrogels that enable for dynamic presentation of biochemical cues, we have synthesized PEG hydrogels that were homogeneously functionalized with addition-fragmentation-chain transfer capable allyl sulfide functional groups, as presented in Chapter 5. Photo-patterning of peptide motifs on to the allyl sulfide functional group via cytocompatible thiol-ene photoclick chemistry was successfully demonstrated via sterolithography and 2-photon lithography techniques. Biochemical functionalization of the hydrogels was characterized using a thiol-containing RGD peptide motif found in the ECM protein fibronectin using wavelengths, initiator concentrations and time lengths previously shown to be cytocompatible.<sup>10-12</sup> Conditions were identified that allowed patterning of the peptide at concentrations that have been previously shown to be capable to induce cell migration, cell attachment and differentiation.<sup>13-17</sup> Photo-lithographic techniques used to pattern adhesive peptides allowed to achieve sub-micron size of the features with high fidelity in

pattern transfer within 10 minutes time scale. Further, reversible exchange of the patterned peptide motifs was demonstrated and the kinetics of the reversible exchange was characterized. By controlling the imaging parameters of 2-photon laser, we demonstrated the ability over complete control of the amount of the peptide exchanged. While the cytocompatibility of the conditions and reactions used in this study has been extensively established previously, the ability of to conduct the exchange reactions in the presence of cells should be an immediate goal of the future experiments.

The methods and conditions studied in this chapter allowed us to use exchange reactions to form opposing step gradients of two peptide motifs demonstrated by RGDS peptides tagged with two different fluorophores. All of the exchange reactions developed in this thesis were based on the allyl sulfide functional group presented as a backbone of the network in the crosslinker. Hence, upon conducting a thiol-ene reaction with this functional group, it undergoes fragmentation and results in scission of the cross-link. This characteristic property of the hydrogel networks could be exploited to form physical channels or topographies functionalized with biochemical cues simply by controlling the photo-patterning process. However, the lower molar absorptivity of the initiator used in chapter 5, I2959,<sup>18</sup> at 365 nm requires very long exposure times (>30 min for the hydrogel formulation studied) to produce radical concentration required to get the required mass loss to form physical channels. Instead, the high molar absorptivity of LAP photoinitiator used in chapter 4 can be exploited to form the physical channels with less exposure times (< 10 min for the hydrogel formulation studied). Additionally, the biochemical functionalization of the formed channels or topographies would be reversible resulting, in hydrogels that might be used to conduct experiments focused on guiding cell

migration dynamically and in 3D and/or understanding the interplay between topography and biochemical cues on differentiation of hMSCs.

Finally, this thesis used linear allyl sulfide functional group cross-linkers to form ideal step growth hydrogel networks, so repeated patterning of the biochemical cues could potentially lead to a significant reduction in the substrate elasticity, which limits some of the applicability and control of the biomaterial properties. Alternatively, the allyl sulfide functional group could be tethered to the backbone of the network, as shown in Figure 6.1a, to avoid the scission of cross-links upon biochemical functionalization of the network. Note that the proposed scheme utilizes cyclic allyl sulfide as opposed to linear version used in this thesis, but would allow for biofunctionalization of the network without altering the network. Further, the allyl sulfide functional group used in this thesis is symmetric about the double bond and probabilistically leads to the addition of the external thiol-containing peptide. This could potentially pose difficulties during further exchange reactions with the already patterned cues. Although we demonstrated stable exchange of the peptide motifs using the material formulations developed in this thesis. However, to achieve more clean and robust exchange reactions, the functional group could be designed to be asymmetric about the double bond, conceptually depicted in Figure 6.1b, to direct the  $\beta$ -scission.

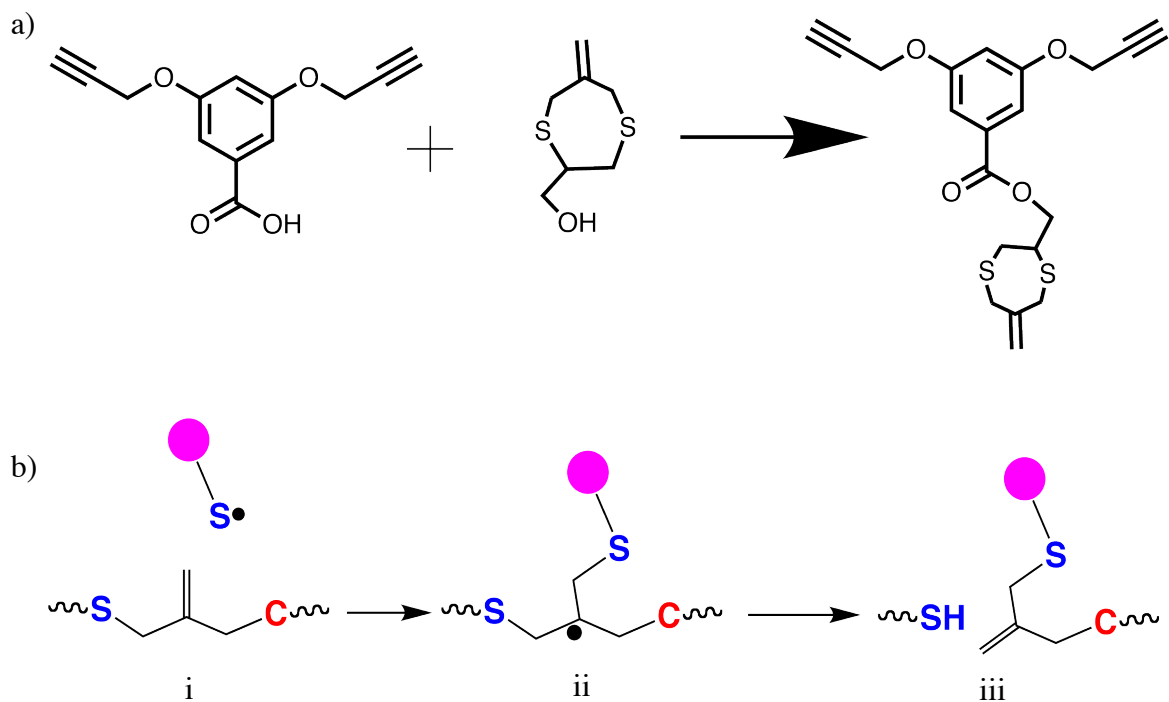


**Figure 6.1.** a) Development of addition-fragmentation-chain transfer (AFCT) capable hydrogels to achieve independent control of reversible patterning and substrate elasticity. A cyclic allyl sulfide can be covalently tethered to the cross-linker used to form the hydrogels reported in Chapter 5. b) Controlling the direction of  $\beta$ -scission of allyl sulfide intermediate upon attack by a thiyl radical. Asymmetric allyl sulfide functional group (i) upon attack by thiyl radical forms an intermediate (ii) that undergoes  $\beta$ -scission only in the direction of sulphur atom resulting in (iii)

Towards the application of these adaptable networks, recent seminal studies on geometric control of hMSC differentiation program have generated great interest in trying to define the underlying mechanisms.<sup>19</sup> While these studies have demonstrated a causal role of these cues on the terminal fate of hMSCs, they have been limited to cultures on static materials, and the methods cannot be readily extended to control these cues dynamically. Thus, towards understanding the underlying mechanism during the translation of geometric cues into controlling key regulators of cell fate, dynamic control of material properties can prove beneficial. As one example, although the geometric

shape of a cell can be similar, the cytoskeleton organization will be highly dependent on the distribution of the integrin binding to the underlying substrate. This was recently demonstrated by Théry and colleagues (Figure 6.2)<sup>20</sup> where the distribution of an adhesive ligand dictated the spatial organization of the focal adhesions and actin network in retinal pigment epithelial cells (RPE1) while the overall geometry of the cells remained same. Ultimately, actin organization regulates the force distributions exerted and experienced by cells. It has been shown that Rac activation induces cell membrane ruffling i.e., formation of membrane protrusions containing a meshwork of newly formed stress fibers (confined to the sites of adhesion) and Rho activation controls the contractility of the stress fibers.<sup>21,22</sup> Hence, the spatial distribution of the focal adhesions and actin stress fibers will differentially regulate the activation of Rho and Rac proteins which are known to play a role in genetic program of cells including hMSCs.<sup>6</sup> Hence, we hypothesize that the geometric control of hMSC fate may be due to the differences in the distribution of the actin cytoskeleton organization.

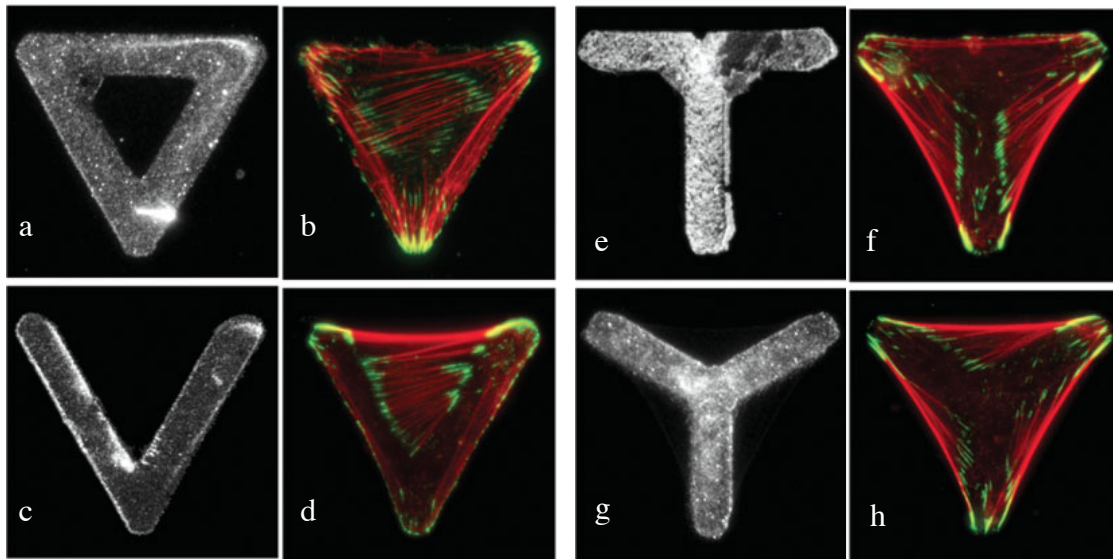


**Figure 6.2. Adhesive patterns define actin-organization maintaining the geometric shape of cell.** Brightfield images (a,c,e,g) show geometric shapes of adhesive patterns. Immunostained images (b,d,f,h) show vinculin (green) and f-actin (red) organization in on different geometric patterns studied. Images clearly show variation of f-actin organization and focal adhesion localization in retinal pigment epithelial cells with same geometric shape.<sup>9</sup>

We propose that the materials developed in this thesis (Chapter 5) allow a ‘living’ strategy towards cell scaffolds that should be suitable to conduct unique experiments that allows for independent control over the geometry and actin organization of hMSCs dynamically (Figure 6.3). Such studies could provide a great deal of insight into the timeline of matrix signal presentation, and the proposed strategy could allow one to gain unique information towards the understanding of how geometric signals, especially dynamic changes in these signals, can be exploited to control and manipulate cell fate.

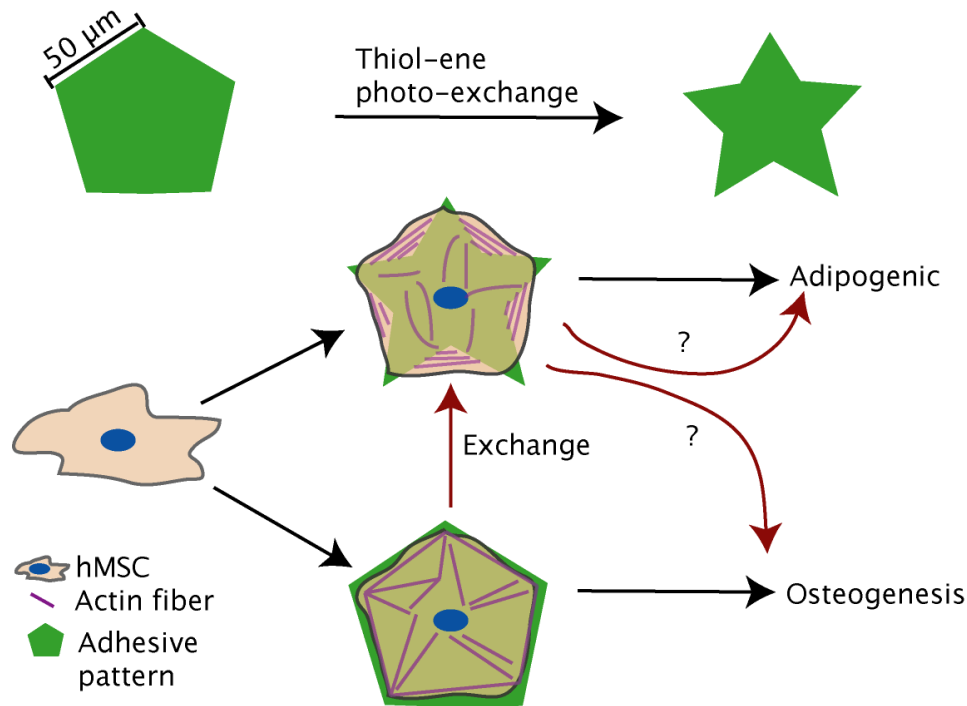


**Figure 6.3. Two-dimensional modulation of f-actin and vinculin organization maintaining the geometric shape.** A) Cells can be initially seeded onto adhesive patterns (e.g. pentagon pattern shown) formed on allyl sulfide containing PEG gels. At a later time point, specific regions of the adhesive pattern can be exchanged with a non-adhesive peptide in the presence of cells, resulting in a new pattern. Cells should re-modulate the f-actin and vinculin organization. Such dynamic modulation of f-actin organization could be used to study the interplay of cell geometry and f-actin organization on hMSC differentiation.

Finally, the reversible exchange strategy can be exploited to construct a time-line map of role of specific integrin signaling on genetic program of hMSCs. Particularly,  $\alpha 5$  integrin priming hydrogels developed in chapter 4 can be programmed to be exchanged with a promiscuous integrin binding RGD peptide at specific time points during culture and osteogenic differentiation can be studied as conceptually depicted in Figure 6.4. Combined with the results presented in chapter 4, such studies would answer

fundamental biological questions related to the sensitivity of the  $\alpha 5\beta 1$  integrin signaling on hMSC osteogenic differentiation.

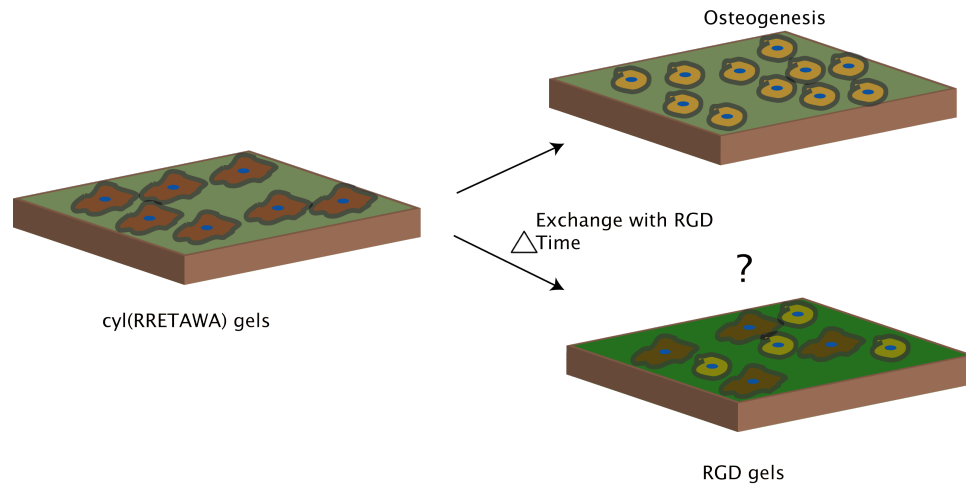


**Figure 6.4. Mapping osteogenic differentiation of hMSCs on  $\alpha 5$  integrin priming cyl(RRETAWA) gels.** At specific time points, cyl(RRETAWA) peptide can be exchanged with a non-specific integrin binding CRGDS peptide, and osteogenic differentiation assayed to map osteogenic differentiation of hMSCs induced by  $\alpha 5$  integrin signaling.

### 6.1 References:

1. Benoit, D. S. W., Schwartz, M. P., Durney, A. R. & Anseth, K. S. Small functional groups for controlled differentiation of hydrogel-encapsulated human mesenchymal stem cells. *Nat Mater* **7**, 816–823 (2008).
2. Kloxin, A. M., Kasko, A. M., Salinas, C. N. & Anseth, K. S. Photodegradable Hydrogels for Dynamic Tuning of Physical and Chemical Properties. *Science* **324**, 59–63 (2009).
3. Kirschner, C. M. & Anseth, K. S. In Situ Control of Cell Substrate Microtopographies Using Photolabile Hydrogels. *Small* (2012).doi:10.1002/sml.201201841
4. Hamidouche, Z. *et al.* Priming integrin alpha5 promotes human mesenchymal stromal cell osteoblast differentiation and osteogenesis. *Proc. Natl. Acad. Sci. U.S.A.* **106**, 18587–18591 (2009).
5. Engler, A. J., Sen, S., Sweeney, H. L. & Discher, D. E. Matrix elasticity directs stem cell lineage specification. *Cell* **126**, 677–689 (2006).



6. McBeath, R., Pirone, D. M., Nelson, C. M., Bhadriraju, K. & Chen, C. S. Cell shape, cytoskeletal tension, and RhoA regulate stem cell lineage commitment. *Dev. Cell* **6**, 483–495 (2004).
7. Petit, V. & Thiery, J. P. Focal adhesions: structure and dynamics. *Biol. Cell* **92**, 477–494 (2000).
8. Xu, B. *et al.* RhoA/ROCK, cytoskeletal dynamics, and focal adhesion kinase are required for mechanical stretch-induced tenogenic differentiation of human mesenchymal stem cells. *J. Cell. Physiol.* **227**, 2722–2729 (2012).
9. Dupont, S. *et al.* Role of YAP/TAZ in mechanotransduction. *Nature* **474**, 179–183 (2011).
10. DeForest, C. A. & Anseth, K. S. Cytocompatible click-based hydrogels with dynamically tunable properties through orthogonal photoconjugation and photocleavage reactions. *Nature Chemistry* **3**, 925–931 (2011).
11. DeForest, C. A., Sims, E. A. & Anseth, K. S. Peptide-Functionalized Click Hydrogels with Independently Tunable Mechanics and Chemical Functionality for 3D Cell Culture. *Chem. Mater.* **22**, 4783–4790 (2010).
12. Bryant, S. J., Nuttelman, C. R. & Anseth, K. S. Cytocompatibility of UV and visible light photoinitiating systems on cultured NIH/3T3 fibroblasts in vitro. *J Biomater Sci Polym Ed* **11**, 439–457 (2000).
13. Hahn, M. S., Miller, J. S. & West, J. L. Three-Dimensional Biochemical and Biomechanical Patterning of Hydrogels for Guiding Cell Behavior. *Advanced Materials* **18**, 2679–2684 (2006).
14. Mann, B. K., Gobin, A. S., Tsai, A. T., Schmedlen, R. H. & West, J. L. Smooth muscle cell growth in photopolymerized hydrogels with cell adhesive and proteolytically degradable domains: synthetic ECM analogs for tissue engineering. *Biomaterials* **22**, 3045–3051 (2001).
15. Leslie-Barbick, J. E., Shen, C., Chen, C. & West, J. L. Micron-scale spatially patterned, covalently immobilized vascular endothelial growth factor on hydrogels accelerates endothelial tubulogenesis and increases cellular angiogenic responses. *Tissue Eng Part A* **17**, 221–229 (2011).
16. Gobin, A. S. & West, J. L. Cell migration through defined, synthetic ECM analogs. *FASEB J.* **16**, 751–753 (2002).
17. DeForest, C. A., Polizzotti, B. D. & Anseth, K. S. Sequential click reactions for synthesizing and patterning three-dimensional cell microenvironments. *Nature Materials* **8**, 659–664 (2009).

18. Fairbanks, B. D., Schwartz, M. P., Bowman, C. N. & Anseth, K. S. Photoinitiated polymerization of PEG-diacrylate with lithium phenyl-2,4,6-trimethylbenzoylphosphinate: polymerization rate and cytocompatibility. *Biomaterials* **30**, 6702–6707 (2009).
19. Kilian, K. A., Bugarija, B., Lahn, B. T. & Mrksich, M. Geometric cues for directing the differentiation of mesenchymal stem cells. *PNAS* **107**, 4872–4877 (2010).
20. Théry, M., Pépin, A., Dressaire, E., Chen, Y. & Bornens, M. Cell distribution of stress fibres in response to the geometry of the adhesive environment. *Cell Motil. Cytoskeleton* **63**, 341–355 (2006).
21. Ridley, A. J. Membrane ruffling and signal transduction. *BioEssays* **16**, 321–327 (1994).
22. Katoh, K. *et al.* Rho-Kinase-Mediated Contraction of Isolated Stress Fibers. *J Cell Biol* **153**, 569–584 (2001).

## CHAPTER 7

### BIBLIOGRAPHY

---

- Abdelrazik, Heba, Grazia M Spaggiari, Laura Chiossone, and Lorenzo Moretta. 2011. "Mesenchymal Stem Cells Expanded in Human Platelet Lysate Display a Decreased Inhibitory Capacity on T- and NK-cell Proliferation and Function." *European Journal of Immunology* 41 (11) (November): 3281–3290. doi:10.1002/eji.201141542.
- Adzima, Brian J., H. Alan Aguirre, Christopher J. Kloxin, Timothy F. Scott, and Christopher N. Bowman. 2008. "Rheological and Chemical Analysis of Reverse Gelation in a Covalently Cross-Linked Diels–Alder Polymer Network." *Macromolecules* 41 (23) (December 9): 9112–9117. doi:10.1021/ma801863d.
- Aimetti, Alex A., Alexandra J. Machen, and Kristi S. Anseth. 2009. "Poly(ethylene Glycol) Hydrogels Formed by Thiol-ene Photopolymerization for Enzyme-responsive Protein Delivery." *Biomaterials* 30 (30) (October): 6048–6054. doi:10.1016/j.biomaterials.2009.07.043.
- Aizawa, Yukie, Ryan Wylie, and Molly Shoichet. 2010. "Endothelial Cell Guidance in 3D Patterned Scaffolds." *Advanced Materials* 22 (43): 4831–4835. doi:10.1002/adma.201001855.
- Albrecht, Dirk R, Valerie Liu Tsang, Robert L Sah, and Sangeeta N Bhatia. 2005. "Photo- and Electropatterning of Hydrogel-encapsulated Living Cell Arrays." *Lab on a Chip* 5 (1) (January): 111–118. doi:10.1039/b406953f.
- An, Chunhou, Yang Cheng, Quan Yuan, and Jianjun Li. 2010. "IGF-1 and BMP-2 Induces Differentiation of Adipose-derived Mesenchymal Stem Cells into Chondrocytes-like Cells." *Annals of Biomedical Engineering* 38 (4) (April): 1647–1654. doi:10.1007/s10439-009-9892-x.
- Anderson, Daniel G, Shulamit Levenberg, and Robert Langer. 2004. "Nanoliter-scale Synthesis of Arrayed Biomaterials and Application to Human Embryonic Stem Cells." *Nat Biotech* 22 (7) (July): 863–866. doi:10.1038/nbt981.
- Anderson, Sarah B, Chien-Chi Lin, Donna V Kuntzler, and Kristi S Anseth. 2011. "The Performance of Human Mesenchymal Stem Cells Encapsulated in Cell-degradable Polymer-peptide Hydrogels." *Biomaterials* 32 (14) (May): 3564–3574. doi:10.1016/j.biomaterials.2011.01.064.
- Anselme, K., and M. Biggerelle. 2005. "Topography Effects of Pure Titanium Substrates on Human Osteoblast Long-term Adhesion." *Acta Biomaterialia* 1 (2) (March): 211–222. doi:10.1016/j.actbio.2004.11.009.

- Anseth, Kristi S, Cynthia M Wang, and Christopher N Bowman. 1994. "Reaction Behaviour and Kinetic Constants for Photopolymerizations of Multi(meth)acrylate Monomers." *Polymer* 35 (15) (July): 3243–3250. doi:10.1016/0032-3861(94)90129-5.
- Arumugam, Selvanathan, and Vladimir V. Popik. 2012. "Attach, Remove, or Replace: Reversible Surface Functionalization Using Thiol–Quinone Methide Photoclick Chemistry." *Journal of the American Chemical Society* 134 (20) (May 23): 8408–8411. doi:10.1021/ja302970x.
- Asmussen, Silvana, Gustavo Arenas, Wayne D. Cook, and Claudia Vallo. 2009. "Photoinitiation Rate Profiles During Polymerization of a Dimethacrylate-based Resin Photoinitiated with Camphorquinone/amine. Influence of Initiator Photobleaching Rate." *European Polymer Journal* 45 (2) (February): 515–522. doi:10.1016/j.eurpolymj.2008.11.005.
- Athanassiou, G, and D Deligianni. 2001. "Adhesion Strength of Individual Human Bone Marrow Cells to Fibronectin. Integrin Beta1-mediated Adhesion." *Journal of Materials Science. Materials in Medicine* 12 (10-12) (December): 965–970.
- Aubin, Jane E., and Kursad Turksen. 1996. "Monoclonal Antibodies as Tools for Studying the Osteoblast Lineage." *Microscopy Research and Technique* 33 (2): 128–140. doi:10.1002/(SICI)1097-0029(19960201)33:2<128::AID-JEMT4>3.0.CO;2-P.
- Azagarsamy, Malar A., Daniel L. Alge, Srinidhi J. Radhakrishnan, Mark W. Tibbitt, and Kristi S. Anseth. 2012. "Photocontrolled Nanoparticles for On-Demand Release of Proteins." *Biomacromolecules* 13 (8) (August 13): 2219–2224. doi:10.1021/bm300646q.
- Bai, Xiaodan, Guangze Li, Can Zhao, Hongzhang Duan, and Fujun Qu. 2011. "BMP7 Induces the Differentiation of Bone Marrow-derived Mesenchymal Cells into Chondrocytes." *Medical & Biological Engineering & Computing* 49 (6) (June): 687–692. doi:10.1007/s11517-010-0729-4.
- Barry, Frank P, and J Mary Murphy. 2004. "Mesenchymal Stem Cells: Clinical Applications and Biological Characterization." *The International Journal of Biochemistry & Cell Biology* 36 (4) (April): 568–584. doi:10.1016/j.biocel.2003.11.001.
- Beamish, Jeffrey A, Junmin Zhu, Kandice Kottke-Marchant, and Roger E Marchant. 2010. "The Effects of Monoacrylated Poly(ethylene Glycol) on the Properties of Poly(ethylene Glycol) Diacrylate Hydrogels Used for Tissue Engineering." *Journal of Biomedical Materials Research. Part A* 92 (2) (February): 441–450. doi:10.1002/jbm.a.32353.
- Benoit, Danielle S W, Michael P Schwartz, Andrew R Durney, and Kristi S Anseth. 2008. "Small Functional Groups for Controlled Differentiation of Hydrogel-encapsulated Human Mesenchymal Stem Cells." *Nature Materials* 7 (10) (October): 816–823. doi:10.1038/nmat2269.
- Benoit, Danielle S W, Margaret C Tripodi, James O Blanchette, Steve J Langer, Leslie A Leinwand, and Kristi S Anseth. 2007. "Integrin-linked Kinase Production Prevents

- Anoikis in Human Mesenchymal Stem Cells.” *Journal of Biomedical Materials Research. Part A* 81 (2) (May): 259–268. doi:10.1002/jbm.a.31292.
- Bianco, Paolo, Mara Riminucci, Stan Gronthos, and Pamela Gehron Robey. 2001. “Bone Marrow Stromal Stem Cells: Nature, Biology, and Potential Applications.” *STEM CELLS* 19 (3): 180–192. doi:10.1634/stemcells.19-3-180.
- Bruder, S P, K H Kraus, V M Goldberg, and S Kadiyala. 1998. “The Effect of Implants Loaded with Autologous Mesenchymal Stem Cells on the Healing of Canine Segmental Bone Defects.” *The Journal of Bone and Joint Surgery. American Volume* 80 (7) (July): 985–996.
- Bryant, S J, C R Nuttelman, and K S Anseth. 2000a. “Cytocompatibility of UV and Visible Light Photoinitiating Systems on Cultured NIH/3T3 Fibroblasts in Vitro.” *Journal of Biomaterials Science. Polymer Edition* 11 (5): 439–457.
- Burdick, Jason A, and Kristi S Anseth. 2002a. “Photoencapsulation of Osteoblasts in Injectable RGD-modified PEG Hydrogels for Bone Tissue Engineering.” *Biomaterials* 23 (22) (November): 4315–4323.
- Buxton, Amanda N, Junmin Zhu, Roger Marchant, Jennifer L West, Jung U Yoo, and Brian Johnstone. 2007. “Design and Characterization of Poly(ethylene Glycol) Photopolymerizable Semi-interpenetrating Networks for Chondrogenesis of Human Mesenchymal Stem Cells.” *Tissue Engineering* 13 (10) (October): 2549–2560. doi:10.1089/ten.2007.0075.
- Campbell, Iain D., and Martin J. Humphries. 2011. “Integrin Structure, Activation, and Interactions.” *Cold Spring Harbor Perspectives in Biology* 3 (3) (March 1). doi:10.1101/cshperspect.a004994. <http://cshperspectives.cshlp.org/content/3/3/a004994>.
- Center for History and New Media. “Zotero Quick Start Guide.” [http://zotero.org/support/quick\\_start\\_guide](http://zotero.org/support/quick_start_guide).
- Chen, Zixian, Xiaofeng Wang, Yunchao Shao, Deyuan Shi, Tongyi Chen, Dafu Cui, and Xiaoxing Jiang. 2011. “Synthetic Osteogenic Growth Peptide Promotes Differentiation of Human Bone Marrow Mesenchymal Stem Cells to Osteoblasts via RhoA/ROCK Pathway.” *Molecular and Cellular Biochemistry* 358 (1): 221–227. doi:10.1007/s11010-011-0938-7.
- Cheng, S L, C F Lai, S D Blystone, and L V Avioli. 2001. “Bone Mineralization and Osteoblast Differentiation Are Negatively Modulated by Integrin Alpha(v)beta3.” *Journal of Bone and Mineral Research: The Official Journal of the American Society for Bone and Mineral Research* 16 (2) (February): 277–288. doi:10.1359/jbmr.2001.16.2.277.
- Chiefari, John, Y. K. (Bill) Chong, Frances Ercole, Julia Krstina, Justine Jeffery, Tam P. T. Le, Roshan T. A. Mayadunne, et al. 1998. “Living Free-Radical Polymerization by Reversible Addition–Fragmentation Chain Transfer: The RAFT Process.” *Macromolecules* 31 (16) (August 1): 5559–5562. doi:10.1021/ma9804951.

- Choi, Seung-Cheol, Su-Jin Kim, Ji-Hyun Choi, Chi-Yeon Park, Wan-Joo Shim, and Do-Sun Lim. 2008. "Fibroblast Growth Factor-2 and -4 Promote the Proliferation of Bone Marrow Mesenchymal Stem Cells by the Activation of the PI3K-Akt and ERK1/2 Signaling Pathways." *Stem Cells and Development* 17 (4) (August): 725–736. doi:10.1089/scd.2007.0230.
- Clark, Katherine, Roumen Pankov, Mark A. Travis, Janet A. Askari, A. Paul Mould, Susan E. Craig, Peter Newham, Kenneth M. Yamada, and Martin J. Humphries. 2005. "A Specific A5 $\beta$ 1 Integrin Conformation Promotes Directional Integrin Translocation and Fibronectin Matrix Formation." *Journal of Cell Science* 118 (Pt 2) (January 15): 291–300. doi:10.1242/jcs.01623.
- Corallini, Federica, Paola Secchiero, Antonio Paolo Beltrami, Daniela Cesselli, Elisa Puppato, Roberto Ferrari, Carlo Alberto Beltrami, and Giorgio Zauli. 2010. "TNF-alpha Modulates the Migratory Response of Mesenchymal Stem Cells to TRAIL." *Cellular and Molecular Life Sciences: CMLS* 67 (8) (April): 1307–1314. doi:10.1007/s00018-009-0246-5.
- Cramer, Neil B., Tanner Davies, Allison K. O'Brien, and Christopher N. Bowman. 2003. "Mechanism and Modeling of a Thiol–Ene Photopolymerization." *Macromolecules* 36 (12) (June 1): 4631–4636. doi:10.1021/ma034072x.
- Culver, James C., Joseph C. Hoffmann, Ross A. Poché, John H. Slater, Jennifer L. West, and Mary E. Dickinson. 2012a. "Three-Dimensional Biomimetic Patterning in Hydrogels to Guide Cellular Organization." *Advanced Materials* 24 (17): 2344–2348. doi:10.1002/adma.201200395.
- Dalby, Matthew J., Nikolaj Gadegaard, Rahul Tare, Abhay Andar, Mathis O. Riehle, Pawel Herzyk, Chris D. W. Wilkinson, and Richard O. C. Oreffo. 2007. "The Control of Human Mesenchymal Cell Differentiation Using Nanoscale Symmetry and Disorder." *Nature Materials* 6 (12): 997–1003. doi:10.1038/nmat2013.
- Danen, E H, S Aota, A A van Kraats, K M Yamada, D J Ruiter, and G N van Muijen. 1995. "Requirement for the Synergy Site for Cell Adhesion to Fibronectin Depends on the Activation State of Integrin Alpha 5 Beta 1." *The Journal of Biological Chemistry* 270 (37) (September 15): 21612–21618.
- Danišovič, L, I Varga, and S Polák. 2012. "Growth Factors and Chondrogenic Differentiation of Mesenchymal Stem Cells." *Tissue & Cell* 44 (2) (April): 69–73. doi:10.1016/j.tice.2011.11.005.
- DeForest, Cole A., and Kristi S. Anseth. 2011. "Cytocompatible Click-based Hydrogels with Dynamically Tunable Properties Through Orthogonal Photoconjugation and Photocleavage Reactions." *Nature Chemistry* 3 (12): 925–931. doi:10.1038/nchem.1174.
- DeForest, Cole A., and Kristi S. Anseth. 2012. "Photoreversible Patterning of Biomolecules Within Click-Based Hydrogels." *Angewandte Chemie International Edition* 51 (8): 1816–1819. doi:10.1002/anie.201106463.

- DeForest, Cole A., Brian D. Polizzotti, and Kristi S. Anseth. 2009. "Sequential Click Reactions for Synthesizing and Patterning Three-dimensional Cell Microenvironments." *Nature Materials* 8 (8): 659–664. doi:10.1038/nmat2473.
- DeForest, Cole A., Evan A. Sims, and Kristi S. Anseth. 2010. "Peptide-Functionalized Click Hydrogels with Independently Tunable Mechanics and Chemical Functionality for 3D Cell Culture." *Chemistry of Materials* 22 (16) (August 24): 4783–4790. doi:10.1021/cm101391y.
- DeLong, Solitaire A, James J Moon, and Jennifer L West. 2005. "Covalently Immobilized Gradients of bFGF on Hydrogel Scaffolds for Directed Cell Migration." *Biomaterials* 26 (16) (June): 3227–3234. doi:10.1016/j.biomaterials.2004.09.021.
- Drumheller, P D, D L Elbert, and J A Hubbell. 1994. "Multifunctional Poly(ethylene Glycol) Semi-interpenetrating Polymer Networks as Highly Selective Adhesive Substrates for Bioadhesive Peptide Grafting." *Biotechnology and Bioengineering* 43 (8) (April 5): 772–780. doi:10.1002/bit.260430812.
- Drumheller, P D, and J A Hubbell. 1994a. "Polymer Networks with Grafted Cell Adhesion Peptides for Highly Biospecific Cell Adhesive Substrates." *Analytical Biochemistry* 222 (2) (November 1): 380–388. doi:10.1006/abio.1994.1506.
- Ducy, Patricia, Michael Starbuck, Matthias Priemel, Jianhe Shen, Gerald Pinero, Valerie Geoffroy, Michael Amling, and Gerard Karsenty. 1999. "A Cbfa1-dependent Genetic Pathway Controls Bone Formation Beyond Embryonic Development." *Genes & Development* 13 (8) (April 15): 1025–1036.
- Dupont, Sirio, Leonardo Morsut, Mariaceleste Aragona, Elena Enzo, Stefano Giullitti, Michelangelo Cordenonsi, Francesca Zanconato, et al. 2011. "Role of YAP/TAZ in Mechanotransduction." *Nature* 474 (7350) (June 9): 179–183. doi:10.1038/nature10137.
- Ehrbar, Martin, Simone C Rizzi, Ruslan Hlushchuk, Valentin Djonov, Andreas H Zisch, Jeffrey A Hubbell, Franz E Weber, and Matthias P Lutolf. 2007. "Enzymatic Formation of Modular Cell-instructive Fibrin Analogs for Tissue Engineering." *Biomaterials* 28 (26) (September): 3856–3866. doi:10.1016/j.biomaterials.2007.03.027.
- Elisseeff, J, K Anseth, D Sims, W McIntosh, M Randolph, and R Langer. 1999. "Transdermal Photopolymerization for Minimally Invasive Implantation." *Proceedings of the National Academy of Sciences of the United States of America* 96 (6) (March 16): 3104–3107.
- Engler, Adam J, Shamik Sen, H Lee Sweeney, and Dennis E Discher. 2006. "Matrix Elasticity Directs Stem Cell Lineage Specification." *Cell* 126 (4) (August 25): 677–689. doi:10.1016/j.cell.2006.06.044.
- Evans, Richard A., Graeme Moad, Ezio Rizzardo, and San H. Thang. 1994. "New Free-Radical Ring-Opening Acrylate Monomers." *Macromolecules* 27 (26) (December 1): 7935–7937. doi:10.1021/ma00104a062.

- Evans, Richard A., and Ezio Rizzardo. 2001. "Free Radical Ring-opening Polymerization of Cyclic Allylic Sulfides: Liquid Monomers with Low Polymerization Volume Shrinkage." *Journal of Polymer Science Part A: Polymer Chemistry* 39 (1): 202–215. doi:10.1002/1099-0518(20010101)39:1<202::AID-POLA230>3.0.CO;2-6.
- Fairbanks, Benjamin D., Michael P. Schwartz, Christopher N. Bowman, and Kristi S. Anseth. 2009. "Photoinitiated Polymerization of PEG-diacrylate with Lithium Phenyl-2,4,6-trimethylbenzoylphosphinate: Polymerization Rate and Cytocompatibility." *Biomaterials* 30 (35) (December): 6702–6707. doi:10.1016/j.biomaterials.2009.08.055.
- Fairbanks, Benjamin D., Michael P. Schwartz, Alexandra E. Halevi, Charles R. Nuttelman, Christopher N. Bowman, and Kristi S. Anseth. 2009. "A Versatile Synthetic Extracellular Matrix Mimic via Thiol-Norbornene Photopolymerization." *Advanced Materials* 21 (48): 5005–5010. doi:10.1002/adma.200901808.
- Fink, Trine, and Vladimir Zachar. 2011. "Adipogenic Differentiation of Human Mesenchymal Stem Cells." *Methods in Molecular Biology (Clifton, N.J.)* 698: 243–251. doi:10.1007/978-1-60761-999-4\_19.
- Fisher, John P, David Dean, Paul S Engel, and Antonios G Mikos. 2001. "Photoinitiated Polymerization of Biomaterials." *Annual Review of Materials Research* 31 (1): 171–181. doi:10.1146/annurev.matsci.31.1.171.
- Fittkau, M H, P Zilla, D Bezuidenhout, M P Lutolf, P Human, J A Hubbell, and N Davies. 2005. "The Selective Modulation of Endothelial Cell Mobility on RGD Peptide Containing Surfaces by YIGSR Peptides." *Biomaterials* 26 (2) (January): 167–174. doi:10.1016/j.biomaterials.2004.02.012.
- Frantz, Christian, Kathleen M. Stewart, and Valerie M. Weaver. 2010. "The Extracellular Matrix at a Glance." *Journal of Cell Science* 123 (24) (December 15): 4195–4200. doi:10.1242/jcs.023820.
- Friedenstein, A. J., R. K. Chailakhyan, and U. V. Gerasimov. 1987. "Bone Marrow Osteogenic Stem Cells: In Vitro Cultivation and Transplantation in Diffusion Chambers." *Cell Proliferation* 20 (3): 263–272. doi:10.1111/j.1365-2184.1987.tb01309.x.
- Friedland, Julie C, Mark H Lee, and David Boettiger. 2009. "Mechanically Activated Integrin Switch Controls Alpha5beta1 Function." *Science (New York, N.Y.)* 323 (5914) (January 30): 642–644. doi:10.1126/science.1168441.
- Fromigué, Olivia, Julia Brun, Caroline Marty, Sophie Da Nascimento, Pascal Sonnet, and Pierre J Marie. 2012a. "Peptide-based Activation of Alpha5 Integrin for Promoting Osteogenesis." *Journal of Cellular Biochemistry* 113 (9) (September): 3029–3038. doi:10.1002/jcb.24181.
- Fu, Xiaobing, Bing Han, Sa Cai, Yonghong Lei, Tongzhu Sun, and Zhiyong Sheng. 2009. "Migration of Bone Marrow-derived Mesenchymal Stem Cells Induced by Tumor Necrosis Factor-alpha and Its Possible Role in Wound Healing." *Wound Repair and*



*Regeneration: Official Publication of the Wound Healing Society [and] the European Tissue Repair Society* 17 (2) (April): 185–191. doi:10.1111/j.1524-475X.2009.00454.x.

- Gavara, Núria, Pere Roca-Cusachs, Raimon Sunyer, Ramon Farré, and Daniel Navajas. 2008. “Mapping Cell-Matrix Stresses During Stretch Reveals Inelastic Reorganization of the Cytoskeleton.” *Biophysical Journal* 95 (1) (July 1): 464–471. doi:10.1529/biophysj.107.124180.
- Gelse, K, E Pöschl, and T Aigner. 2003. “Collagens--structure, Function, and Biosynthesis.” *Advanced Drug Delivery Reviews* 55 (12) (November 28): 1531–1546.
- Giancotti, F G, and E Ruoslahti. 1999a. “Integrin Signaling.” *Science (New York, N.Y.)* 285 (5430) (August 13): 1028–1032.
- Globus, R K, S B Doty, J C Lull, E Holmuhamedov, M J Humphries, and C H Damsky. 1998. “Fibronectin Is a Survival Factor for Differentiated Osteoblasts.” *Journal of Cell Science* 111 ( Pt 10) (May): 1385–1393.
- Gobin, Andrea S, and Jennifer L West. 2002. “Cell Migration Through Defined, Synthetic ECM Analogs.” *FASEB Journal: Official Publication of the Federation of American Societies for Experimental Biology* 16 (7) (May): 751–753. doi:10.1096/fj.01-0759fje.
- Gould, Sarah T, Nicole J Darling, and Kristi S Anseth. 2012. “Small Peptide Functionalized Thiol-ene Hydrogels as Culture Substrates for Understanding Valvular Interstitial Cell Activation and De Novo Tissue Deposition.” *Acta Biomaterialia* 8 (9) (September): 3201–3209. doi:10.1016/j.actbio.2012.05.009.
- Gronthos, S, P J Simmons, S E Graves, and P G Robey. 2001. “Integrin-mediated Interactions Between Human Bone Marrow Stromal Precursor Cells and the Extracellular Matrix.” *Bone* 28 (2) (February): 174–181.
- Gruber, Reinhard, Florian Karreth, Barbara Kandler, Gabor Fuerst, Antal Rot, Michael B Fischer, and Georg Watzek. 2004. “Platelet-released Supernatants Increase Migration and Proliferation, and Decrease Osteogenic Differentiation of Bone Marrow-derived Mesenchymal Progenitor Cells Under in Vitro Conditions.” *Platelets* 15 (1) (February): 29–35. doi:10.1080/09537100310001643999.
- Guerra, Nayrim Brizuela, Cristina González-García, Virginia Llopis, Jose Carlos Rodríguez-Hernández, David Moratal, Patricia Rico, and Manuel Salmerón-Sánchez. 2010. “Subtle Variations in Polymer Chemistry Modulate Substrate Stiffness and Fibronectin Activity.” *Soft Matter* 6 (19) (September 21): 4748–4755. doi:10.1039/C0SM00074D.
- Hahn, M. S., J. S. Miller, and J. L. West. 2006. “Three-Dimensional Biochemical and Biomechanical Patterning of Hydrogels for Guiding Cell Behavior.” *Advanced Materials* 18 (20): 2679–2684. doi:10.1002/adma.200600647.
- Hahn, Mariah S, Melissa K McHale, Eva Wang, Rachael H Schmedlen, and Jennifer L West. 2007. “Physiologic Pulsatile Flow Bioreactor Conditioning of Poly(ethylene Glycol)-

- based Tissue Engineered Vascular Grafts.” *Annals of Biomedical Engineering* 35 (2) (February): 190–200. doi:10.1007/s10439-006-9099-3.
- Hahn, Mariah S, Lakeshia J Taite, James J Moon, Maude C Rowland, Katie A Ruffino, and Jennifer L West. 2006. “Photolithographic Patterning of Polyethylene Glycol Hydrogels.” *Biomaterials* 27 (12) (April): 2519–2524. doi:10.1016/j.biomaterials.2005.11.045.
- Hamidouche, Zahia, Olivia Fromigué, Jochen Ringe, Thomas Häupl, and Pierre J. Marie. 2010. “Crosstalks Between Integrin Alpha 5 and IGF2/IGFBP2 Signalling Trigger Human Bone Marrow-derived Mesenchymal Stromal Osteogenic Differentiation.” *BMC Cell Biology* 11 (1) (June 23): 44. doi:10.1186/1471-2121-11-44.
- Hamidouche, Zahia, Olivia Fromigué, Jochen Ringe, Thomas Häupl, Pascal Vaudin, Jean-Christophe Pagès, Samer Srouji, Erella Livne, and Pierre J Marie. 2009a. “Priming Integrin Alpha5 Promotes Human Mesenchymal Stromal Cell Osteoblast Differentiation and Osteogenesis.” *Proceedings of the National Academy of Sciences of the United States of America* 106 (44) (November 3): 18587–18591. doi:10.1073/pnas.0812334106.
- Hamidouche, Zahia, Olivia Fromigué, Jochen Ringe, Thomas Häupl, Pascal Vaudin, Jean-Christophe Pagès, Samer Srouji, Erella Livne, and Pierre J. Marie. 2009b. “Priming Integrin A5 Promotes Human Mesenchymal Stromal Cell Osteoblast Differentiation and Osteogenesis.” *Proceedings of the National Academy of Sciences of the United States of America* 106 (44) (November 3): 18587–18591. doi:10.1073/pnas.0812334106.
- Handorf, Andrew M., and Wan-Ju Li. 2011. “Fibroblast Growth Factor-2 Primes Human Mesenchymal Stem Cells for Enhanced Chondrogenesis.” *PLoS ONE* 6 (7) (July 27): e22887. doi:10.1371/journal.pone.0022887.
- Hern, D L, and J A Hubbell. 1998. “Incorporation of Adhesion Peptides into Nonadhesive Hydrogels Useful for Tissue Resurfacing.” *Journal of Biomedical Materials Research* 39 (2) (February): 266–276.
- Hoffmann, Joseph C., and Jennifer L. West. 2010. “Three-dimensional Photolithographic Patterning of Multiple Bioactive Ligands in Poly(ethylene Glycol) Hydrogels.” *Soft Matter* 6 (20) (October 5): 5056–5063. doi:10.1039/C0SM00140F.
- Horwitz, Edwin M., Patricia L. Gordon, Winston K. K. Koo, Jeffrey C. Marx, Michael D. Neel, Rene Y. McNall, Linda Muul, and Ted Hofmann. 2002. “Isolated Allogeneic Bone Marrow-derived Mesenchymal Cells Engraft and Stimulate Growth in Children with Osteogenesis Imperfecta: Implications for Cell Therapy of Bone.” *Proceedings of the National Academy of Sciences* 99 (13) (June 25): 8932–8937. doi:10.1073/pnas.132252399.
- Hoyle, Charles E., and Christopher N. Bowman. 2010. “Thiol–Ene Click Chemistry.” *Angewandte Chemie International Edition* 49 (9): 1540–1573. doi:10.1002/anie.200903924.

- Hu, Bi-Huang, Jing Su, and Phillip B. Messersmith. 2009. "Hydrogels Cross-Linked by Native Chemical Ligation." *Biomacromolecules* 10 (8) (August 10): 2194–2200. doi:10.1021/bm900366e.
- Hu, Diane, Chuanyong Lu, Anna Sapozhnikova, Michael Barnett, Carolyn Sparrey, Theodore Mclau, and Ralph S Marcucio. 2010. "Absence of Beta3 Integrin Accelerates Early Skeletal Repair." *Journal of Orthopaedic Research: Official Publication of the Orthopaedic Research Society* 28 (1) (January): 32–37. doi:10.1002/jor.20955.
- Hubbell, Jeffrey A. 1998. "Synthetic Biodegradable Polymers for Tissue Engineering and Drug Delivery." *Current Opinion in Solid State and Materials Science* 3 (3) (June): 246–251. doi:10.1016/S1359-0286(98)80098-3.
- Humphries, J D, J A Askari, X P Zhang, Y Takada, M J Humphries, and A P Mould. 2000. "Molecular Basis of Ligand Recognition by Integrin Alpha5beta 1. II. Specificity of arg-gly-Asp Binding Is Determined by Trp157 OF THE Alpha Subunit." *The Journal of Biological Chemistry* 275 (27) (July 7): 20337–20345. doi:10.1074/jbc.M000568200.
- Humphries, Jonathan D., Adam Byron, and Martin J. Humphries. 2006. "Integrin Ligands at a Glance." *Journal of Cell Science* 119 (19) (October 1): 3901–3903. doi:10.1242/jcs.03098.
- Hynd, Matthew R, John P Frampton, Natalie Dowell-Mesfin, James N Turner, and William Shain. 2007. "Directed Cell Growth on Protein-functionalized Hydrogel Surfaces." *Journal of Neuroscience Methods* 162 (1-2) (May 15): 255–263. doi:10.1016/j.jneumeth.2007.01.024.
- Hynes, Richard O. 2002. "Integrins: Bidirectional, Allosteric Signaling Machines." *Cell* 110 (6) (September 20): 673–687.
- Impellitteri, Nicholas A, Michael W Toepke, Sheeny K Lan Levengood, and William L Murphy. 2012. "Specific VEGF Sequestering and Release Using Peptide-functionalized Hydrogel Microspheres." *Biomaterials* 33 (12) (April): 3475–3484. doi:10.1016/j.biomaterials.2012.01.032.
- Jaiswal, Neelam, Stephen E. Haynesworth, Arnold I. Caplan, and Scott P. Bruder. 1997. "Osteogenic Differentiation of Purified, Culture-expanded Human Mesenchymal Stem Cells in Vitro." *Journal of Cellular Biochemistry* 64 (2): 295–312. doi:10.1002/(SICI)1097-4644(199702)64:2<295::AID-JCB12>3.0.CO;2-I.
- Jung, Sunghoon, Arindom Sen, Lawrence Rosenberg, and Leo A Behie. 2010. "Identification of Growth and Attachment Factors for the Serum-free Isolation and Expansion of Human Mesenchymal Stromal Cells." *Cytotherapy* 12 (5) (September): 637–657. doi:10.3109/14653249.2010.495113.
- Kaabeche, Karim, Hind Guenou, Daniel Bouvard, Nadège Didelot, Antoine Listrat, and Pierre J Marie. 2005. "Cbl-mediated Ubiquitination of Alpha5 Integrin Subunit Mediates Fibronectin-dependent Osteoblast Detachment and Apoptosis Induced by FGFR2

Activation.” *Journal of Cell Science* 118 (Pt 6) (March 15): 1223–1232. doi:10.1242/jcs.01679.

Katayama, Yoshio, Michela Battista, Wei-Ming Kao, Andrés Hidalgo, Anna J. Peired, Steven A. Thomas, and Paul S. Frenette. 2006. “Signals from the Sympathetic Nervous System Regulate Hematopoietic Stem Cell Egress from Bone Marrow.” *Cell* 124 (2) (January 27): 407–421. doi:10.1016/j.cell.2005.10.041.

Katoh, Kazuo, Yumiko Kano, Mutsuki Amano, Hirofumi Onishi, Kozo Kaibuchi, and Keigi Fujiwara. 2001. “Rho-Kinase–Mediated Contraction of Isolated Stress Fibers.” *The Journal of Cell Biology* 153 (3) (April 30): 569–584. doi:10.1083/jcb.153.3.569.

Keselowsky, Benjamin G, David M Collard, and Andrés J García. 2003. “Surface Chemistry Modulates Fibronectin Conformation and Directs Integrin Binding and Specificity to Control Cell Adhesion.” *Journal of Biomedical Materials Research. Part A* 66 (2) (August 1): 247–259. doi:10.1002/jbm.a.10537.

Keselowsky, Benjamin G., David M. Collard, and Andrés J. García. 2005. “Integrin Binding Specificity Regulates Biomaterial Surface Chemistry Effects on Cell Differentiation.” *Proceedings of the National Academy of Sciences* 102 (17) (April 26): 5953–5957. doi:10.1073/pnas.0407356102.

Khetan, Sudhir, and Jason A. Burdick. 2010. “Patterning Network Structure to Spatially Control Cellular Remodeling and Stem Cell Fate Within 3-dimensional Hydrogels.” *Biomaterials* 31 (32) (November): 8228–8234. doi:10.1016/j.biomaterials.2010.07.035.

Kilian, Kristopher A., Branimir Bugarija, Bruce T. Lahn, and Milan Mrksich. 2010. “Geometric Cues for Directing the Differentiation of Mesenchymal Stem Cells.” *Proceedings of the National Academy of Sciences* 107 (11) (March 16): 4872–4877. doi:10.1073/pnas.0903269107.

Kirschner, Chelsea M., and Kristi S. Anseth. 2012. “In Situ Control of Cell Substrate Microtopographies Using Photolabile Hydrogels.” *Small*: n/a–n/a. doi:10.1002/smll.201201841.

Klees, Robert F, Roman M Salaszyk, Karl Kingsley, William A Williams, Adele Boskey, and George E Plopper. 2005. “Laminin-5 Induces Osteogenic Gene Expression in Human Mesenchymal Stem Cells Through an ERK-dependent Pathway.” *Molecular Biology of the Cell* 16 (2) (February): 881–890. doi:10.1091/mbc.E04-08-0695.

Kloxin, April M., Andrea M. Kasko, Chelsea N. Salinas, and Kristi S. Anseth. 2009. “Photodegradable Hydrogels for Dynamic Tuning of Physical and Chemical Properties.” *Science* 324 (5923) (April 3): 59–63. doi:10.1126/science.1169494.

Kloxin, Christopher J., Timothy F. Scott, Brian J. Adzima, and Christopher N. Bowman. 2010. “Covalent Adaptable Networks (CANs): A Unique Paradigm in Cross-Linked Polymers.” *Macromolecules* 43 (6) (March 23): 2643–2653. doi:10.1021/ma902596s.

- Kloxin, Christopher J., Timothy F. Scott, and Christopher N. Bowman. 2009. "Stress Relaxation via Addition-fragmentation Chain Transfer in a Thiol-ene Photopolymerization." *Macromolecules* 42 (7) (April 14): 2551–2556. doi:10.1021/ma802771b.
- Kloxin, Christopher J., Timothy F. Scott, Hee Young Park, and Christopher N. Bowman. 2011. "Mechanophotopatterning on a Photoresponsive Elastomer." *Advanced Materials* 23 (17): 1977–1981. doi:10.1002/adma.201100323.
- Kobel, Stefan, Monika Limacher, Samy Gobaa, Thierry Laroche, and Matthias P. Lutolf. 2009. "Micropatterning of Hydrogels by Soft Embossing†." *Langmuir* 25 (15) (August 4): 8774–8779. doi:10.1021/la9002115.
- Kocgozlu, Leyla, Philippe Lavalle, Géraldine Koenig, Bernard Senger, Youssef Haikel, Pierre Schaaf, Jean-Claude Voegel, Henri Tenenbaum, and Dominique Vautier. 2010. "Selective and Uncoupled Role of Substrate Elasticity in the Regulation of Replication and Transcription in Epithelial Cells." *Journal of Cell Science* 123 (Pt 1) (January 1): 29–39. doi:10.1242/jcs.053520.
- Koivunen, E, B Wang, and E Ruoslahti. 1994. "Isolation of a Highly Specific Ligand for the Alpha 5 Beta 1 Integrin from a Phage Display Library." *The Journal of Cell Biology* 124 (3) (February): 373–380.
- Kollar, Katarina, Matthew M. Cook, Kerry Atkinson, and Gary Brooke. 2009. "Molecular Mechanisms Involved in Mesenchymal Stem Cell Migration to the Site of Acute Myocardial Infarction." *International Journal of Cell Biology* 2009: 1–8. doi:10.1155/2009/904682.
- Kulterer, Birgit, Gerald Friedl, Anita Jandrositz, Fatima Sanchez-Cabo, Andreas Prokesch, Christine Paar, Marcel Scheideler, Reinhard Windhager, Karl-Heinz Preisegger, and Zlatko Trajanoski. 2007. "Gene Expression Profiling of Human Mesenchymal Stem Cells Derived from Bone Marrow During Expansion and Osteoblast Differentiation." *BMC Genomics* 8 (1) (March 12): 70. doi:10.1186/1471-2164-8-70.
- Larsen, Coby C., Faina Kligman, Chad Tang, Kandice Kottke-Marchant, and Roger E. Marchant. 2007. "A Biomimetic Peptide Fluorosurfactant Polymer for Endothelialization of ePTFE with Limited Platelet Adhesion." *Biomaterials* 28 (24) (August): 3537–3548. doi:10.1016/j.biomaterials.2007.04.026.
- Lee, Sang Hun, Yu Jin Lee, Chang Hun Song, Young Keun Ahn, and Ho Jae Han. 2010. "Role of FAK Phosphorylation in Hypoxia-induced hMSCS Migration: Involvement of VEGF as Well as MAPKS and eNOS Pathways." *American Journal of Physiology - Cell Physiology* 298 (4) (April 1): C847–C856. doi:10.1152/ajpcell.00418.2009.
- Lee, Soo-Hong, James J. Moon, Jordan S. Miller, and Jennifer L. West. 2007. "Poly(ethylene Glycol) Hydrogels Conjugated with a Collagenase-sensitive Fluorogenic Substrate to Visualize Collagenase Activity During Three-dimensional Cell Migration." *Biomaterials* 28 (20) (July): 3163–3170. doi:10.1016/j.biomaterials.2007.03.004.

- Lee, W, TG Lee, and WG Koh. 2007. "Grafting of Poly(acrylic Acid) on the Poly(ethylene Glycol) Hydrogel Using Surface-initiated Photopolymerization for Covalent Immobilization of Collagen." *Journal of Industrial Engineering Chemistry* 13 (7): 1195–1200.
- Leslie-Barbick, Julia E, James J Moon, and Jennifer L West. 2009. "Covalently-immobilized Vascular Endothelial Growth Factor Promotes Endothelial Cell Tubulogenesis in Poly(ethylene Glycol) Diacrylate Hydrogels." *Journal of Biomaterials Science. Polymer Edition* 20 (12): 1763–1779. doi:10.1163/156856208X386381.
- Leslie-Barbick, Julia E, Colette Shen, Christopher Chen, and Jennifer L West. 2011. "Micron-scale Spatially Patterned, Covalently Immobilized Vascular Endothelial Growth Factor on Hydrogels Accelerates Endothelial Tubulogenesis and Increases Cellular Angiogenic Responses." *Tissue Engineering. Part A* 17 (1-2) (January): 221–229. doi:10.1089/ten.TEA.2010.0202.
- Li, Yu-Ming, Tatjana Schilling, Peggy Benisch, Sabine Zeck, Jutta Meissner-Weigl, Doris Schneider, Catarina Limbert, et al. 2007. "Effects of High Glucose on Mesenchymal Stem Cell Proliferation and Differentiation." *Biochemical and Biophysical Research Communications* 363 (1) (November 9): 209–215. doi:10.1016/j.bbrc.2007.08.161.
- Lin, Chien-Chi, and Kristi S Anseth. 2009a. "PEG Hydrogels for the Controlled Release of Biomolecules in Regenerative Medicine." *Pharmaceutical Research* 26 (3) (March): 631–643. doi:10.1007/s11095-008-9801-2.
- Lin, Chien-Chi, and Kristi S. Anseth. 2009d. "Glucagon-Like Peptide-1 Functionalized PEG Hydrogels Promote Survival and Function of Encapsulated Pancreatic  $\beta$ -Cells." *Biomacromolecules* 10 (9) (September 14): 2460–2467. doi:10.1021/bm900420f.
- Lin, Chien-Chi, Andrew T Metters, and Kristi S Anseth. 2009. "Functional PEG-peptide Hydrogels to Modulate Local Inflammation Induced by the Pro-inflammatory Cytokine TNFalpha." *Biomaterials* 30 (28) (October): 4907–4914. doi:10.1016/j.biomaterials.2009.05.083.
- Lin, Chien-Chi, Asad Raza, and Han Shih. 2011a. "PEG Hydrogels Formed by Thiol-ene Photo-click Chemistry and Their Effect on the Formation and Recovery of Insulin-secreting Cell Spheroids." *Biomaterials* 32 (36) (December): 9685–9695. doi:10.1016/j.biomaterials.2011.08.083.
- Lin, Chien-Chi, and Kristi S Anseth. 2011b. "PEG Hydrogels Formed by Thiol-ene Photo-click Chemistry and Their Effect on the Formation and Recovery of Insulin-secreting Cell Spheroids." *Biomaterials* 32 (36) (December): 9685–9695. doi:10.1016/j.biomaterials.2011.08.083.
- Lin, Chien-Chi, and Kristi S Anseth. 2012b. "Controlling Affinity Binding with Peptide-Functionalized Poly(ethylene Glycol) Hydrogels." *Advanced Functional Materials* 19 (14) (July 24): 2325. doi:10.1002/adfm.200900107.

- Lin, Chien-Chi, Suzanne M Sawicki, and Andrew T Metters. 2008. "Free-radical-mediated Protein Inactivation and Recovery During Protein Photoencapsulation." *Biomacromolecules* 9 (1) (January): 75–83. doi:10.1021/bm700782c.
- Lin-Gibson, Sheng, Ronald L. Jones, Newell R. Washburn, and Ferenc Horkay. 2005. "Structure–Property Relationships of Photopolymerizable Poly(ethylene Glycol) Dimethacrylate Hydrogels." *Macromolecules* 38 (7) (April 1): 2897–2902. doi:10.1021/ma0487002.
- Luo, Ying, and Molly S. Shoichet. 2004. "A Photolabile Hydrogel for Guided Three-dimensional Cell Growth and Migration." *Nature Materials* 3 (4): 249–253. doi:10.1038/nmat1092.
- Lutolf, M. P., and J. A. Hubbell. 2005. "Synthetic Biomaterials as Instructive Extracellular Microenvironments for Morphogenesis in Tissue Engineering." *Nature Biotechnology* 23 (1): 47–55. doi:10.1038/nbt1055.
- Lutolf, M. P., J. L. Lauer-Fields, H. G. Schmoekel, A. T. Metters, F. E. Weber, G. B. Fields, and J. A. Hubbell. 2003. "Synthetic Matrix Metalloproteinase-sensitive Hydrogels for the Conduction of Tissue Regeneration: Engineering Cell-invasion Characteristics." *Proceedings of the National Academy of Sciences* 100 (9) (April 29): 5413–5418. doi:10.1073/pnas.0737381100.
- Lutolf, M. P., N. Tirelli, S. Cerritelli, L. Cavalli, and J. A. Hubbell. 2001. "Systematic Modulation of Michael-Type Reactivity of Thiols Through the Use of Charged Amino Acids." *Bioconjugate Chemistry* 12 (6) (November 1): 1051–1056. doi:10.1021/bc015519e.
- Lutolf, Matthias P., Regis Doyonnas, Karen Havenstrite, Kassie Koleckar, and Helen M. Blau. 2009. "Perturbation of Single Hematopoietic Stem Cell Fates in Artificial Niches." *Integrative Biology* 1 (1) (January 1): 59–69. doi:10.1039/B815718A.
- Ma, Peter X., and Jennifer H. Elisseeff. 2005. *Scaffolding In Tissue Engineering*. CRC Press.
- Malkoch, Michael, Robert Vestberg, Nalini Gupta, Laetitia Mespouille, Philippe Dubois, Andrew F. Mason, James L. Hedrick, et al. 2006a. "Synthesis of Well-defined Hydrogel Networks Using Click Chemistry." *Chemical Communications* (26) (June 26): 2774–2776. doi:10.1039/B603438A.
- Mammoto, Tadanori, and Donald E Ingber. 2010. "Mechanical Control of Tissue and Organ Development." *Development (Cambridge, England)* 137 (9) (May): 1407–1420. doi:10.1242/dev.024166.
- Mann, Brenda K, Rachael H Schmedlen, and Jennifer L West. 2001. "Tethered-TGF- $\beta$  Increases Extracellular Matrix Production of Vascular Smooth Muscle Cells." *Biomaterials* 22 (5) (March): 439–444. doi:10.1016/S0142-9612(00)00196-4.

- Mann, Brenda K., Andrea S. Gobin, Annabel T. Tsai, Rachael H. Schmedlen, and Jennifer L. West. 2001. "Smooth Muscle Cell Growth in Photopolymerized Hydrogels with Cell Adhesive and Proteolytically Degradable Domains: Synthetic ECM Analogs for Tissue Engineering." *Biomaterials* 22 (22) (November 15): 3045–3051. doi:10.1016/S0142-9612(01)00051-5.
- Martens, Penny J., Stephanie J. Bryant, and Kristi S. Anseth. 2003. "Tailoring the Degradation of Hydrogels Formed from Multivinyl Poly(ethylene Glycol) and Poly(vinyl Alcohol) Macromers for Cartilage Tissue Engineering." *Biomacromolecules* 4 (2) (March 1): 283–292. doi:10.1021/bm025666v.
- Martino, Mikaël M., Mayumi Mochizuki, Dominique A Rothenfluh, Sandra A Rempel, Jeffrey A Hubbell, and Thomas H Barker. 2009. "Controlling Integrin Specificity and Stem Cell Differentiation in 2D and 3D Environments Through Regulation of Fibronectin Domain Stability." *Biomaterials* 30 (6) (February): 1089–1097. doi:10.1016/j.biomaterials.2008.10.047.
- McBeath, Rowena, Dana M Pirone, Celeste M Nelson, Kiran Bhadriraju, and Christopher S Chen. 2004. "Cell Shape, Cytoskeletal Tension, and RhoA Regulate Stem Cell Lineage Commitment." *Developmental Cell* 6 (4) (April): 483–495.
- McCall, Joshua D., and Kristi S. Anseth. 2012. "Thiol–Ene Photopolymerizations Provide a Facile Method To Encapsulate Proteins and Maintain Their Bioactivity." *Biomacromolecules* 13 (8) (August 13): 2410–2417. doi:10.1021/bm300671s.
- McCall, Joshua D., Chien-Chi Lin, and Kristi S. Anseth. 2011. "Affinity Peptides Protect Transforming Growth Factor Beta During Encapsulation in Poly(ethylene Glycol) Hydrogels." *Biomacromolecules* 12 (4) (April 11): 1051–1057. doi:10.1021/bm101379v.
- McHugh, K P, K Hodivala-Dilke, M H Zheng, N Namba, J Lam, D Novack, X Feng, F P Ross, R O Hynes, and S L Teitelbaum. 2000. "Mice Lacking Beta3 Integrins Are Osteosclerotic Because of Dysfunctional Osteoclasts." *The Journal of Clinical Investigation* 105 (4) (February): 433–440. doi:10.1172/JCI8905.
- Meijs, Gordon F., Ezio Rizzardo, and San H. Thang. 1988. "Preparation of Controlled-molecular-weight, Olefin-terminated Polymers by Free Radical Methods. Chain Transfer Using Allylic Sulfides." *Macromolecules* 21 (10) (October 1): 3122–3124. doi:10.1021/ma00188a039.
- Metters, Andrew, and Jeffrey Hubbell. 2005. "Network Formation and Degradation Behavior of Hydrogels Formed by Michael-type Addition Reactions." *Biomacromolecules* 6 (1) (February): 290–301. doi:10.1021/bm049607o.
- Mimura, Sumiyo, Naohiro Kimura, Mitsuhi Hirata, Daiki Tateyama, Midori Hayashida, Akihiro Umezawa, Arihiro Kohara, Hiroki Nikawa, Tetsuji Okamoto, and Miho K Furue. 2011. "Growth Factor-defined Culture Medium for Human Mesenchymal Stem Cells." *The*



*International Journal of Developmental Biology* 55 (2): 181–187.  
doi:10.1387/ijdb.103232sm.

- Mizuno, M, R Fujisawa, and Y Kuboki. 2000. “Type I Collagen-induced Osteoblastic Differentiation of Bone-marrow Cells Mediated by Collagen-alpha2beta1 Integrin Interaction.” *Journal of Cellular Physiology* 184 (2) (August): 207–213. doi:10.1002/1097-4652(200008)184:2<207::AID-JCP8>3.0.CO;2-U.
- Moon, James J., Mariah S. Hahn, Iris Kim, Barbara A. Nsiah, and Jennifer L. West. 2009. “Micropatterning of Poly(Ethylene Glycol) Diacrylate Hydrogels with Biomolecules to Regulate and Guide Endothelial Morphogenesis.” *Tissue Engineering Part A* 15 (3) (March): 579–585. doi:10.1089/ten.tea.2008.0196.
- Mostafa, Nesrine Z, Ross Fitzsimmons, Paul W Major, Adetola Adesida, Nadr Jomha, Hongxing Jiang, and Hasan Uludağ. 2012. “Osteogenic Differentiation of Human Mesenchymal Stem Cells Cultured with Dexamethasone, Vitamin D3, Basic Fibroblast Growth Factor, and Bone Morphogenetic Protein-2.” *Connective Tissue Research* 53 (2): 117–131. doi:10.3109/03008207.2011.611601.
- Mould, A P, J A Askari, and M J Humphries. 2000. “Molecular Basis of Ligand Recognition by Integrin Alpha 5beta 1. I. Specificity of Ligand Binding Is Determined by Amino Acid Sequences in the Second and Third NH2-terminal Repeats of the Alpha Subunit.” *The Journal of Biological Chemistry* 275 (27) (July 7): 20324–20336. doi:10.1074/jbc.M000572200.
- Mould, A P, L Burrows, and M J Humphries. 1998. “Identification of Amino Acid Residues That Form Part of the Ligand-binding Pocket of Integrin Alpha5 Beta1.” *The Journal of Biological Chemistry* 273 (40) (October 2): 25664–25672.
- Moursi, A M, R K Globus, and C H Damsky. 1997. “Interactions Between Integrin Receptors and Fibronectin Are Required for Calvarial Osteoblast Differentiation in Vitro.” *Journal of Cell Science* 110 ( Pt 18) (September): 2187–2196.
- Nemir, Stephanie, and Jennifer L West. 2010. “Synthetic Materials in the Study of Cell Response to Substrate Rigidity.” *Annals of Biomedical Engineering* 38 (1) (January): 2–20. doi:10.1007/s10439-009-9811-1.
- Neuss, Sabine, Eva Becher, Michael Wöltje, Lothar Tietze, and Willi Jahnen-Dechent. 2004. “Functional Expression of HGF and HGF Receptor/c-met in Adult Human Mesenchymal Stem Cells Suggests a Role in Cell Mobilization, Tissue Repair, and Wound Healing.” *Stem Cells (Dayton, Ohio)* 22 (3): 405–414. doi:10.1634/stemcells.22-3-405.
- Ng, Felicia, Shayne Boucher, Susie Koh, Konduru S R Sastry, Lucas Chase, Uma Lakshmiopathy, Cleo Choong, et al. 2008. “PDGF, TGF-beta, and FGF Signaling Is Important for Differentiation and Growth of Mesenchymal Stem Cells (MSCs): Transcriptional Profiling Can Identify Markers and Signaling Pathways Important in Differentiation of

- MSCs into Adipogenic, Chondrogenic, and Osteogenic Lineages.” *Blood* 112 (2) (July 15): 295–307. doi:10.1182/blood-2007-07-103697.
- Nimmo, Chelsea M., and Molly S. Shoichet. 2011. “Regenerative Biomaterials That ‘Click’: Simple, Aqueous-Based Protocols for Hydrogel Synthesis, Surface Immobilization, and 3D Patterning.” *Bioconjugate Chemistry* 22 (11) (November 16): 2199–2209. doi:10.1021/bc200281k.
- Nuttelman, C. PhD Thesis, University of Colorado at Boulder, 2005.
- Odian, George G. 2004. *Principles of polymerization*. Hoboken, N.J.: Wiley. <http://public.eblib.com/EBLPublic/PublicView.do?ptiID=469767>.
- Park, Yongdoo, Matthias P Lutolf, Jeffrey A Hubbell, Ernst B Hunziker, and Marcy Wong. 2004. “Bovine Primary Chondrocyte Culture in Synthetic Matrix Metalloproteinase-sensitive Poly(ethylene Glycol)-based Hydrogels as a Scaffold for Cartilage Repair.” *Tissue Engineering* 10 (3-4) (April): 515–522. doi:10.1089/107632704323061870.
- Pauloehrl, Thomas, Guillaume Delaittre, Volker Winkler, Alexander Welle, Michael Bruns, Hans G. Börner, Alexandra M. Greiner, Martin Bastmeyer, and Christopher Barner-Kowollik. 2012. “Adding Spatial Control to Click Chemistry: Phototriggered Diels–Alder Surface (Bio)functionalization at Ambient Temperature.” *Angewandte Chemie International Edition* 51 (4): 1071–1074. doi:10.1002/anie.201107095.
- Peppas, N. A., J. Z. Hilt, A. Khademhosseini, and R. Langer. 2006. “Hydrogels in Biology and Medicine: From Molecular Principles to Bionanotechnology.” *Advanced Materials* 18 (11): 1345–1360. doi:10.1002/adma.200501612.
- Perl, András, David N. Reinhoudt, and Jurriaan Huskens. 2009. “Microcontact Printing: Limitations and Achievements.” *Advanced Materials* 21 (22): 2257–2268. doi:10.1002/adma.200801864.
- Petit, V, and J P Thiery. 2000. “Focal Adhesions: Structure and Dynamics.” *Biology of the Cell / Under the Auspices of the European Cell Biology Organization* 92 (7) (October): 477–494.
- Petrie, Timothy A, Jeffrey R Capadona, Catherine D Reyes, and Andrés J García. 2006. “Integrin Specificity and Enhanced Cellular Activities Associated with Surfaces Presenting a Recombinant Fibronectin Fragment Compared to RGD Supports.” *Biomaterials* 27 (31) (November): 5459–5470. doi:10.1016/j.biomaterials.2006.06.027.
- Petrie, Timothy A, Catherine D Reyes, Kellie L Burns, and Andrés J García. 2009. “Simple Application of Fibronectin-mimetic Coating Enhances Osseointegration of Titanium Implants.” *Journal of Cellular and Molecular Medicine* 13 (8B) (August): 2602–2612. doi:10.1111/j.1582-4934.2008.00476.x.
- Petrie, Timothy A., Jenny E. Raynor, Catherine D. Reyes, Kellie L. Burns, David M. Collard, and Andrés J. García. 2008. “The Effect of Integrin-specific Bioactive Coatings on

- Tissue Healing and Implant Osseointegration.” *Biomaterials* 29 (19) (July): 2849–2857. doi:10.1016/j.biomaterials.2008.03.036.
- Phelps, Edward A., Nduka O. Enemchukwu, Vincent F. Fiore, Jay C. Sy, Niren Murthy, Todd A. Sulchek, Thomas H. Barker, and Andrés J. García. 2012. “Maleimide Cross-Linked Bioactive PEG Hydrogel Exhibits Improved Reaction Kinetics and Cross-Linking for Cell Encapsulation and In Situ Delivery.” *Advanced Materials* 24 (1): 64–70. doi:10.1002/adma.201103574.
- Pittenger, M F, A M Mackay, S C Beck, R K Jaiswal, R Douglas, J D Mosca, M A Moorman, D W Simonetti, S Craig, and D R Marshak. 1999. “Multilineage Potential of Adult Human Mesenchymal Stem Cells.” *Science (New York, N.Y.)* 284 (5411) (April 2): 143–147.
- Polizzotti, Brian D, Benjiman D Fairbanks, and Kristi S Anseth. 2008a. “Three-dimensional Biochemical Patterning of Click-based Composite Hydrogels via Thiolene Photopolymerization.” *Biomacromolecules* 9 (4) (April): 1084–1087. doi:10.1021/bm7012636.
- Popov, C, T Radic, F Haasters, W C Prall, A Aszodi, D Gullberg, M Schieker, and D Docheva. 2011. “Integrins A2 $\beta$ 1 and A11 $\beta$ 1 Regulate the Survival of Mesenchymal Stem Cells on Collagen I.” *Cell Death & Disease* 2: e186. doi:10.1038/cddis.2011.71.
- Quist, Arjan P, Elisabeth Pavlovic, and Sven Oscarsson. 2005. “Recent Advances in Microcontact Printing.” *Analytical and Bioanalytical Chemistry* 381 (3) (February): 591–600. doi:10.1007/s00216-004-2847-z.
- Ratner, Buddy D., and Stephanie J. Bryant. 2004. “BIOMATERIALS: Where We Have Been and Where We Are Going.” *Annual Review of Biomedical Engineering* 6 (1): 41–75. doi:10.1146/annurev.bioeng.6.040803.140027.
- Ridley, Anne J. 1994. “Membrane Ruffling and Signal Transduction.” *BioEssays* 16 (5): 321–327. doi:10.1002/bies.950160506.
- Roberts, M J, M D Bentley, and J M Harris. 2002. “Chemistry for Peptide and Protein PEGylation.” *Advanced Drug Delivery Reviews* 54 (4) (June 17): 459–476.
- Ruiz, Sami Alom, and Christopher S. Chen. 2008. “Emergence of Patterned Stem Cell Differentiation Within Multicellular Structures.” *STEM CELLS* 26 (11): 2921–2927. doi:10.1634/stemcells.2008-0432.
- Rydholm, Amber E., Christopher N. Bowman, and Kristi S. Anseth. 2005. “Degradable Thiol-acrylate Photopolymers: Polymerization and Degradation Behavior of an in Situ Forming Biomaterial.” *Biomaterials* 26 (22) (August): 4495–4506. doi:10.1016/j.biomaterials.2004.11.046.
- Saik, Jennifer E, Daniel J Gould, Emily M Watkins, Mary E Dickinson, and Jennifer L West. 2011. “Covalently Immobilized Platelet-derived Growth factor-BB Promotes

- Angiogenesis in Biomimetic Poly(ethylene Glycol) Hydrogels.” *Acta Biomaterialia* 7 (1) (January): 133–143. doi:10.1016/j.actbio.2010.08.018.
- Salasznyk, Roman M, Robert F Klees, William A Williams, Adele Boskey, and George E Plopper. 2007. “Focal Adhesion Kinase Signaling Pathways Regulate the Osteogenic Differentiation of Human Mesenchymal Stem Cells.” *Experimental Cell Research* 313 (1) (January 1): 22–37. doi:10.1016/j.yexcr.2006.09.013.
- Salinas, Chelsea N, and Kristi S Anseth. 2008a. “The Influence of the RGD Peptide Motif and Its Contextual Presentation in PEG Gels on Human Mesenchymal Stem Cell Viability.” *Journal of Tissue Engineering and Regenerative Medicine* 2 (5) (July): 296–304. doi:10.1002/term.95.
- Salinas, Chelsea N., and Kristi S. Anseth. 2008b. “The Enhancement of Chondrogenic Differentiation of Human Mesenchymal Stem Cells by Enzymatically Regulated RGD Functionalities.” *Biomaterials* 29 (15) (May): 2370–2377. doi:10.1016/j.biomaterials.2008.01.035.
- Salinas, Chelsea N., and Kristi S. Anseth. 2008c. “Mixed Mode Thiol–Acrylate Photopolymerizations for the Synthesis of PEG–Peptide Hydrogels.” *Macromolecules* 41 (16) (August 1): 6019–6026. doi:10.1021/ma800621h.
- Salter, D M, J E Robb, and M O Wright. 1997. “Electrophysiological Responses of Human Bone Cells to Mechanical Stimulation: Evidence for Specific Integrin Function in Mechanotransduction.” *Journal of Bone and Mineral Research: The Official Journal of the American Society for Bone and Mineral Research* 12 (7) (July): 1133–1141. doi:10.1359/jbmr.1997.12.7.1133.
- Sanborn, Tracy J., Phillip B. Messersmith, and Annelise E. Barron. 2002. “In Situ Crosslinking of a Biomimetic peptide-PEG Hydrogel via Thermally Triggered Activation of Factor XIII.” *Biomaterials* 23 (13) (July): 2703–2710. doi:10.1016/S0142-9612(02)00002-9.
- Sawhney, Amarpreet S., Chandrashekhar P. Pathak, and Jeffrey A. Hubbell. 1993. “Bioerodible Hydrogels Based on Photopolymerized Poly(ethylene Glycol)-co-poly(.alpha.-hydroxy Acid) Diacrylate Macromers.” *Macromolecules* 26 (4) (February 1): 581–587. doi:10.1021/ma00056a005.
- Schmedlen, Rachael H., Kristyn S. Masters, and Jennifer L. West. 2002. “Photocrosslinkable Polyvinyl Alcohol Hydrogels That Can Be Modified with Cell Adhesion Peptides for Use in Tissue Engineering.” *Biomaterials* 23 (22) (November): 4325–4332. doi:10.1016/S0142-9612(02)00177-1.
- Schmidt, David Richard, and Weiyuan John Kao. 2007. “Monocyte Activation in Response to Polyethylene Glycol Hydrogels Grafted with RGD and PHSRN Separated by Interpositional Spacers of Various Lengths.” *Journal of Biomedical Materials Research. Part A* 83 (3) (December 1): 617–625. doi:10.1002/jbm.a.31270.

- Schwartz, Martin A, and Douglas W DeSimone. 2008. "Cell Adhesion Receptors in Mechanotransduction." *Current Opinion in Cell Biology* 20 (5) (October): 551–556. doi:10.1016/j.ceb.2008.05.005.
- Schwartz, Martin A, and Mark H Ginsberg. 2002. "Networks and Crosstalk: Integrin Signalling Spreads." *Nature Cell Biology* 4 (4) (April): E65–68. doi:10.1038/ncb0402-e65.
- Scott, Michelle A, Virginia T Nguyen, Benjamin Levi, and Aaron W James. 2011. "Current Methods of Adipogenic Differentiation of Mesenchymal Stem Cells." *Stem Cells and Development* 20 (10) (October): 1793–1804. doi:10.1089/scd.2011.0040.
- Scott, Timothy F., Andrew D. Schneider, Wayne D. Cook, and Christopher N. Bowman. 2005. "Photoinduced Plasticity in Cross-Linked Polymers." *Science* 308 (5728) (June 10): 1615–1617. doi:10.1126/science.1110505.
- Seidlits, Stephanie K., Christine E. Schmidt, and Jason B. Shear. 2009. "High-Resolution Patterning of Hydrogels in Three Dimensions Using Direct-Write Photofabrication for Cell Guidance." *Advanced Functional Materials* 19 (22): 3543–3551. doi:10.1002/adfm.200901115.
- Sekiya, Ichiro, Benjamin L Larson, Jussi T Vuoristo, Jian-Guo Cui, and Darwin J Prockop. 2004. "Adipogenic Differentiation of Human Adult Stem Cells from Bone Marrow Stroma (MSCs)." *Journal of Bone and Mineral Research: The Official Journal of the American Society for Bone and Mineral Research* 19 (2) (February): 256–264. doi:10.1359/JBMR.0301220.
- Shekaran, Asha, and Andrés J. García. 2011a. "Extracellular Matrix-mimetic Adhesive Biomaterials for Bone Repair." *Journal of Biomedical Materials Research Part A* 96A (1): 261–272. doi:10.1002/jbm.a.32979.
- Shih, Yu-Ru V, Kuo-Fung Tseng, Hsiu-Yu Lai, Chi-Hung Lin, and Oscar K Lee. 2011. "Matrix Stiffness Regulation of Integrin-mediated Mechanotransduction During Osteogenic Differentiation of Human Mesenchymal Stem Cells." *Journal of Bone and Mineral Research: The Official Journal of the American Society for Bone and Mineral Research* 26 (4) (April): 730–738. doi:10.1002/jbmr.278.
- Shintani, Nahoko, and Ernst B Hunziker. 2007. "Chondrogenic Differentiation of Bovine Synovium: Bone Morphogenetic Proteins 2 and 7 and Transforming Growth Factor Beta1 Induce the Formation of Different Types of Cartilaginous Tissue." *Arthritis and Rheumatism* 56 (6) (June): 1869–1879. doi:10.1002/art.22701.
- Skardal, Aleksander, David Mack, Anthony Atala, and Shay Soker. 2013. "Substrate Elasticity Controls Cell Proliferation, Surface Marker Expression and Motile Phenotype in Amniotic Fluid-derived Stem Cells." *Journal of the Mechanical Behavior of Biomedical Materials* 17 (January): 307–316. doi:10.1016/j.jmbbm.2012.10.001.

- Slaughter, Brandon V., Shahana S. Khurshid, Omar Z. Fisher, Ali Khademhosseini, and Nicholas A. Peppas. 2009. "Hydrogels in Regenerative Medicine." *Advanced Materials* 21 (32-33): 3307–3329. doi:10.1002/adma.200802106.
- Solchaga, Luis A, Kitsie Penick, Victor M Goldberg, Arnold I Caplan, and Jean F Welter. 2010. "Fibroblast Growth Factor-2 Enhances Proliferation and Delays Loss of Chondrogenic Potential in Human Adult Bone-marrow-derived Mesenchymal Stem Cells." *Tissue Engineering. Part A* 16 (3) (March): 1009–1019. doi:10.1089/ten.TEA.2009.0100.
- Stockmayer, Walter H. 1944. "Theory of Molecular Size Distribution and Gel Formation in Branched Polymers II. General Cross Linking." *The Journal of Chemical Physics* 12 (4): 125–131. doi:10.1063/1.1723922.
- Takada, Ichiro, Alexander P Kouzmenko, and Shigeaki Kato. 2009. "Molecular Switching of Osteoblastogenesis Versus Adipogenesis: Implications for Targeted Therapies." *Expert Opinion on Therapeutic Targets* 13 (5) (May): 593–603. doi:10.1517/14728220902915310.
- Takeuchi, Y, M Suzawa, T Kikuchi, E Nishida, T Fujita, and T Matsumoto. 1997. "Differentiation and Transforming Growth Factor-beta Receptor Down-regulation by Collagen-alpha2beta1 Integrin Interaction Is Mediated by Focal Adhesion Kinase and Its Downstream Signals in Murine Osteoblastic Cells." *The Journal of Biological Chemistry* 272 (46) (November 14): 29309–29316.
- Tamama, Kenichi, Haruhisa Kawasaki, and Alan Wells. 2010. "Epidermal Growth Factor (EGF) Treatment on Multipotential Stromal Cells (MSCs). Possible Enhancement of Therapeutic Potential of MSC." *Journal of Biomedicine and Biotechnology* 2010: 1–11. doi:10.1155/2010/795385.
- Tayalia, Prakriti, and David J Mooney. 2009. "Controlled Growth Factor Delivery for Tissue Engineering." *Advanced Materials (Deerfield Beach, Fla.)* 21 (32-33) (September 4): 3269–3285. doi:10.1002/adma.200900241.
- "The Small GTP-binding Protein Rho Regulates the Assembly of Focal Adhesions and Actin Stress Fibers in Response to Growth Factors." 1992. *Cell* 70 (3) (August 7): 389–399. doi:10.1016/0092-8674(92)90163-7.
- Théry, Manuel, Anne Pépin, Emilie Dressaire, Yong Chen, and Michel Bornens. 2006. "Cell Distribution of Stress Fibres in Response to the Geometry of the Adhesive Environment." *Cell Motility and the Cytoskeleton* 63 (6) (June): 341–355. doi:10.1002/cm.20126.
- Tibbitt, Mark W, and Kristi S Anseth. 2009a. "Hydrogels as Extracellular Matrix Mimics for 3D Cell Culture." *Biotechnology and Bioengineering* 103 (4) (July 1): 655–663. doi:10.1002/bit.22361.
- Liu Tsang, Valerie, Alice A Chen, Lisa M Cho, Kyle D Jadin, Robert L Sah, Solitaire DeLong, Jennifer L West, and Sangeeta N Bhatia. 2007. "Fabrication of 3D Hepatic Tissues by Additive Photopatterning of Cellular Hydrogels." *FASEB Journal: Official Publication of*

*the Federation of American Societies for Experimental Biology* 21 (3) (March): 790–801. doi:10.1096/fj.06-7117com.

- Tse, Justin R., and Adam J. Engler. 2011. “Stiffness Gradients Mimicking In Vivo Tissue Variation Regulate Mesenchymal Stem Cell Fate.” *PLoS ONE* 6 (1) (January 5): e15978. doi:10.1371/journal.pone.0015978.
- Tsutsumi, S, A Shimazu, K Miyazaki, H Pan, C Koike, E Yoshida, K Takagishi, and Y Kato. 2001a. “Retention of Multilineage Differentiation Potential of Mesenchymal Cells During Proliferation in Response to FGF.” *Biochemical and Biophysical Research Communications* 288 (2) (October 26): 413–419. doi:10.1006/bbrc.2001.5777.
- Veevers-Lowe, Jennifer, Stephen G Ball, Adrian Shuttleworth, and Cay M Kielty. 2011. “Mesenchymal Stem Cell Migration Is Regulated by Fibronectin Through A5 $\beta$ 1-integrin-mediated Activation of PDGFR- $\beta$  and Potentiation of Growth Factor Signals.” *Journal of Cell Science* 124 (Pt 8) (April 15): 1288–1300. doi:10.1242/jcs.076935.
- Van der Velde-Zimmermann, D, M A Verdaasdonk, L H Rademakers, R A De Weger, J G Van den Tweel, and P Joling. 1997a. “Fibronectin Distribution in Human Bone Marrow Stroma: Matrix Assembly and Tumor Cell Adhesion via Alpha5 Beta1 Integrin.” *Experimental Cell Research* 230 (1) (January 10): 111–120. doi:10.1006/excr.1996.3405.
- Vogel, Viola, and Michael Sheetz. 2006. “Local Force and Geometry Sensing Regulate Cell Functions.” *Nature Reviews. Molecular Cell Biology* 7 (4) (April): 265–275. doi:10.1038/nrm1890.
- Walcott, Sam, and Sean X. Sun. 2010. “A Mechanical Model of Actin Stress Fiber Formation and Substrate Elasticity Sensing in Adherent Cells.” *Proceedings of the National Academy of Sciences* 107 (17) (April 27): 7757–7762. doi:10.1073/pnas.0912739107.
- Weber, Laney M, Kirsten N Hayda, Kathryn Haskins, and Kristi S Anseth. 2007. “The Effects of Cell-matrix Interactions on Encapsulated Beta-cell Function Within Hydrogels Functionalized with Matrix-derived Adhesive Peptides.” *Biomaterials* 28 (19) (July): 3004–3011. doi:10.1016/j.biomaterials.2007.03.005.
- Winer, Jessamine P, Paul A Janmey, Margaret E McCormick, and Makoto Funaki. 2009. “Bone Marrow-derived Human Mesenchymal Stem Cells Become Quiescent on Soft Substrates but Remain Responsive to Chemical or Mechanical Stimuli.” *Tissue Engineering. Part A* 15 (1) (January): 147–154. doi:10.1089/ten.tea.2007.0388.
- Wozniak, Michele A., and Christopher S. Chen. 2009. “Mechanotransduction in Development: a Growing Role for Contractility.” *Nature Reviews. Molecular Cell Biology* 10 (1) (January): 34–43. doi:10.1038/nrm2592.
- Wylie, Ryan G., Shoeb Ahsan, Yukie Aizawa, Karen L. Maxwell, Cindi M. Morshead, and Molly S. Shoichet. 2011. “Spatially Controlled Simultaneous Patterning of Multiple Growth Factors in Three-dimensional Hydrogels.” *Nature Materials* 10 (10): 799–806. doi:10.1038/nmat3101.

- Xu, Baiyao, Guanbin Song, Yang Ju, Xian Li, Yuanhui Song, and Sachi Watanabe. 2012. "RhoA/ROCK, Cytoskeletal Dynamics, and Focal Adhesion Kinase Are Required for Mechanical Stretch-induced Tenogenic Differentiation of Human Mesenchymal Stem Cells." *Journal of Cellular Physiology* 227 (6) (June): 2722–2729. doi:10.1002/jcp.23016.
- Yun, Seung Pil, Jung Min Ryu, and Ho Jae Han. 2011. "Involvement of B1-integrin via PIP Complex and FAK/paxillin in Dexamethasone-induced Human Mesenchymal Stem Cells Migration." *Journal of Cellular Physiology* 226 (3) (March): 683–692. doi:10.1002/jcp.22383.
- Zhu, Junmin. 2010. "Bioactive Modification of Poly(ethylene Glycol) Hydrogels for Tissue Engineering." *Biomaterials* 31 (17) (June): 4639–4656. doi:10.1016/j.biomaterials.2010.02.044.
- Zimmerman, D, F Jin, P Leboy, S Hardy, and C Damsky. 2000. "Impaired Bone Formation in Transgenic Mice Resulting from Altered Integrin Function in Osteoblasts." *Developmental Biology* 220 (1) (April 1): 2–15. doi:10.1006/dbio.2000.9633.
- Zou, Chengyu, Guanbin Song, Qing Luo, Lin Yuan, and Li Yang. 2011. "Mesenchymal Stem Cells Require Integrin B1 for Directed Migration Induced by Osteopontin in Vitro." *In Vitro Cellular & Developmental Biology - Animal* 47 (3) (March 1): 241–250. doi:10.1007/s11626-010-9377-0.